THE COMBINATION OF CARBOXYLESTERASE-EXPRESSING ONCOLYTIC VACCINIA VIRUS AND IRINOTECAN

By

Michelle Caitlin Becker

A thesis submitted in partial fulfillment of the requirements for the degree of

Master of Science in Biochemistry with Specialization in Human and Molecular Genetics

University of Ottawa

Faculty of Medicine

December 28th, 2012

Supervisor: Dr. John Bell

ABSTRACT

This project combines oncolytic Vaccinia virus (VV) with irinotecan (CPT-11) for the treatment of cancer. VV can infect, replicate in and destroy cancer cells, yet leave healthy cells relatively unaffected. CPT-11 is a chemotherapeutic of which ~5% is converted to the more active chemotherapeutic SN-38 by endogenous carboxylesterase (CE) enzymes. SN-38 is a topoisomerase I inhibitor that induces DNA double strand breaks, leading to growth arrest and apoptosis. Consequently, VV has been engineered to express a more effective isoform of the CE enzyme. The virus' tumour tropism should restrict enhanced conversion of CPT-11 to the tumour.

Neither CPT-11 nor SN-38 interfered with VV replication or spread. Engineered recombinants expressed CE enzyme which, when combined with CPT-11, produced DNA double strand breaks and cancer cell death. *In vitro*, the combination of CE-virus and CPT-11 killed more K-562 cancer cells than its non-CE counterpart and CPT-11.

ACKNOWLEDGEMENTS

Although my name stands alone on the title page of this document, it was completed with the help of many. First and foremost, I'd like to thank Dr. Bell for the opportunity to work in an extremely exciting field, in a lab that is constantly pushing the field in new directions, filled with gifted and dedicated researchers. I'd also like to thank him for his guidance, time and constructive criticism. I'd also like to thank the entire extended Bell lab for their help, discussions and time throughout. In particular, Chris Storbeck, Carolina Ilkow, Julia Rintoul, Rozanne Arulanandam, Naomi De Silva, Dominic Roy, Dr. Atkins, Jean-Simon Diallo, Fabrice LeBoeuf, Theresa Falls, Jiahu Wang, Chantal Lemay, Judith Paget, Madison Foster, Marianne Stanford and Manijeh Daneshmand, as well as my TAC committee, Dr. Atkins and Dr. Parks. I'd also like to thank Danielle Dewar-Darch and the University of Ottawa's Animal Care Veterinary Services for their part in animal experiments.

Finally, I want to thank my family for providing a kind and supportive environment to come home to.

TABLE OF CONTENTS

LIST OF ABBREVIATIONS

5-FC – 5-fluorocytosine

5-FU – 5-fluorouracil

Ad – Adenovirus

ADR – adriamycin

BLAST – Basic Local Alignment Search Tool

CE – carboxylesterase

CEV – cell-associated enveloped virion(s)

Chemo – chemotherapeutic drug(s)

C*max* – maximum concentration attained

CPT-11 – irinotecan

DMEM – Dulbecco's modified Eagle's medium

DMSO – dimethyl sulfoxide

DSBs – double strand breaks

EEV – extracellular enveloped virion(s)

EGF – epidermal growth factor

eGFP – enhanced green fluorescent protein

EM – electron microscopy

ES1-SCID – severe combined immunodeficient mice homozygous for $ES1^e$ allele

Fa – fraction of cells affected by the dose

FBS – fetal bovine serum

FL – full length CE

H & E(s) – Hematoxylin and eosin stain(s)

hCES1 – human liver CE

hCES1m6 – mutant human liver CE

hCES2 – human intestinal CE

HIF-1α – hypoxia-inducible factor 1α

HPLC – high-performance liquid chromatography

IHC – immunohistochemistry

IMV – intracellular mature virion(s)

IT – intratumoural(ly)

IV – intravenous(ly)

LC50 – median lethal concentration

Log – common logarithm

mAb – monoclonal antibody

MHC-1 – major histocompatibility complex class I

MOI – multiplicity of infection

NCBI – National Center for Biotechnology Information

o-NPA – *o*-nitrophenolic acid

OV(s) – oncolytic virus(es)

PBS – phosphate-buffered saline

rCE – rabbit CE

SQ – subcutaneous(ly)

TK – thymidine kinase

topo I – topoisomerase I

VEGF – vascular endothelial growth factor

VEGF-E – Orf virus VEGF

VEGFR – VEGF receptor

VGF – Vaccinia growth factor

VSV – Vesicular stomatitis virus

VV – Vaccinia virus

vvDD – double deleted Vaccinia virus

YFP – yellow fluorescent protein

WT – wild type

Wy_{TK-} – TK-disrupted Wyeth strain Vaccinia virus

ΔHIEL – secreted CE

LIST OF FIGURES

LIST OF TABLES

GENERAL INTRODUCTION

Cancer

The Canadian Cancer Society estimates that, in Canada alone, year 2012 will bring approximately 186,400 new cases of cancer and 75,700 cancer-related deaths (Canadian Cancer Society 2012). Although the numbers are concerning, far more devastating is the idea that many people are about to have their lives derailed by cancer, either being diagnosed themselves or witnessing a loved one engage in the battle.

Cancer is defined by cells that divide unencumbered by restraints built into the normal cell cycle and that invade and colonize new tissues. Cancerous cells are thought to arise from a cell that has experienced a mutation and then undergoes cycles of mutations and natural selection, adapting progressively to an independent life. These mutations can provide the cell with growth advantages such as self-sufficiency in growth signals, insensitivity to anti-growth signals, limitless replication potential, ability to evade apoptosis, induce angiogenesis and invade tissues and metastasize (Hanahan and Weinberg, 2000). Another emerging cancer hallmark is the ability to evade the immune system (Dunn et al., 2002; Hanahan and Weinberg, 2011). Although cells must accumulate multiple mutations in crucial cellular genes before they can replicate autonomously and invade other tissues, most cancers are genetically unstable, enhancing their mutation rate and probability of tumour progression (Bertram, 2000; Alberts et al., 2002).

Initially, nutrients are supplied to tumour cells by simple diffusion. Subsequently, the cells produce angiogenic factors that create a vascular network; this is necessary for a tumour to exceed 1-2 mm in diameter (Folkman, 1986). Tumour cells then detach from the primary tumour and invade surrounding tissues, intravasating into blood or lymph vessels. Some circulating tumour cells survive to arrest in distant organs, extravasate and proliferate in the

new microenvironment. These metastases can also evade immunity, develop their own vascular network and produce additional metastases (Fidler, 2003; Chaffer and Weinberg, 2011). Finally, as the cancer cells continue to proliferate and invade, they can interfere with or damage relevant organs, eventually leading to organ failure.

Current Cancer Treatment

Conventional cancer therapies include surgery, chemotherapy, radiation therapy, targeted therapy and immunotherapy. Surgery, the oldest form of cancer treatment, is effective if the primary tumour is localized. However, if any tumour cells were left behind, recurrence can occur. In fact, studies have shown that surgery-induced immunosuppression can promote metastasis (Neeman and Ben-Eliyahu, 2012).

In general, chemotherapeutic drugs (chemo) impair DNA synthesis or cell division and thus are toxic to any fast-diving cell. Chemo is a systemic therapy; although beneficial for the treatment of disseminated or undiscovered disease, it also results in many side effects. Furthermore, cancer cells can develop resistance to chemo, often by the following mechanisms: intracellular transport disturbances, drug inactivation, alterations in the drug target, DNA damage repair and evasion of apoptosis (Stefanko and Wróbel, 2010).

Radiation therapy uses ionizing radiation to damage the DNA of cells in a specific location, preventing them from proliferating if not killing them. Radiation also damages normal cells in the in the area, but because they are more efficient at DNA repair, they are better able to recover (Baskar et al., 2012). However, hypoxia, which is common in tumours, increases radiation therapy resistance (Begg et al., 2011). Moreover, the DNA-damaging effects of some forms of chemo and radiation therapy render them carcinogenic; they can

increase the risk of secondary cancers (Tucker et al., 1987 ; Tucker et al., 1988 ; Froelich et al., 1999).

Advances in cancer research have led to a better understanding of tumour development and progression, as well as its major players. Targeted therapy is a systemic therapy that inhibits specific molecular factors needed for cancer growth. Its selectivity results in less severe side effects than chemotherapy. Targeted therapies can be small molecules or antibodies directed against such factors as tyrosine kinase receptors, angiogenic factors, proteasomes, intracellular signaling molecules or apoptotic factors. However, cancer heterogeneity presents a hurdle and means rational combinations might be necessary. (Arkenau, et al., 2008; Riley and Desai, 2009; Ciavarella et al., 2010)

Immunotherapy stimulates the immune system to eliminate the tumour. Immunotherapeutic agents can include cytokines, antibodies, therapeutic cancer vaccines and low dose chemo. They can activate the immune system in general or specifically against the tumour by stimulating immune cell types, increasing tumour cell immunogenicity, supplying exogenously produced antibodies or increasing immune recognition of tumour cells. Drawbacks of immunotherapy include inadvertently selecting for immune-evasive tumour cells and the risk of autoimmunity (Skeel et al., 1997; Baxevanis et al., 2009; Fry and Lankester, 2010; Sheng and Huang, 2011).

Research into the aforementioned fields has improved survival rates, but disease progression and relapse are still common. Current treatments often produce severe side effects or target just one molecule. Cancers evolve to use multiple different signaling pathways, therefore, it is unlikely that a single target will be effective long-term (Jones et al., 2008). Furthermore, tumor cells are sculpted by their microenvironment and can become heterogeneous, even within a single tumour (Subarsky and Hill, 2003; Gerlinger et al.,

2012). However, many of the pathways activated during tumour progression benefit viral replication (Kim et al., 2010). Viruses also inherently activate both innate and adaptive immune responses (Parato et al., 2005), which can potentially recognize malignant cells (Cheever et al., 2009). These characteristics of viruses suggest that they have the potential to be powerful cancer treatment modalities (Melcher et al., 2011).

Oncolytic Viruses

Oncolytic viruses (OVs) are viruses that infect and replicate in tumour cells, resulting in their destruction, yet leave normal cells largely unaffected. They usurp the cancer cell's machinery for their own replication, ultimately leading to cell necrosis or apoptosis (Parato et al., 2005). The concept of using viruses to treat cancer emerged in the 19th century from cases of brief remission coinciding with naturally acquired viral infections; some properties of viral therapeutics were promising, such as moderate local tumour responses and lack of serious side effects, while others proved undesirable, such as short-lived efficacy and unpredictable side-effects (Wildner, 2001; Kelly and Russell, 2007). Once *in vivo* tumour models in rodents became feasible, OVs that showed promise in preclinical models progressed to clinical trials; disappointingly, OVs proved more effective in mice than human patients (Kelly and Russell, 2007). Overall, OVs had potential, but needed manipulation to increase tumour specificity.

In the 1990s, recombinant DNA technology became common and scientists were now able to manipulate the viral genome (Kelly and Russell, 2007), which meant they could gain a better understanding of the therapeutic as well as engineer it. As a result, the field of oncolytic virotherapy progressed rapidly.

OV tumour selectivity can be inherent or the result of genetic engineering. The specific mechanism of tumour selectivity depends on the virus. Some OVs are restricted to cancer cells because their entry depends on extracellular proteins that are unique or overexpressed on cancer cells. Others are engineered to place critical viral genes under the control of tumour-specific promoters (Mullen and Tanabe, 2002). But, in general, OVs take advantage of the cellular defects that promote tumour growth, such as constitutively activated signalling pathways, deregulated cell cycle, stimulated DNA synthesis, mutations in anti-viral defence and blocked apoptosis (Parato et al., 2005). As a result, OV manipulation often involves the removal of viral genes which are necessary to infect normal cells but are dispensable for cancer cells.

Oncolytic virotherapy has several advantages over conventional cancer therapy. First and foremost, it has a high therapeutic index; OVs have a therapeutic index of up to 10,000 (Chiocca, 2002); for every 10,000 cancer cells killed, one normal cell is killed. This is in contrast to typical chemotherapeutics which have a narrow therapeutic index (Parato et al., 2012). OVs are also self-amplifying; in theory, they should continue to replicate in the body as long as there are cancerous cells to support their replication. In addition, they act on entire pathways rather than a single molecule, therefore, it is harder for a cancer cell to acquire resistance. As alluded to, OVs can be manipulated with DNA technology, allowing for the addition or removal of specific traits. Furthermore, they are a multi-modality treatment: OVs can directly lyse cancer cells by replicating in them, deliver therapeutic transgenes such as suicide genes, disrupt tumour vasculature, promote tumour-specific inflammation, induce non-specific and specific antitumour immunity that lead to the destruction of infected and non-infected cancer cells and sensitize tumour cells to chemotherapy and radiation therapy.

(Mullen and Tanabe, 2002; Kirn and Thorne, 2009) Finally, toxicities are usually limited to mild flu-like symptoms.

Despite great promise, OVs have drawbacks: replication cannot always easily be shut-off potentially leading to serious side effects and not every gene of every virus has had its function elucidated (Chiocca, 2002). Furthermore, virus-host interactions are complex; innate and acquired immunity have evolved to restrict viral delivery and replication, as well as mediate viral clearance (Mullen and Tanabe, 2002). OVs can be cleared from the tumour before they have had a chance to substantially damage it. For some OVs, pre-existing viral immunity can curtail efficacy, while others are unaffected by it (Mullen and Tanabe, 2002; Parato et al., 2005).

In 2005, Chinese regulators approved the world's first OV therapy - adenovirus H101 (Garber, 2006). OVs have yet to be approved in North America and Europe; nonetheless, several OVs have generated promising phase II clinical trials data. Frontrunners are oncolytic versions of Herpes simplex virus (T-Vec by Amgen), Reovirus (Reolysin by Oncolytics Biotech) and Vaccinia virus (JX-594 by Jennerex Biotherapeutics) (Bell, 2010). The first two have entered phase III clinical trials, while JX-594 is set to do so.

Ongoing research continuously strives to refine and improve OVs for the next generation of clinical trials. Such areas include improving OV delivery, specificity and efficacy, shielding OVs from the immune system, arming OVs with therapeutics transgenes and combining OVs with chemotherapy, radiation therapy, other OVs, vascular disrupting agents or immunotherapy (Chiocca, 2002; Parato et al., 2005; Power and Bell, 2007; Bridle et al., 2010; De Silva et al., 2010; Le Boeuf and Bell, 2010; Ottolino-Perry et al., 2010; Melcher et al., 2011; Ferguson et al., 2012). Overall, it is believed that in the near future, oncolytic viruses will be used in the clinic, in combination with other standard therapies.

Vaccinia virus

This particular research focuses on oncolytic Vaccinia virus (VV). VV is a member of the poxvirus family and although its natural host is unknown, it is derived from cowpox virus. It became famous as the first widely used vaccine and resulted in the eradication of smallpox in 1977, at which point vaccination was discontinued (Fenner et al., 1988; Shen and Nemunaitis, 2004). VV is a large, complex enveloped virus with a double-stranded DNA genome that encodes over 200 genes, many of which are of unknown function. VV replication occurs entirely in the host cell's cytoplasm – replication and transcription proceed autonomously (Guse et al., 2011). VV produces 3 types of infectious particles: intracellular mature virions (IMV), cell-associated enveloped virions (CEV) and extracellular enveloped virions (EEV). The majority of the VV particles are IMV, which have a single envelope and are maintained within the infected cells until lysis. CEV and EEV have an additional envelope and bud from the infected cell prior to lysis; CEV adheres to the cell surface while EEV is completely released. CEV aid in cell-to-cell spread and EEV provide long-range dissemination (Moss, 2001). In addition, VV encodes many genes that interact with the host environment such as modulators of complement or inhibitors of interferon, apoptosis, chemokines, etc. (Moss, 2001).

VV is naturally selective for tumour cells (Yu et al., 2004; Thorne et al., 2007), as most tumours have an activated EGFR-Ras pathway which is conducive to VV replication (Kirn and Thorne, 2009). Furthermore, this virus' large size may mean more effective delivery to tumours via their leaky vasculature (Breitbach et al., 2011b). Genetic engineering has improved VV selectivity. Although a variety of VV manipulations can increase selectivity, the most common are deletion of the genes encoding thymidine kinase (TK) and

vaccinia growth factor (VGF). These genes are necessary for VV replication in normal cells but are dispensable in cancer cells. TK is involved in the synthesis of deoxyribonucleotides for DNA replication and VGF is an epidermal growth factor (EGF) homolog that is secreted from infected cells and binds EGF receptors on surrounding cells, stimulating cell proliferation (Kirn and Thorne, 2009; Guse et al., 2011). Cancer cells, which are naturally proliferating, already have high concentrations of nucleotides (Guse et al., 2011) and are in a state that supports viral production.

VV is an attractive OV candidate. It is capable of infecting most cell types: binding to host cells is mediated by heparan sulphate and cellular uptake by macropinocytosis, both of which are ubiquitous. Selectivity is thus a result of replication within the cell (Shen and Nemunaitis, 2004; Guse et al., 2011; Parato et al., 2012). VV also has efficient gene expression and can accommodate up to 25 kb of foreign DNA (Smith and Moss, 1983). Replication occurs exclusively within the cytoplasm, eliminating the possibility of integration with host DNA. VV can replicate and lyse tumour cells rapidly as well as spread throughout the bloodstream. VV is also able to induce vascular collapse and innate and adaptive anti-tumour responses. Finally, it has the longest and most extensive history of use in humans of any virus and there are approved antiviral agents in case of uncontrolled replication. (Shen and Nemunaitis, 2004; Kirn and Thorne, 2009; Guse et al., 2011; Parato et al., 2012). However, due to the smallpox vaccination program, a large portion of the population likely has neutralizing antibodies against VV (Parato et al., 2005), but studies have emerged showing productive VV replication in patients despite neutralizing antibodies (Mukherjee et al., 2000; Breitbach et al., 2011b).

This work primarily involves arming VV with therapeutics transgenes, to increase efficacy. This work is divided into three projects; the main project examines VV encoding

carboxylesterase, the second project combines VV and Orf virus vascular endothelial growth factor and the third examines and improves the plaque purification procedure. Herein, the projects are presented separately and further background information is provided in the appropriate project section.

MATERIALS AND METHODS

Cell lines:

All cell lines were purchased from the American Type Culture Collection (Manassas, USA) and were cultured in HyQ high glucose Dulbecco's modified Eagle's medium (DMEM) (HyClone, Logan, USA) supplemented with 10% fetal bovine serum (FBS) (CanSera, Etobicoke, Canada). MIA PaCa-2 cells were additionally supplemented with 2.5% horse serum (GIBCO, Carlsbad, USA) while NCI-H226 cells were grown in RPMI-1640 (Hyclone) with 10% FBS. The following cell lines were used 786-0, ACHN, HCT-116, HCT-15, HT-29, HeLa, NCI-H226, SW-620, U2OS, MIA PaCa-2 and K-562. Cell types are listed in Table 1.1. CT26WT and CT26LacZ (also known as CT26.CL25), both mouse colon carcinomas, were also used.

Viruses:

Wy_{TK-} is Wyeth strain VV with a disruption of its TK region. VV-YFP and the VV-CE recombinants are of the Copenhagen strain but contain their TK region disrupted by the addition of genes encoding luciferase for VV-YFP or the indicated CE for VV-CE recombinants. All Copenhagen recombinants contain the gene encoding yellow fluorescent protein (YFP). The CE gene is controlled by a synthetic late promoter, p004. Cloning was verified by sequencing. vvDD, also termed vvDD-eGFP, has been described previously (McCart, J. A. et al. 2001). vvDD-mCherry contains mCherry instead of enhanced green fluorescent protein (eGFP). All viruses used were propagated in HeLa cells and purified by sucrose cushion purification. As a side note, throughout the project, the multiplicity of infection (MOI) corresponds to the plaque forming units determined on U2OS cells.

Drugs:

For *in vitro* studies, CPT-11 (Sigma, St. Louis, USA) and SN-38 (Sigma) were diluted in dimethyl sulfoxide (DMSO) (Fisher Scientific, Hampton, USA). Adriamycin (ADR), provided by Dr. Ian Lorimer (Ottawa Hospital Research Institute), and CPT-11 for *in vivo* studies, were originally obtained from The Ottawa Hospital Cancer Centre Pharmacy.

Growth curves in the presence of CPT-11 and SN-38:

12-well plates were seeded with the indicated cell line at 0.5×10^6 cells/well. The next day, cells were infected with the indicated virus at either a high MOI, 3, or a low MOI, 0.01, for 2 hrs at 37°C. The inoculum was replaced with media containing either vehicle or the indicated concentration of CPT-11 or SN-38. Drugs were left in the media for the duration of the experiment. Samples (both cells and sup) were collected at the indicated time point, freeze/thawed 3 times and titered on U2OS cells. To see the effect of SN-38 in the absence of virus, 96-well plates were seeded with 10^4 cells/well (8×10^3 cells/well for HT-29). The next day, the cells were treated with either vehicle or the indicated concentration of SN-38. At the indicated time point, metabolic activity was measured by Alamar Blue (AbD Serotec, Raleigh, USA), according to the manufacturer's protocol, to estimate viability.

Combination Index for the combination of Wy_{TK-} and CPT-11:

HCT-116, SW-620, HCT-15 and HT-29 cells were plated at 1.5×10^4 cells/well in 96-well plates. The next day, serial dilutions of Wy_{TK-} (6000 to 750 PFU) and CPT-11 (40 to 5 µM) were added, with a fixed-ratio of 150 PFU of Wy_{TK-} : 1 µM CPT-11. Three days later, Alamar Blue was used to assess metabolic activity. Combination indices were calculated

according to the method of Chou and Talaly using Calcusyn Software (Biosoft, Ferguson, USA).

Determination of the median lethal concentration (LC50) of CPT-11, SN-38 and VV-YFP: The indicated cells were plated in 96-well plates at a density of 10^4 cells/well (2×10^3 cells/well for 786-0, 8×10^3 cells/well for HT-29 and K-562). The next day, cells were treated with a range of concentrations of either CPT-11 or SN-38 or a range of VV-YFP MOIs. The drugs or virus were left in the media for the duration of the experiment. Three days post-treatment, metabolic activity was measured by Alamar Blue.

CE Protein Expression from VV-CE recombinants:
SW-620 cells were plated in 10 cm dishes at a cell density of 7×10^6 cells per dish. The next day, cells were infected with the indicated virus at an MOI of 0.1. After infection, inoculum was replaced with media supplemented with 1% FBS. At either 2 or 3 days post-infection, both supernatant and cell fractions were collected. The cell fraction was lysed using ProteoJET Mammalian Cell Lysis Reagent (Fermentas, Burlington, Canada) containing ProteoBlock Protease Inhibitor Cocktail (Fermentas) and the supernatant was concentrated using 100 and 50 kDa centrifugal filters (Amicon, Billerica, USA). The fraction between 50 and 100 kDa was then desalted with a 1M Tris, pH = 6.8 solution. Specifically, the samples (35 µg of protein for the lysates and 22.5 µl of concentrated/desalted supernatant) were separated on a precast 4-20% SDS-PAGE gel (Invitrogen, Carlsbad, USA) and transferred onto a PVDF membrane (Amersham, Amersham, UK). CE was detected by Western blot using a monoclonal rabbit anti-human ACAT antibody (Epitomics, Burlingame, USA) at a dilution of 1:1000. This antibody recognizes residues on the C-terminus of hCES1. A

peroxidase-conjugated goat anti-rabbit secondary antibody (Jackson Immunoresearch, West Grove, USA) was used at a dilution of 1:3000. Bands were visualized with Supersignal West Pico Chemiluminscent Substrate (Pierce) using FluorChem FC2 imaging system (Alpha Innotech, San Leandro, USA). Loading was verified with a polyclonal goat anti-human β-tubulin antibody (Abcam, Cambrige, UK) at a dilution of 1:2000.

VV-CE induction of DNA DSBs in target cells:

For the direct infection experiment, 10 cm dishes were seeded with 7×10^6 SW-620 cells. The next day, cells were infected with the indicated virus at an MOI of 3. Following infection, inoculum was replaced with media containing either 0.1 μM CPT-11, 0.1 μM SN-38 or 0.5 μM adriamycin (ADR), which was left on the cells for the duration of the experiment. Three days post-infection, cells were collected and lysed. For the supernatant transfer experiment, inoculum, in addition to virus, contained either vehicle, 2.2 μM CPT-11, 0.06 μM SN-38. Following the 2 hour infection, inoculum was replaced with media containing the same concentration of drug. Six hours later, media was replaced with drug-free media. Three days post-infection, the supernatant was collected and filtered through a 0.22 μm filter to remove any virus particles. This supernatant, which may or may not contain newly formed SN-38, was then transferred onto fresh SW-620 target cells which had been plated in 10 cm dishes the day before. For the positive control, mock-infected supernatant was transferred onto target cells which were subsequently treated with ADR. Two days later, the target SW-620 cell fraction was collected, lysed and a Western Blot was performed as described above, for the detection of γ-H2A.X, a marker for DNA DSBs. A monoclonal mouse anti-human γ-H2A.X antibody (Millipore, Billerica, USA) was used at a dilution of 1:1000. This antibody recognizes amino acids 134 – 142 of human γ-H2A.X, phosphorylated

at Ser139. Loading was verified with polyclonal rabbit anti-human GAPDH (Abcam) at a dilution of 1:5000. Densitometry was performed with Alphaview software (Alpha Innotech).

Supernatant transfer assay to show CE bystander killing:

SW-620 cells were plated in 10 cm dishes using a cell density of 7×10^6 cells per dish. The next day, cells were mock infected or infected with the indicated virus at an MOI of 0.1. Three days later, this CE-containing supernatant was collected, filtered through a 0.22 µm filter and transferred onto fresh SW-620 target cells, which had been plated in 96-well plates the day before at a cell density of 2.5×10^3 cells/well, so that the added supernatant accounted for 50% of the final volume. Either vehicle, 2.2 µM CPT-11 or 0.06 µM SN-38 were added to target cells for 8 hours at which point media was replaced with drug-free media. Five days following transfer, metabolic activity of target cells was measured using Alamar Blue.

Modified supernatant transfer assay to show SN-38 bystander killing:

SW-620 cells were plated in 10 cm dishes and, the next day, cells were mock infected or infected with the indicated virus at an MOI of 0.1. For brief exposure, either vehicle, 2.2 µM CPT-11 or 0.06 µM SN-38 was added to the inoculum and following the infection, the inoculum was replaced with media containing the same drug. Six hours later, media was replaced with drug-free media. Three days post-infection, the SN-38 containing supernatant was collected, filtered through a 0.22 µm filter and added to fresh SW-620 target cells, which had been plated in 96-well plates the day before. Two or three days later, metabolic activity of target cells was measured using Alamar Blue.

In vitro efficacy of VV-CE recombinants in K-562 cells:

K-562 cells were either mock infected or infected with the indicated virus at an MOI of 3. Cells were then centrifuged, inoculum was replaced with fresh media, cells were counted and seeded at 0.5×10^6 cells/well in a 12-well plate. For the 5-day experiment, cells were treated with either vehicle, 0.1 µM CPT-11 or 0.1 µM SN-38 and cell viability was assessed by trypan blue exclusion 5 days post-infection. For the 10-day experiment, cells were treated with either vehicle, 0.05 µM, 0.1 µM or 0.25 µM CPT-11 or 0.05 µM SN-38 and every three days, the entire contents of the well were collected (K-562 is a suspension cell line), centrifuged and the supernatant was replaced with fresh media containing the same drug. Viability was assessed 10 days post-infection.

In vitro efficacy of VV-CE recombinants in K-562 and U2OS co-cultures:

Twelve-well plates were seeded with 0.29×10^6 U2OS cells/well. The next day, they were mock infected or infected with the indicated virus at an MOI of 0.01 or 3. After the infection, the inoculum was replaced with a suspension of 0.5×10^6 K-562 cells/well. The wells were then treated with either vehicle, 0.1 µM, 0.25 µM or 0.5 µM CPT-11 or 0.1 µM SN-38. Either 3, 4 or 5 days post-treatment, cell viability was assessed by trypan blue exclusion.

In vivo VV-CE experiments in ES1-SCID mice:

ES1-SCID mice were a gift from Dr. Philip Potter (St. Jude Children's Research Hospital). Mice were bred by Danielle Dewar-Darch (Ottawa Hospital Research Institute) at the University of Ottawa Animal Care and Veterinary Service and all experiments were conducted with their approval. These mice are homozygous for the $Es\text{-}1^e$ allele, which

reduces their plasma carboxylesterase activity, comparable with that of humans. These mice do not have any discernable health problems (Soares, 1979; Morton et al., 2005).

ES1-SCID mice were injected with 5×10^6 K-562 cells subcutaneously (SQ). Once tumours were palpable, treatment began and this was set as Day 0. Tumour measurements were taken on the indicated days using calipers and tumour volume was calculated by (length $\times$ width^2)/2.

For the preliminary intratumoural (IT) efficacy study, mice were injected IT with 10^4 PFU of the indicated virus on days 0 and 7, and with 0.3 mg/kg of CPT-11 IT on days 2 and 9. Mice were sacrificed on day 10, their tumours were excised, embedded in Optimal Cutting Temperature (Tissue-Tek, Alphen aan den Rijn, Netherlands), frozen at -80°C and sectioned into 6 µm slices using a Microm HM500 OM cryostat (Microm, Walldorf, Germany). Immunohistochemistry (IHC) was performed on these sections; VV infected cells were detected by a polyclonal rabbit anti-VV antibody (1:15000, Quartett, Berlin, Germany) using the Vectastain ABC kit (Vector Labs, Burlingame, USA) for rabbit primary antibodies, according to the manufacturer's protocol. To detect apoptotic cells, a polyclonal rabbit anti-human active caspase-3 antibody (BD Biosciences, Mississauga, Canada) was used at a dilution of 1:500. Nuclei were counterstained in hematoxylin. Staining was digitized using Aperio ScanScope (Axiovision Technologies, Toronto, Canada) and analyzed using Aperio ImageScope software.

vvDD-VEGF-E cloning:

VEGF-E was amplified from Orf virus DNA and inserted into the pSC65-Luc plasmid using XhoI and BamHI restriction sites. The VEGF-E and luciferase genes were inserted into

vvDD's TK region by homologous recombination and recombinants were selected by luciferase expression and plaque purified on U2OS cells.

In vivo experiments with VEGF-E and vvDD in BALB/c mice:

Female 6-week-old BALB/c mice were purchased from Charles River Laboratories (Wilmington, USA). Mice were injected with 3×10^5 cells SQ (either CT26LacZ or CT26WT).

For the Orf pre-treatment experiment, mice bearing CT26LacZ tumours were given 5×10^6 PFU of Orf virus (± VEGF-E) IT on days 0 and 2. On day 4, 10^7 PFU of vvDD was given either IT or IV. On day 7, mice were sacrificed, tumours were excised, weighed, homogenized in PBS and titered on U2OS cells.

For the experiment where viral spread was examined, mice bearing CT26WT tumours were given 400 ng of recombinant VEGF-E protein (Prospec, Rehovot, Israel) IT. On day 4, they received 10^7 PFU of vvDD IT. On day 7, mice were sacrificed, tumours were excised, weighed, homogenized in PBS and titered on U2OS cells.

For the experiment where viral delivery was examined, mice bearing CT26WT tumours were given 650 ng of recombinant VEGF-E protein IT. On day 4, some mice received 10^7 PFU of vvDD IV while the other mice were sacrificed, to observe tumour histology and perfusion at the time point when the first group of mice received virus. The latter group was injected IV with 100 µl of a 50% solution of 100 nm diameter orange fluorescent microspheres (Molecular Probes, Burlington, Canada) in PBS. Five minutes later, animals were sacrificed, tumours were excised and frozen at -80°C. For quantification of blood vessels, tumours were sectioned into 6 µm sections and stained with hematoxylin and eosin (H & E) according to standard protocols. Staining was digitized using Aperio

ScanScope and analyzed using Aperio ImageScope software. For assessment of tumour perfusion, tumours were sectioned into 10 µm sections and fluorescent microspheres in the vasculature were visualized using a ScanArray Express microarray scanner with a standard Cy3 laser (Packard Bioscience, Waltham, USA). The mice that received virus on day 4 were sacrificed on day 5, had their tumours excised, weighed, homogenized in PBS and titered on U2OS cells.

% aggregation of sucrose-purified virus:

Six well plates were seeded with 0.6×10^6 U2OS cells/well. The next day, cells were infected with a mixture containing equal parts vvDD-eGFP and vvDD-mCherry (MOI = 0.005 for each virus). Following infection, inoculum was replaced with an agarose overlay (1:1 2% agarose: 2X DMEM + 20% FBS). Two days post-infection, GFP and mCherry expression were visualized by microscopy and the percentage of total plaques that express both GFP and mCherry is the resulting % aggregation.

% aggregation of infected cell lysate:

Ten cm plates were seeded with 3×10^6 U2OS cells. The next day, cells were infected with a mixture of vvDD-eGFP and vvDD-mCherry (MOI = 0.005 for each virus). Following infection, inoculum was replaced with fresh media. Two days post-infection, the entire contents of the well were collected and freeze/thawed three times. This is referred to as the vvDD-GFP and vvDD-mCherry infected cell lysate and was used to infect U2OS plates using the same protocol as described for the determination of % aggregation of sucrose-purified virus preparations, above.

For the comparison of disaggregation methods, vvDD-GFP and vvDD-mCherry infected cell lysate was either left untreated, sonicated 3 × 1 minute on ice using a probe sonicator (Sonic Dismembrator model 3000 at 35% power) (Fisher), treated with 50 U/ml of Benzonase Nuclease (Sigma) for 30 mins at 37°C followed by a 1:1 Tryp-LE (GIBCO) treatment at room temperature for 1 hour or filtered through a 0.65 µm pore syringe filter (Sartorius, Göttingen, Germany).

For the reaggregation time course experiment, vvDD-GFP and vvDD-mCherry infected cell lysate was split into several fractions, which were stored at 4°C. At the indicated time prior to infection, fractions were filtered and put back at 4°C. For the reaggregation after freeze/thaw cycles experiment, fractions were either filtered or left untreated and then freeze/thawed for the indicated number of freeze/thaw cycles. All fractions were then used to infect U2OS 6-well plates as described above.

Determination of % aggregation in the supernatant and lysate:

Ten cm plates were seeded with 3×10^6 U2OS cells. The next day, cells were infected with a mixture of vvDD-eGFP and vvDD-mCherry (MOI = 0.005 for each virus). Following infection, inoculum is replaced with fresh media. Either the supernatant was collected at 16 hrs post-infection or the entire contents of the well were collected two days post-infection. Samples were freeze/thawed 3 times and used to infect U2OS 6-well plates as described above.

Aggregation in the plaque picking procedure:

U2OS cells were infected with vvDD-GFP and vvDD-mCherry infected cell lysate, as described above. Resulting plaques were observed by microscopy and 3 green plaques, 3 red

plaques and 3 mixed plaques were picked according to the lab's plaque picking procedure. These plaques were then split into two fractions, one of which was filtered, the other untreated, and these were then used to infect subsequent U2OS cells, also as described above.

PROJECT 1: THE COMBINATION OF CARBOXYLESTERASE-EXPRESSING ONCOLYTIC VACCINIA VIRUS AND IRINOTECAN

Introduction

This work combines VV with irinotecan (CPT-11), a chemotherapeutic used against various cancers, but mainly colorectal cancer. It is infused intravenously and converted to the more active chemo SN-38 by carboxylesterase (CE) enzymes, high levels of which are in the liver and intestine. CE enzymes hydrolyze ester and amide-containing chemicals and are involved in the detoxification or activation of various drugs or environmental compounds (Satoh and Hosokawa, 1998; Imai, 2006). However, usually less than 5 % of the CPT-11 is converted to SN-38 (Rivory et al., 1997). SN-38 is a topoisomerase I (topoisomerase I) inhibitor; it binds to topoisomerase I – DNA complexes and stabilizes them, preventing topoisomerase I's religation of the temporary single strand nicks. When cells enters S phase; the replication machinery collides with these SN-38 – topoisomerase I – DNA complexes, resulting in DNA double strand breaks (DSBs), leading to growth arrest and apoptosis (Hsiang et al., 1989; te Poele and Joel, 1999). Although CPT-11 and SN-38 are both topoisomerase I inhibitors, SN-38 is 100 – 1000 times more active (Kawato et al., 1991). CPT-11/SN-38 activity shows some degree of selectivity for cancer cells, as these cells tend to proliferate and have higher topoisomerase I activity, which would lead to more DSBs (Jansen et al., 1997; Guichard et al., 1999). Nevertheless, the intestinal isoform of CE produces SN-38 in the colon, leading to gastrointestinal damage and dose-limiting toxicities (Khanna et al., 2000).

In addition to simply combining the oncolytic virus with the chemotherapeutic, VV recombinants have been engineered to express a CE enzyme (termed VV-CE), which should increase the conversion of CPT-11 to SN-38. Moreover, various CE recombinant viruses were made; one recombinant contains rabbit CE (rCE), which is known to be 100 – 1000 times more effective than the human liver isoform (hCES1) (Danks et al., 1999). Another recombinant contains a mutant version of hCES1; this mutant was created after aligning the sequences of rCE and hCES1 and noticing that they were 81 % identical at the amino acid level (Danks et al., 1999). Subsequently, Dr. Philip Potter's group made a mutant derived from hCES1, but containing 8 mutations to make its active site resemble that of rCE. This mutant, termed hCES1m6, shows similar activity to the rCE and, in theory, if it were to be used in the clinic, it would be less likely to generate an immune response than rCE (Wierdl et al., 2008). In addition to these two isoforms, there are two versions of the isoforms; retained (FL) and secreted (ΔHIEL). CE's last four amino acids, HIEL, cause it to be retained within the cell. Thus, the secreted versions have these amino acids removed (Potter et al., 1998; Wierdl et al., 2001). Since the CE-expressing viruses are tumour tropic, the enhanced conversion of CPT-11 should only be occurring in the tumour; viral CE may improve the safety of CPT-11 as lower doses can be administered yet its activity should remain high in the tumour. And since some of the recombinants have a secreted version of CE, this should allow for bystander killing of uninfected tumour cells.

Hypothesis and objectives

We suspect that virally-encoded CE will potentiate the combination of VV and CPT-11. The objectives of the project are to determine if CPT-11 and the SN-38 its converted to negatively affect the VV backbone (in the absence of CE); confirm the functionality of VV-

CE recombinants and determine if viral expression of CE provides an advantage in the presence of CPT-11 *in vitro* and *in vivo*.

Results

Preliminary work by Marianne Stanford, PhD, had showed that 1 µM CPT-11 had no effect on Wy_{TK-} spread, alleviating concerns that CPT-11 might inhibit the viral topoisomerase I and subsequently impede the combination. She also showed the combination to be synergistic in HCT-116 cells and a pilot experiment in mice bearing HCT-116 tumours showed that the combination reduced tumour volume and extended survival more than either agent alone.

These findings were repeated; growth curves confirmed that CPT-11 does not affect Wy_{TK-} spread, Figure 1.1A. Growth curves in the presence of SN-38 (Figure 1.1B) were also performed since viral CE would be producing SN-38. Only the highest concentration of SN-38 affected Wy_{TK-} spread in HCT-116 and SW-620 cells. This SN-38 concentration also decreased host cell viability in the absence of virus (Figure 1.1C). However, it can be observed that 0.06 µM SN-38, the second highest concentration, is almost as toxic as 0.6 µM SN-38 on its own, but does not impact viral spread as drastically. It was also confirmed that the combination was slightly synergistic in HCT-116 cells, Figure 1.1D. At concentrations of CPT-11 and Wy_{TK-} high enough to affect roughly 30% of cells (Fa = 0.3), the combination index dips below 1, indicative of an additive interaction. After reaching Fa = 0.7, the combination index is lower than 0.7, implying a synergistic interaction.

Subsequently, Chris Storbeck, PhD, cloned a TK disrupted Copenhagen, termed VV-YFP; TK was disrupted by the addition of genes encoding YFP and luciferase.

A preliminary cell line screen was done by determining the LC50s of CPT-11, SN-38 and VV-YFP in each cell line, Table 1.1. The ideal cell line would be much more sensitive to SN-38 than VV or CPT-11, that way, the production of SN-38 would have a drastic effect on

Figure 1.1: Only high concentrations of topo I inhibitors CPT-11 and SN-38 affect Wy_{TK-} replication. A) and B) HCT-116, SW-620, HCT-15 and HT-29 cells were infected with Wy_{TK-} at an MOI of 0.01 and then treated with the indicated amount of CPT-11 (A), SN-38 (B) or vehicle control. The drugs were left on the cells for the duration of the experiment. Samples were collected at the indicated time points and viral titer was determined by titering on U2OS cells. For A) and B), data was obtained from one experiment, but is representative of two separate experiments. C) HCT-116, SW-620, HCT-15 and HT-29 cells were treated with the indicated amount of SN-38 or vehicle control. The drugs remained in the media for the duration of the experiment. At the indicated time point, metabolic activity was assessed by Alamar Blue. Data was obtained from one independent experiment done in quadruplicate; data points represent means. D) HCT-116 cells were treated with serial dilutions of a mixture of a fixed ratio of Wy_{TK-} to CPT-11 (150 PFU to 1 µM CPT-11). Metabolic activity was assessed 3 days post-treatment using Alamar Blue. The combination index was generated with Calcusyn software, using a method described previously (Chou, T. C. and Talaly, P. 1977). The graph represents the combination index as a function of the fraction of cells affected. Results are obtained from one experiment done in quadruplicate. Data points are means ± SD.

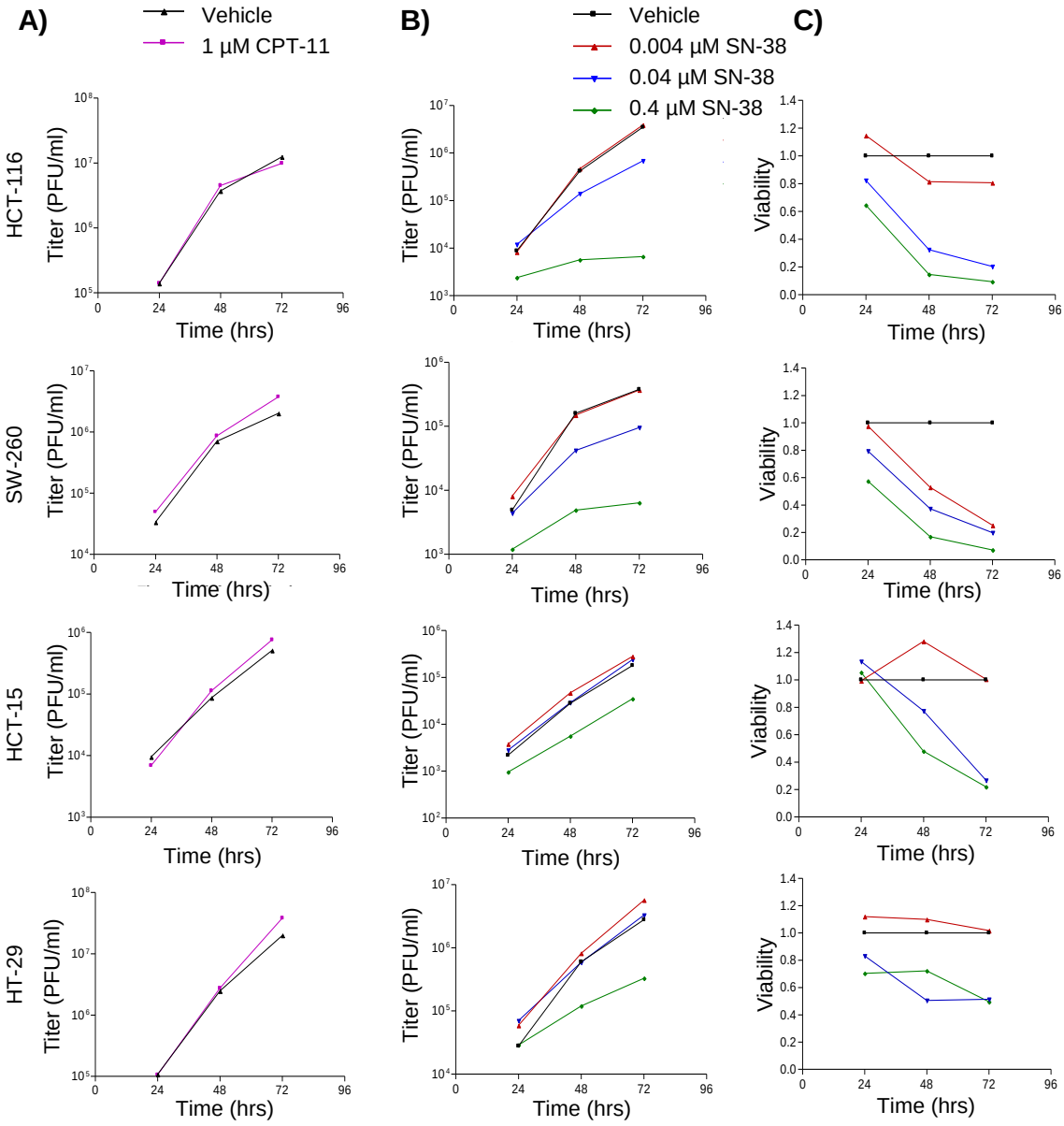
A)
Vehicle
1 µM CPT-11
B)
Vehicle
0.004 µM SN-38
0.04 µM SN-38
0.4 µM SN-38
C)
HCT-116
SW-260
HCT-15
HT-29
Titer (PFU/ml)
Viability
Time (hrs)

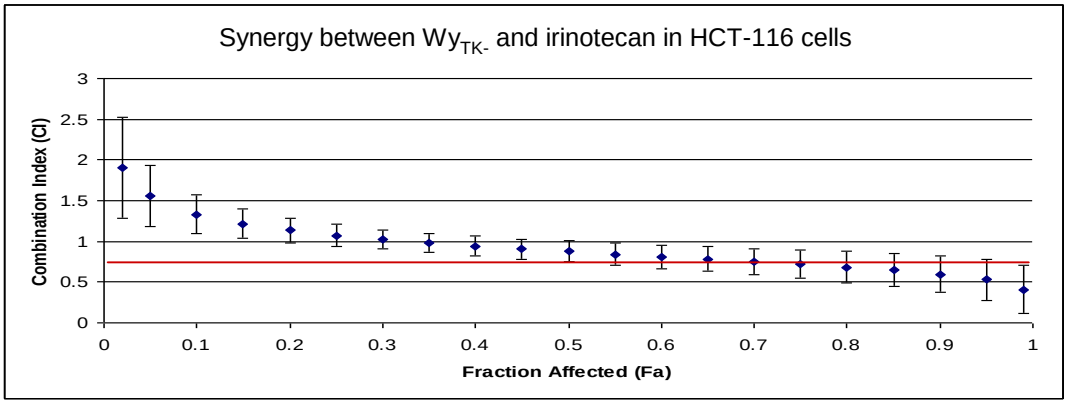
D)
Synergy between Wy$_{TK-}$ and irinotecan in HCT-116 cells
Combination Index (CI)
Fraction Affected (Fa)

Table 1.1A: LC50s of CPT-11, SN-38 and VV-YFP in various human cancer cell lines 3 days post treatment, as assessed by metabolic activity with Alamar Blue

Cell Line	Organism	Source	LC50			CPT-11 / SN-38 [b]	VV-YFP / SN-38 [b]
			CPT-11 (µM)	SN-38 (µM)	VV-YFP (MOI)		
786-0	human	Renal cell adenocarcinoma	2.94	0.004	0.100	679.9	23.07
ACHN	human	Renal cell adenocarcinoma	2.80	0.008	0.011	370.0	1.45
HCT-116	human	Colorectal carcinoma	2.96	0.005	0.041	604.6	8.40
HCT-15	human	Colorectal adenocarcinoma	18.04	0.012	0.304	1489.5	25.09
HeLa	human	Cervical adenocarcinoma	65.16	0.250	0.061	260.6	0.24
HT-29	human	Colorectal adenocarcinoma	123.15	0.258	0.587	476.9	2.27
NCI-H226	human	Lung squamous cell carcinoma	23.10	0.031	0.043	748.8	1.38
SW-620	human	Colorectal adenocarcinoma	1.61	0.003	0.371	628.1	144.34
U2OS	human	Osteosarcoma	53.13	0.668	0.016	79.5	0.02
MIA PaCa-2	human	Pancreatic carcinoma	3.20	0.034	0.196	93.3	5.70
K-562 [a]	human	Chronic myelogenous leukemia	2.72	0.006	1.789	489.3	321.64

Numbers represent the averages of at least 3 independent experiments, done with 6 replicates.

[a] Cell line was not included in the original screen. It was assessed later in the project.

[b] Colour scheme is arbitrary.

Table 1.1B: Legend for Table 1A

Legend		
Excellent		> 100
Good	> 1000	10 - 100
Intermediate	100 - 1000	1 - 10
Poor	<100	<1

cancer cell death. High ratios of both virus LC50 to SN-38 LC50 and CPT-11 LC50 to SN-38 LC50 signify the cell line is more sensitive to SN-38 than the agent it is being compared to. Of note, SW-620, HCT-15 and 786-0 cell lines were most promising. K-562 cells were not assessed until later in the project. SW-620 cells were selected for further studies given they are a colon cancer cell line and are commonly used for *in vivo* studies in our laboratory.

To assess if CPT-11 hinders the Copenhagen backbone, growth curves were done with VV-YFP and either CPT-11 or SN-38 in SW-620 cells. Three concentrations of each drug were used. For CPT-11, this was the average patient plasma C_{max}, 2.2 µM, one tenth of it, 0.22 µM, and the highest patient plasma C_{max} found, 10µM. For SN-38, this was the average patient plasma C_{max}, 0.06 µM, one tenth of it, 0.006 µM, and ten times it, 0.6 µM, given there might be more SN-38 produced than the cells are typically exposed to (de Forni et al., 1994; Catimel et al., 1995; Pitot et al., 2000; Rothenberg et al., 2001; Ueno et al., 2007). A single-step growth curve, Figure 1.2A, showed that the drugs do not affect viral replication and a multi-step growth curve, Figure 1.2B, showed that they do not affect viral spread; all titers are within 1 log of the vehicle sample and any differences are smaller than the sensitivity of the assay and thus considered not different in this assay.

VV recombinants expressing different versions of CE, termed VV-CE recombinants, were cloned. To ensure that they produce CE protein during viral infection, SW-620 cells were infected with the various recombinants and CE expression in the supernatant and cell fraction was assessed by Western Blot using an α-hCES1 mAb. Figure 1.3 shows that the cell fraction of cells infected with VV-hCES1m6 FL and VV-hCES1m6ΔHIEL contained detectable hCES1 at 48 and 72 hrs. The rCEΔHIEL counterpart did not; likely the anti-human antibody failed to react with the rabbit protein. Only the supernatant from cells

Figure 1.2: Topoisomerase I inhibitors CPT-11 and SN-38 do not affect VV-YFP replication nor spread *in vitro* in SW-620 cells. SW-620 cells were infected with VV-YFP at an MOI of 3 (single step growth curve, (A)) or 0.01 (multi step growth curve, (B)) and then treated with the indicated amount of CPT-11, SN-38 or vehicle control. The drugs were left on the cells for the duration of the experiment. Samples were collected at the indicated time points and viral titer was determined by titering on U2OS cells. A) represents data from one experiment. B) represents data from one experiment, done in duplicate, but is representative of two independent experiments. ns $P < 0.05$ (one-way ANOVA with Bonferroni's Multiple Comparison Test, comparing all samples to vehicle).

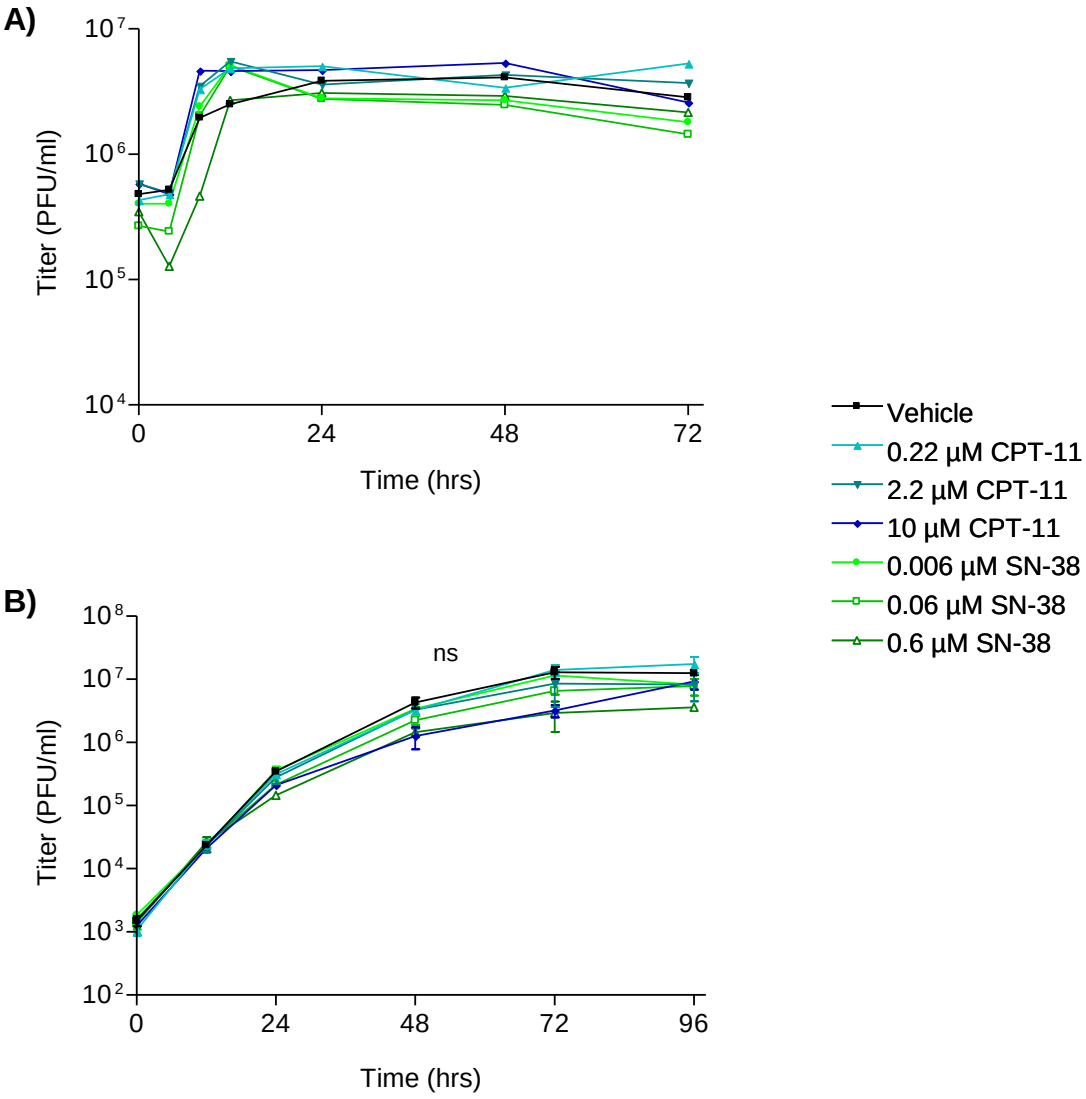
A)
Titer (PFU/ml)
Time (hrs)
B)
ns
Vehicle
0.22 µM CPT-11
2.2 µM CPT-11
10 µM CPT-11
0.006 µM SN-38
0.06 µM SN-38
0.6 µM SN-38

Figure 1.3: VV recombinants encoding human CE produce CE protein. Western blots showing the levels of hCES1 and β-tubulin (loading control) in cell lysates and supernatants collected from SW-620 cells at either 48 (A) or 72 hrs (B) following infection with the indicated VV-CE recombinant at an MOI of 0.1.

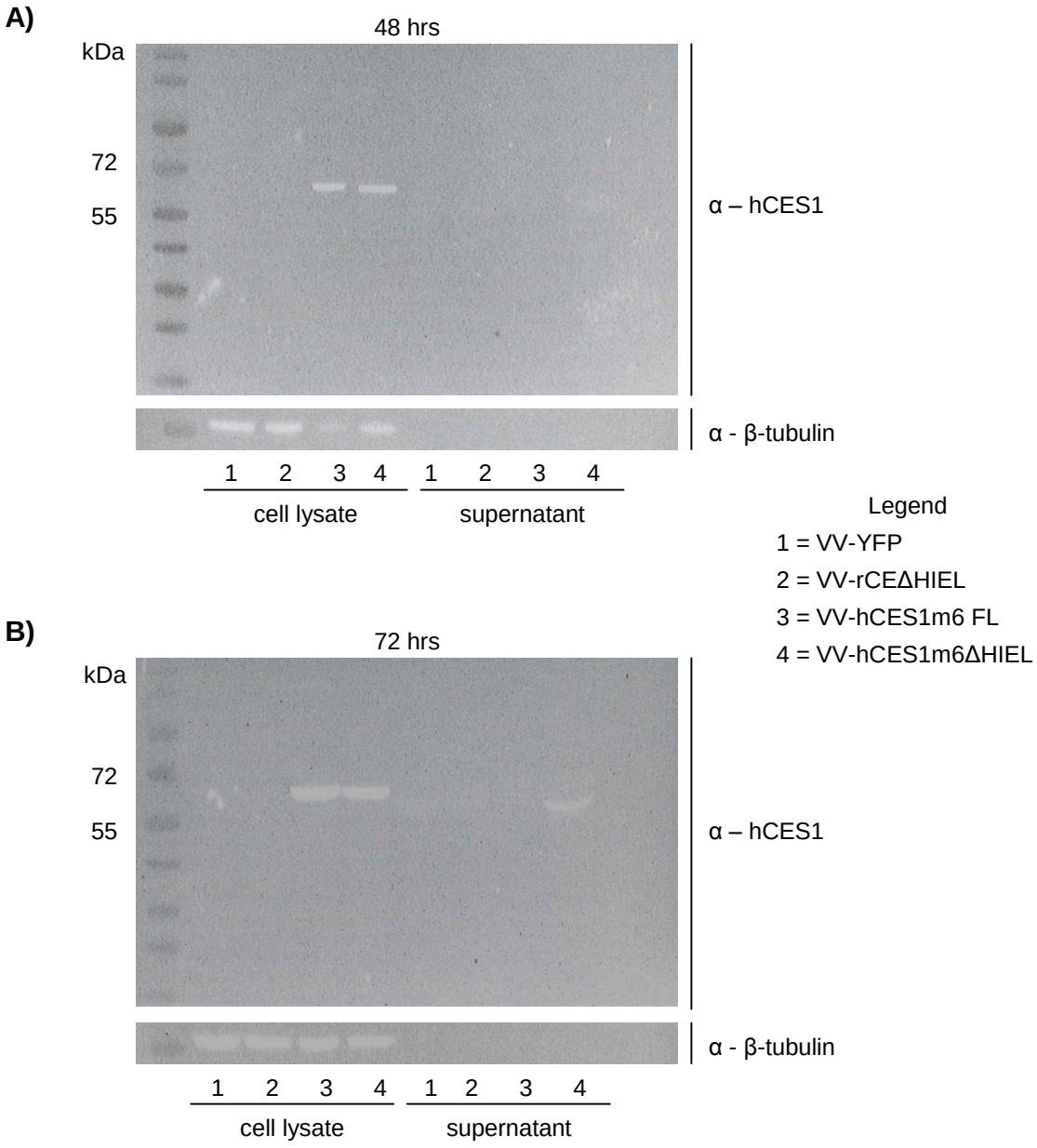
A)
48 hrs
kDa
72
55
α – hCES1
α - β-tubulin
1 2 3 4 1 2 3 4
cell lysate
supernatant
Legend
1 = VV-YFP
2 = VV-rCEΔHIEL
3 = VV-hCES1m6 FL
4 = VV-hCES1m6ΔHIEL
B)
72 hrs
kDa
72
55
α – hCES1
α - β-tubulin
1 2 3 4 1 2 3 4
cell lysate
supernatant

infected with VV-hCES1m6ΔHIEL contained hCES1, as detected faintly at 48 hrs and more obviously at 72 hrs. VV-rCEΔHIEL was nevertheless carried forward into functional assays.

In the literature, CE activity can be measured by SN-38 output using high-performance liquid chromatography (HPLC). Since our lab does not have this technology, SN-38 was detected by its known mechanism of action, the induction of DNA DSBs. Cells were infected with either VV-YFP or VV-hCES1m6ΔHIEL as well as treated with either CPT-11, SN-38 or ADR, given ADR is known to cause DNA DSBs (Byfield et al., 1977; Goldenberg et al., 1986). These cells were then collected, lysed and γ-H2A.X, which is quickly produced in response to DNA DSBs (Rogakou et al., 1998), was detected by Western blot. Figure 1.4A shows that any effects of CPT-11/SN-38 are dwarfed by the virus-mediated induction of γ-H2A.X. In order to focus on the γ-H2A.X induced by the drugs only, cells were infected with either VV-YFP or VV-hCES1m6ΔHIEL and treated with either vehicle, CPT-11 or SN-38. Supernatant from these cells, which may or may not contain SN-38, was collected, filtered to remove virus and added to target SW-620 cells which were examined for γ-H2A.X induction. Figure 1.4B shows that the combination of VV-hCES1m6ΔHIEL and CPT-11 induces γ-H2A.X to a greater extent than the combination of VV-YFP and CPT-11, comparable to cells treated with SN-38. The other VV-CE recombinants did as well (data not shown).

In order to determine if viral CE expression could convert CPT-11 to SN-38 outside of the cell and subsequently induce bystander killing, the supernatant transfer technique was further explored: cells were infected with the various viruses and supernatant from these cells, which may or may not contain CE, was filtered to remove virus and added to fresh target SW-620 cells. Vehicle, 2.2 μM CPT-11 – the average patient plasma C_{max}, or SN-38 were then added to the target cells for 8 hours, which is approximately the half life of the

Figure 1.4: The supernatant from cells infected with VV-CE recombinants and treated with CPT-11 is able to induce γ-H2A.X. Western blot showing the levels of γ-H2A.X, a marker for DNA DSBs, the mechanism by which SN-38 is known to act, and GAPDH (loading control) in SW-620 cell lysates. (A) SW-620 cells were infected at an MOI of 3 and treated with either 0.1 µM CPT-11, 0.1 µM SN-38 or 0.5 µM ADR. The drug was left in the media throughout the experiment. Three days following infection, cells were collected and lysed. (B) Original SW-620 cells were infected at an MOI of 0.1 and treated with either vehicle, 2.2 µM CPT-11 or 0.06 µM SN-38 for 8 hours. Three days following infection, supernatant was collected, filtered to remove virus and added to target SW-620 cells at a final volume of 50%, with or without 0.5 µM ADR. Two days following supernatant transfer, target cells were collected and lysed. For both A) and B), the bottom panel shows quantification of the blot by densitometry; each quantitated γ-H2A.X signal was normalized to that of its GAPDH counterpart and then levels were expressed relative to the sample in lane 1.

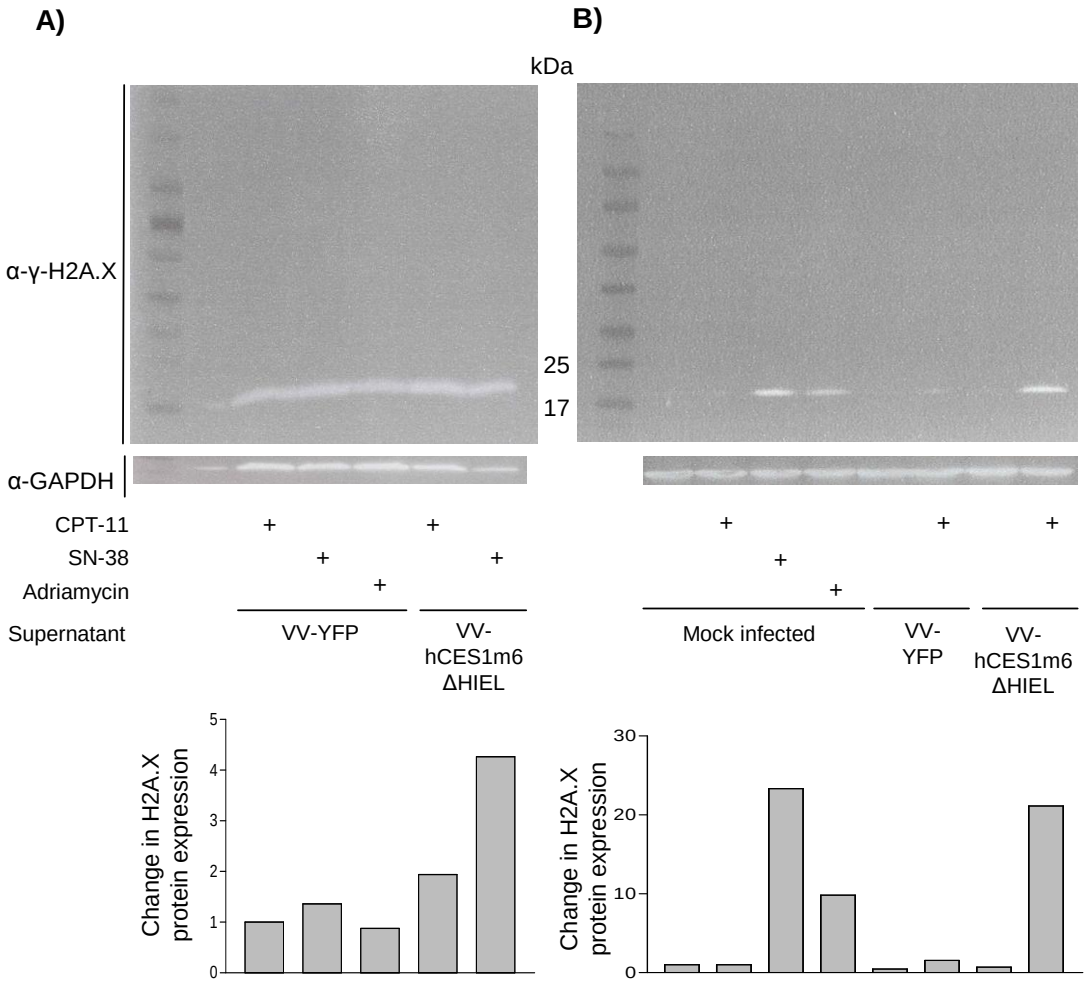
A)
B)
kDa
α-γ-H2A.X
25
17
α-GAPDH
CPT-11
SN-38
Adriamycin
Supernatant
VV-YFP
VV-hCES1m6 ΔHIEL
Mock infected
VV-YFP
VV-hCES1m6 ΔHIEL
Change in H2A.X protein expression
Change in H2A.X protein expression

CPT-11, 9.4 hrs (de Forni et al., 1994; Catimel et al., 1995; Chabot et al., 1995 ; Rivory et al., 1997; Pitot et al., 2000; Rothenberg et al., 2001; Ueno et al., 2007). Figure 1.5A shows that supernatant from cells infected with recombinants expressing a secreted version of CE, and not the retained version, significantly decreased target cell viability.

If CPT-11 exposure is increased, it is toxic on its own (data not shown) and viral CE no longer provides added benefit, meaning there is a window of CPT-11 concentrations in which the effect occurs. Figure 1.5B shows that, in this supernatant transfer assay, viral expression of CE enhances cancer cell killing when combined with 0.1 to 3 μM of CPT-11.

In order to determine if produced SN-38, be it produced intra- or extra-cellularly, induces bystander killing, as well as to compare all recombinants' ability to make SN-38, a set-up similar to the supernatant transfer assay was devised: rather than adding drug to the target cells, drug was added to the original cells and SN-38 containing supernatant was transferred. Since SN-38 can freely cross the plasma membrane (Kobayashi et al., 1999; Wierdl et al., 2001), conversion of CPT-11 can occur inside the cells as well; SN-38 would simply diffuse into the supernatant. This modified version of the supernatant transfer is shown in Figure 1.5C. Conditions where CPT-11 was combined with any of the CE recombinants, including that with a retained version of CE, enhanced target cell death, resulting in approximately equivalent target cell death.

Subsequently, various *in vitro* experiments were undertaken with SW-620 cells. Results showed that SN-38 mediated bystander killing was insignificant in comparison to cell killing caused by the virus (Appendices III, IV, V, VI, VIII). This lead to an expansion of the cell line screen to include cell lines that are more resistant to VV. The LC50 ratios shown in Table 1.1 revealed that although relatively more resistant to VV than SW-620 and 786-0s, K-562 cells are only slightly more resistant to SN-38.

Figure 1.5: The supernatant from cells infected with recombinants expressing a secreted version of CE kills target SW-620 cells *in vitro*, when combined with CPT-11. A) and B) Original cells were either mock infected or infected with the indicated virus at an MOI of 0.1. Three days later, supernatant was collected, filtered to remove virus and transferred to target cells, at a final volume of 50%. A) Either vehicle, 2.2 µM CPT-11 or 0.06 µM SN-38 was added to target cells for 8 hrs. B) Either vehicle or a range of CPT-11 concentrations were added to target cells for 8 hrs. C) Original cells were either mock infected or infected with the indicated virus at an MOI of 0.1, as well as treated with either vehicle, 2.2 µM CPT-11 or 0.06 µM SN-38 for 8 hrs. Three days following infection, supernatant was collected, filtered to remove virus and added to target cells, at a final volume of 50%. A), B) and C) Target cell metabolic activity was assessed by Alamar Blue 5 (A), B)) or 2 (C) days post-supernatant transfer. Viability was normalized to cells receiving supernatant from mock infected cells and treated with vehicle. Panels represent one experiment done with 6 replicates. For A) experiment is representative of 4 independent experiments. For B), graph was obtained from one representative experiment, while LC50 ratios were obtained from 3 independent experiments. Data represents mean ± SD. ns P > 05, *** P < 0.001 (one way ANOVA with Bonferroni's Multiple Comparison Test).

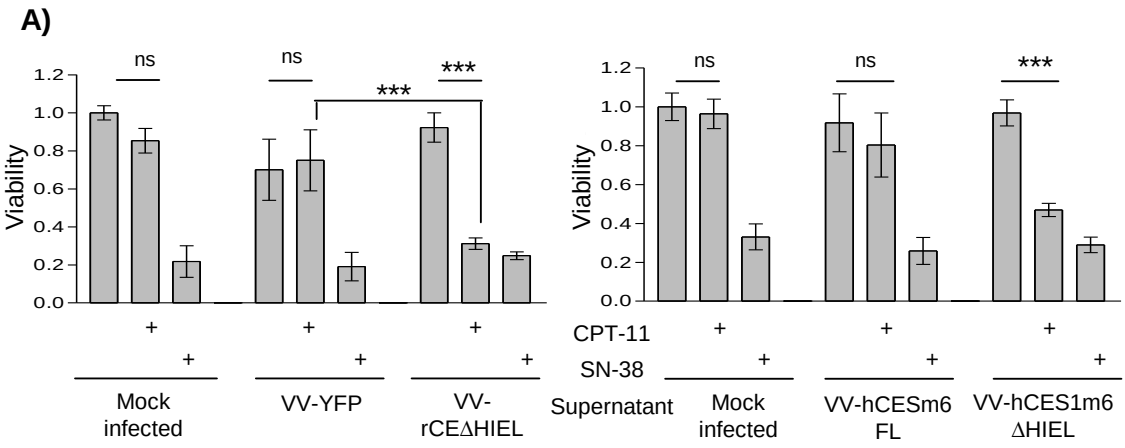
A)
Viability
ns
ns
***
***
CPT-11
SN-38
Supernatant
Mock infected
VV-YFP
VV-rCEΔHIEL
Mock infected
VV-hCESm6 FL
VV-hCES1m6 ΔHIEL

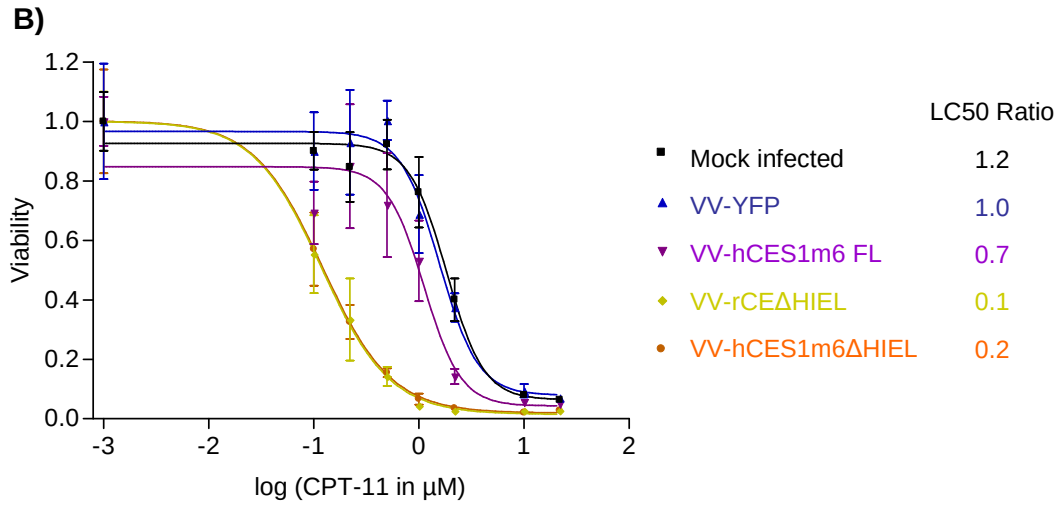
B)
Viability
log (CPT-11 in µM)
LC50 Ratio
Mock infected 1.2
VV-YFP 1.0
VV-hCES1m6 FL 0.7
VV-rCEΔHIEL 0.1
VV-hCES1m6ΔHIEL 0.2

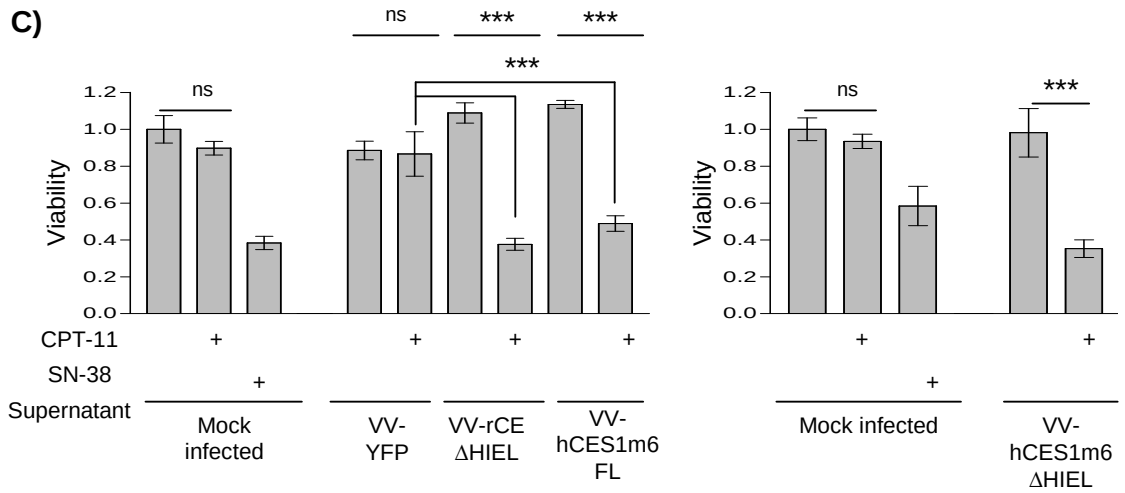
C)
Viability
ns
***
***
***
CPT-11
SN-38
Supernatant
Mock infected
VV-YFP
VV-rCE ΔHIEL
VV-hCES1m6 FL
Mock infected
VV-hCES1m6 ΔHIEL

An *in vitro* efficacy experiment in K-562s, Figure 1.6A, showed a benefit to virally-encoded CE, still present after normalization to remove differences in virus on its own (Figure 1.6B). The % increase in cell death observed with VV-CE over its control counterpart (Figure 1.6C), showed that CE virus is ~10% more toxic on its own and ~30% more toxic with CPT-11, implying that ~20% of this toxicity is due to conversion of CPT-11.

A co-culture experiment was also performed; a monolayer of U2OS cells were infected at either a low or high MOI and, after infection, inoculum was replaced with K-562 suspension cells as well as either vehicle, CPT-11 or SN-38. Figure 1.7 shows only the most effective time points for each MOI, for clarity. The effect of CE is visible (Figure 1.7A) and more obvious upon normalization (Figure 1.7B). Looking at the % increase in cell death observed with VV-CE over its control counterpart (Figure 1.7C), at a low MOI (for 4 days), the CE virus is ~30% more toxic on its own and 75% more toxic with CPT-11, implying that conversion of CPT-11 to SN-38 accounts for ~45% of the toxicity. At a high MOI (for 5 days), CE virus is ~35% more effective in the presence of the drug.

To take advantage of K-562's ability to be persistently infected by VV (Pogo et al., 1991); infected K-562s were treated with either vehicle, CPT-11 or SN-38 and drug-containing media was replaced every 3 days, for a total of 10 days. Figure 1.6D shows that the effect is more drastic in a long-term experiment and still observed upon normalization (Figure 1.6E). The % increase in cell death observed with VV-CE over its control counterpart (Figure 1.6F), shows that, the CE virus is ~20% more toxic on its own and ~90% more toxic with 0.1 μM CPT-11, implying that ~70% of this toxicity is due to CE.

Next, experiments progressed to *in vivo* models. However, these were complicated by the fact that, unlike humans, mice express a serum CE enzyme, which effectively converts CPT-11 to SN-38. There are, however, plasma CE-deficient mice that still have liver and

Figure 1.6: Virally-encoded CE provides an advantage when it comes to *in vitro* K-562 cell killing in the presence of CPT-11. K-562 cells were either mock infected or infected with the indicated virus at an MOI of 3. A)-C) Cells were then treated with either vehicle, 0.1 µM CPT-11 or 0.1 µM SN-38. Five days post-treatment, cell viability was assessed by trypan blue exclusion. A) Raw viability B) Viability is normalized to the sample treated with the same virus and vehicle. C) Change in cell killing of VV-hCES1m6ΔHIEL relative to VV-YFP. Data is obtained from one experiment done in triplicate, but is representative of 2 independent experiments. Data points are means ± SD. ** $P < 0.01$, *** $P < 0.001$ (one way ANOVA with Bonferroni's Multiple Comparison Test). D)-F) Following infection, cells were treated with either vehicle, 0.05 µM, 0.1 µM or 0.25 µM CPT-11 or 0.1 µM SN-38. Every three days, media was replaced with fresh media containing the same amount of drug. Ten days post-infection, cell viability was assessed by trypan blue exclusion. D) Raw viability E) Viability is normalized to the sample treated with the same virus and vehicle. F) Change in cell killing of VV-hCES1m6ΔHIEL relative to VV-YFP. Data is obtained from one experiment.

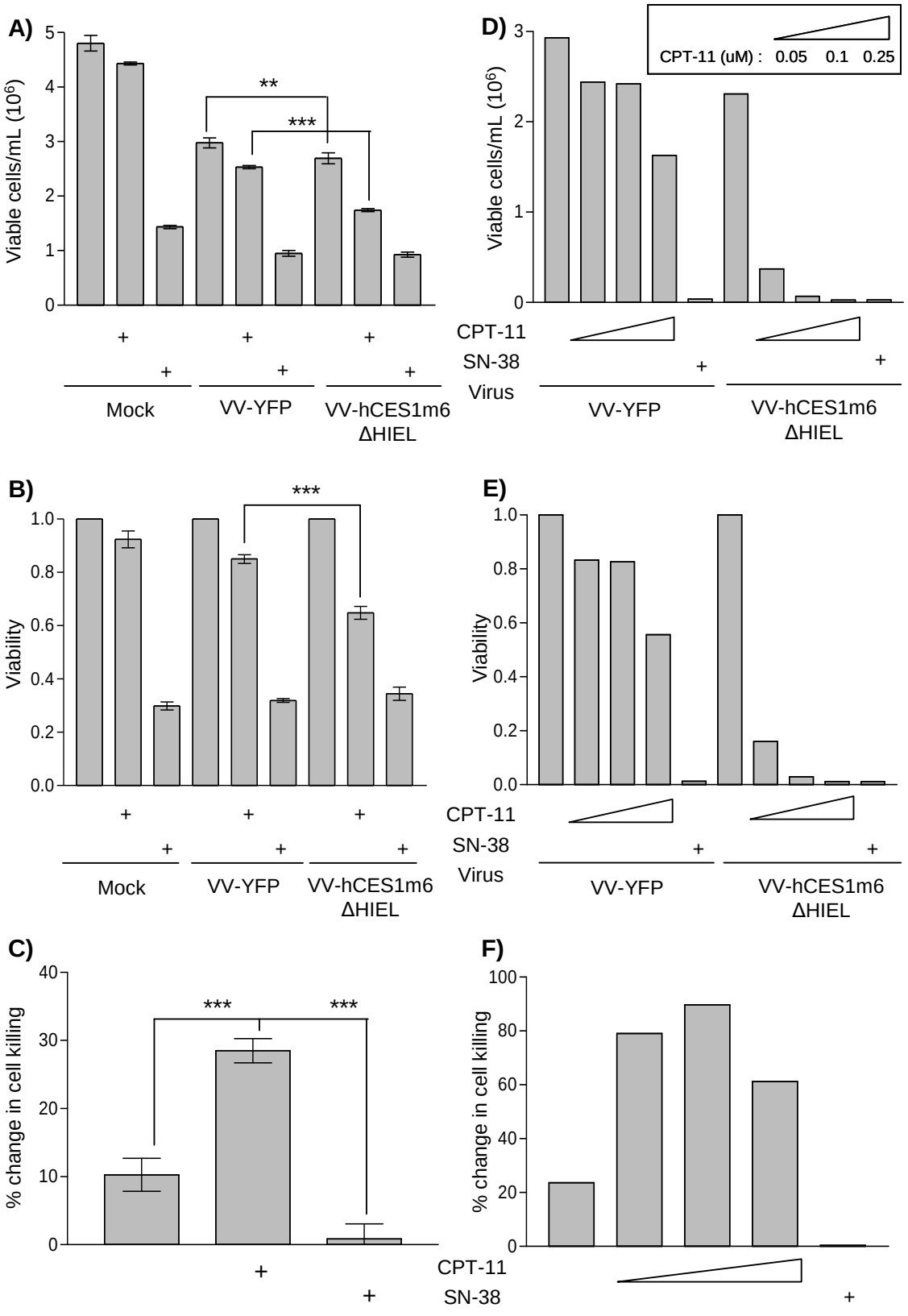
A)
Viable cells/mL (10^6)
**
***
Mock
VV-YFP
VV-hCES1m6 ΔHIEL
D)
CPT-11 (uM) : 0.05 0.1 0.25
CPT-11
SN-38
Virus
VV-YFP
VV-hCES1m6 ΔHIEL
B)
Viability
***
E)
C)
% change in cell killing
***
***
F)

Figure 1.7: Virally-encoded CE provides an advantage in the context of *in vitro* U2OS and K-562 co-cultures. U2OS cells were either mock infected or infected with the indicated virus at an MOI of 0.01 or 3. After the infection, the inoculum was removed and replaced with K-562 cells. The wells were then treated with either vehicle, 0.1 µM, 0.25 µM or 0.5 µM CPT-11 or 0.1 µM SN-38. The drugs were left on the cells for the duration of the experiment. Either 3, 4 or 5 days post-treatment, cell viability was assessed by trypan blue exclusion. For simplicity, for each MOI, only the most effective time point is shown. For A), raw viability is reported. For B), all values are normalized to the no drug control for that particular virus. C) Change in cell killing of VV-hCES1m6ΔHIEL relative to VV-YFP is shown.

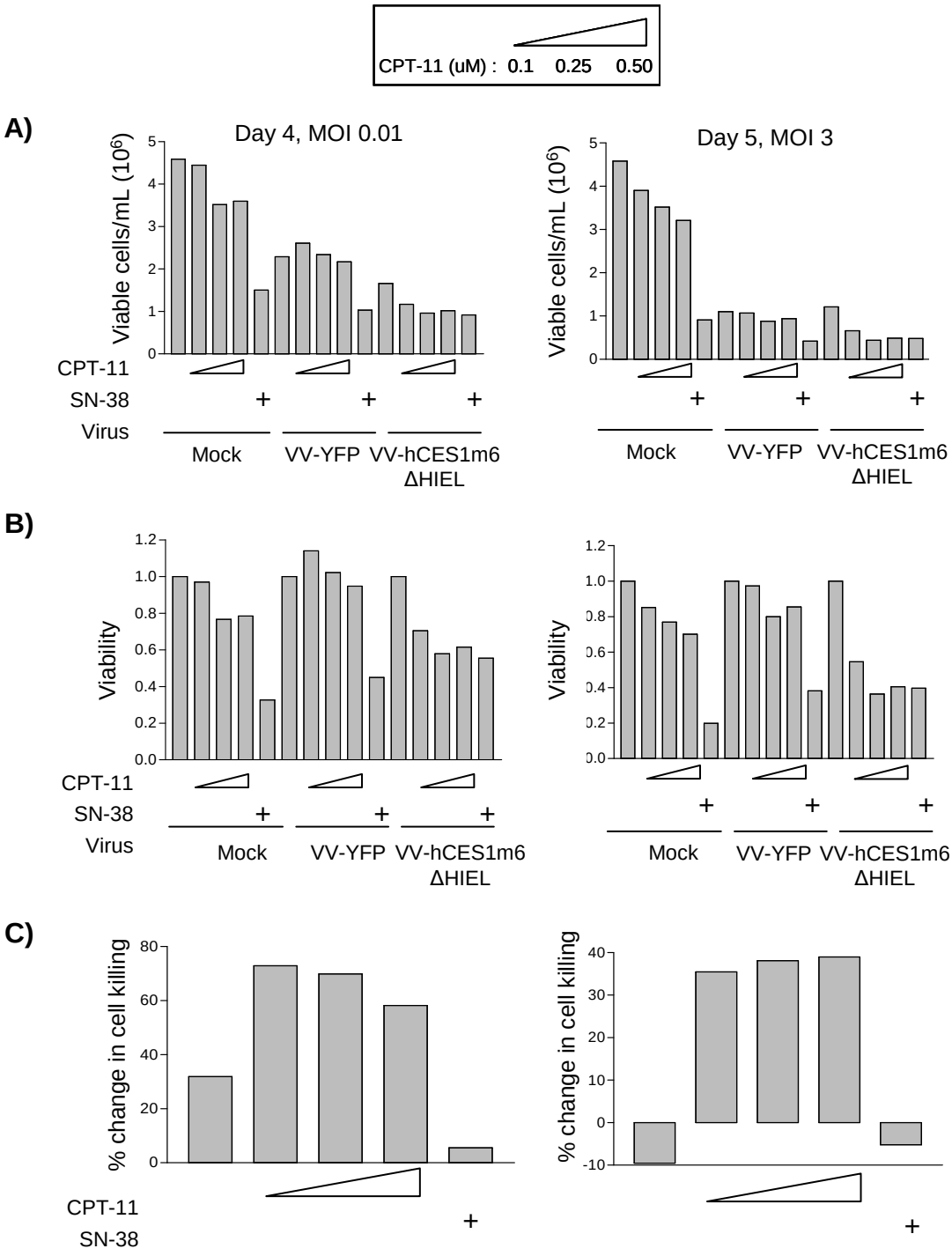
CPT-11 (uM) : 0.1 0.25 0.50
A)
Day 4, MOI 0.01
Day 5, MOI 3
Viable cells/mL (10^6)
CPT-11
SN-38
Virus
Mock
VV-YFP
VV-hCES1m6 ΔHIEL
B)
Viability
C)
% change in cell killing

intestinal CE, like humans, that better model CPT-11 treatment in the clinic (Soares 1979; Morton et al., 2000; Morton et al., 2005). These SCID mice, termed ES1-SCID, had been obtained and but breeding difficulties resulted in small numbers of mice for use in experiments. This meant that experiments could not produce reliable nor significant quantitative data. As a result, high doses of virus and CPT-11 were injected IT and then tumour histopathology was observed. In a pilot *in vivo* K-562 experiment, mice bearing palpable K-562 SQ tumours received either control or CE virus IT, followed by CPT-11 IT, Figure 1.8A. The idea was to treat the tumours with CPT-11 when there was a large amount of CE enzyme in the tumour. The small number of mice meant important control groups such as vehicle, CPT-11 only, control virus only and CE virus only had to be omitted. Tumour volume measurements showed a trend towards CE virus outperforming control virus, Figure 1.8B, however it was not significant. IHC performed on the tumour sections showed that VV staining corresponded with active caspase-3 staining, a marker for apoptosis (Cohen, 1997; Cryns and Yuan, 1998; Slee et al., 1999). Unfortunately, tumours treated with virus encoding a secreted version of CE and CPT-11 did not have more intense active caspase-3 staining nor staining extend beyond the area of VV staining, Figure 1.8C.

Figure 1.8: Virally-encoded CE does not provide an advantage in the presence of CPT-11 for the treatment of K-562 xenograft tumours in this model. A) ES1-SCID mice bearing palpable K-562 SQ tumours were treated according to schedule shown. B) Tumour volume was measured on days 0, 2, 7 and 9. Volume was calculated by (length × width^2)/2. Data points are means ± SD, n = 2. ns P > 0.05 (Welch's corrected unpaired t test). (C) Excised tumours were sectioned, frozen and IHC staining for VV or active caspase-3 was performed. Image is representative of tumours from both groups.

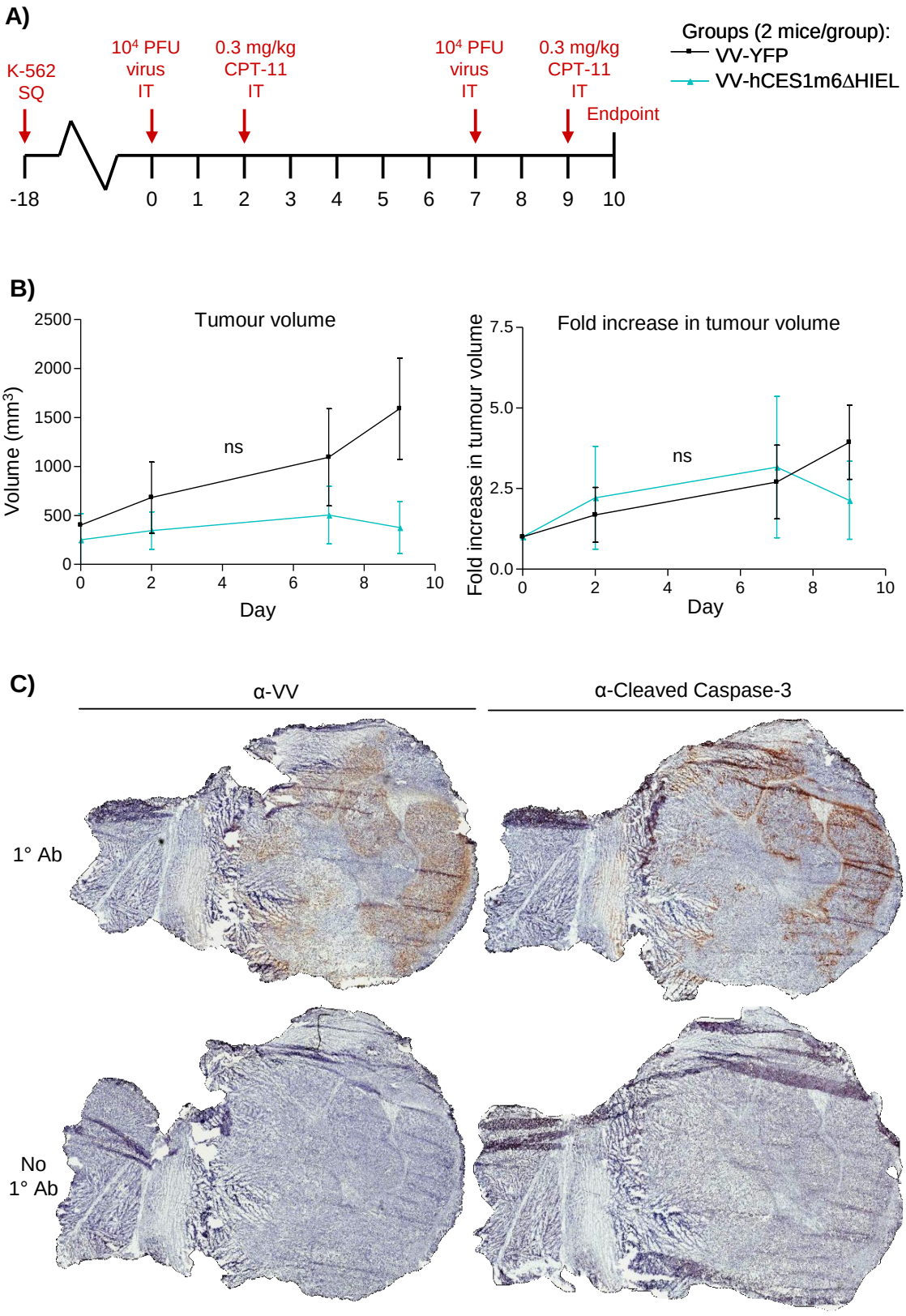
A)
K-562
SQ
10⁴ PFU
virus
IT
0.3 mg/kg
CPT-11
IT
10⁴ PFU
virus
IT
0.3 mg/kg
CPT-11
IT
Endpoint
-18
0
1
2
3
4
5
6
7
8
9
10
Groups (2 mice/group):
VV-YFP
VV-hCES1m6ΔHIEL
B)
Tumour volume
Volume (mm³)
2500
2000
1500
1000
500
0
ns
0
2
4
6
8
10
Day
Fold increase in tumour volume
Fold increase in tumour volume
7.5
5.0
2.5
0.0
ns
0
2
4
6
8
10
Day
C)
α-VV
α-Cleaved Caspase-3
1° Ab
No
1° Ab

Discussion

Initial data with Wy_{TK-} showed that only high concentrations of SN-38 affected viral spread in SW-620 cells. From this data, it can be inferred that only high concentrations of SN-38 affect Wy_{TK-}'s life cycle, likely by inhibiting its viral topoisomerase. In HCT-116 cells, Wy_{TK-} and CPT-11 showed slight synergy at higher concentrations by combination index. This data, although preliminary, justified further pursuit of the combination of VV and CPT-11.

The cell line screen identified K-562 and SW-620 cells as promising; since they are relatively more resistant to VV-YFP but still susceptible to SN-38; as soon as SN-38 is produced, there should be a drastic effect on cancer cell viability. SW-620 cells were selected, because at this point, K-562 cells had not yet been included in the screen.

Initial data with VV-YFP showed that clinically relevant concentrations of CPT-11 and SN-38 did not affect VV-YFP replication or spread in SW-620 cells. Even at concentrations 10X the average patient plasma C_{max}, SN-38 did not affect VV-YFP replication nor spread. This is consistent with reports in the literature which show that the VV topoisomerase I is not inhibited by 100 μM camptothecin, of which CPT-11 is a semi-synthetic analogue, in DNA relaxation assays (Shuman et al., 1988; Gupta et al., 1992). Further work could involve using CPT-11 and SN-38 in this DNA relaxation assay. Although the VV-YFP data conflicts with the Wy_{TK-} data; these viruses are different strains of VV; Wy_{TK-} is Wyeth strain and VV-YFP is Copenhagen. There may be slight differences between the strains' topoisomerases. Although there have not been any reports published comparing the two, use of the National Center for Biotechnology Information's (NCBI) Basic Local Alignment Search Tool (BLAST) shows that these two strains' topoisomerase I

DNA sequences (Genbank AY313847 vs. M35027) only differ by 5 point mutations. Since four of these are silent mutations, the protein sequences are >99% identical. Although not the same point mutation, Gupta et al. have shown that one amino acid substitution can confer camptothecin sensitivity to VV topoisomerase I. Therefore, it is possible that the differences between the Wyeth and Copenhagen topoisomerase I may result in differential sensitivity to CPT-11. For the experiment, SN-38 concentrations ten times those observed in patients were used because having a virally-encoded CE should increase local production of SN-38 beyond what is typically observed in the clinic. It is difficult to estimate from the literature how much SN-38 should be produced from CE; although ~91% conversion of CPT-11 was estimated from our data, to be discussed below, other studies produced different values, depending on the source of CE, how much CE and CPT-11 were present, how long the reaction proceeded for, etc. Danks et al. found that ~68% of CPT-11 was converted to SN-38 by lysate from cells overexpressing rCE with a CE enzymatic activity of 2000 µmol/min/mg. This CE enzymatic activity is higher than typically observed in the literature; most studies observe ~200 – 500 µmol/min/mg (Danks et al., 1998; Danks et al., 1999; Wierdl et al., 2001; Wierdl et al., 2008), which converted ~6% of CPT-11 to SN-38 (Danks et al., 1999). Although the most extreme case may produce concentrations of SN-38 that exceed those tested, most values should fall within the range examined. Again, this is assuming CE enzymatic activity is representative of CPT-11 converting ability, which it is not (Wierdl et al., 2001; Wierdl et al., 2008), and assuming *in vitro* production in the above assays properly models *in vivo* production. Nevertheless, it is important to note that the growth curves were done with continuous drug exposure and that in the body, drugs would be metabolized, SN-38 concentrations would decrease over time and any effect on viral replication/spread would be subtler than if the cells were exposed to the drug continuously. Finally, the lack of effect

of CPT-11 and SN-38 on viral replication is consistent with findings from two other groups who showed that CPT-11 and SN-38 did not inhibit replication-competent adenovirus or herpes simplex virus (Stubdal et al., 2003; Tyminski et al., 2005).

Upon receipt of the VV-CE recombinant viruses, CE protein expression was verified by Western Blot using an anti-human CE antibody that did not cross-react with rabbit CE. Nevertheless, the virus expressing rCE was carried forward into functional tests.

CE-mediated SN-38 production was measured using a functional assay that assessed DNA DSBs, SN-38's known mechanism of action. Virus infection strongly induced γ-H2A.X, a marker for DNA DSBs (Rogakou et al., 1998), corresponding with literature of virus infection activating the DNA damage response via global changes to host chromatin, nuclear architecture and cell structure (Weitzman et al., 2010). Once the assay was done with virus-free supernatant, it showed that the combination of CE virus and CPT-11 produced a factor that could induce γ-H2A.X. Specifically, VV-hCES1m6ΔHIEL combined with 0.1 μM CPT-11 induced γ-H2A.X more than ADR, a known inducer of DNA DSBs (Byfield et al., 1977; Goldenberg et al., 1986) and almost as much as 0.1 μM SN-38 (21.1 vs. 23.3 fold increase over untreated). Since 0.1 μM CPT-11 did not significantly induce γ-H2A.X relative to untreated, this would suggest that ~ 91% conversion occurred under these conditions, an estimate higher than typically observed in the literature (Danks et al., 1998; Danks et al., 1999; Wierdl et al., 2001; Wierdl et al., 2008). It is possible that a lower percentage conversion occurred but that this lesser amount of SN-38 was almost just as effective, given an SN-38 standard curve was never performed. Moreover, detection of DNA DSBs could have been improved by use of fluorescence in situ hybridization, which can detect DNA DSBs directly, on a cell-by-cell basis (Fernández and Gosálvez, 2002). Nevertheless, γ-H2A.X induction suggests that virally-encoded CE is indeed producing SN-38 from CPT-11.

Supernatant transfer experiments were undertaken to demonstrate CE-mediated bystander killing. They showed that, using this particular regimen, only when supernatant from cells infected with virus encoding a secreted version of CE, but not retained, was combined with 0.1 to 3 μM of CPT-11 was target cell death observed, supporting the notion that secreted CE is capable of converting CPT-11 to SN-38 outside of the cell and that this SN-38 can kill uninfected cells.

The modified supernatant transfer experiments where CPT-11 was added to infected cells, rather than target cells, compared the recombinants ability to make SN-38. Since SN-38 can freely cross the plasma membrane (Kobayashi et al., 1999; Wierdl et al., 2001), regardless of whether CE is cell-retained or secreted, the resulting SN-38 can diffuse into the supernatant. The VV-CE recombinants did not differ in SN-38 produced at 72 hrs, as measured by SW-620 target cell viability. In addition, this showed that SN-38 produced within the cell can diffuse out of the cell and kill uninfected cells.

The cell line screen was then expanded to include cell lines that are more resistant to VV infection. Leukemic cell lines are known for this (unpublished data from our lab); alterations in apoptotic pathways render lymphocytic and myelogenous leukemias generally resistant to various agents and conditions (Cotter, 1995; Casas et al., 2003; Chen and Plunkett, 2010) However, one concern was translating *in vitro* leukemic cell line data to the preclinical setting. One of the features of this particular project is that enhanced SN-38 production would only be occurring at the site of viral replication; tumours. Since leukemic cells circulate through the bone marrow and blood stream, the enhanced SN-38 production might produce unwanted side effects throughout the body. Nevertheless, previous studies have shown that K-562 cells, chronic myelogenous leukemia cells, can form solid tumours upon injection of a large number of cells SQ (Lozzio et al., 1983; Iqbal Ahmed et al., 2001;

He et al., 2003; Li et al., 2005; Fu et al., 2007; Gao et al., 2011; Zeng et al., 2012). Furthermore, there is a report of K-562s being persistently infected by VV (Pogo et al., 1991) – a potentially favourable situation: VV could replicate in the cells, producing CE, but does not destroy the population. In the cell line screen, K-562 cells were relatively more resistant to VV than SW-620 and 786-0s, but only slightly more resistant to SN-38.

An *in vitro* efficacy experiment with K-562s showed that the CE virus is ~10% more toxic than YFP virus in the absence of drug. However, differences between observed LC50s of VV-YFP and VV-hCES1m6ΔHIEL were not statistically significant in either K-562 or SW-620 (data not shown). Growth curves comparing VV-YFP and VV-hCES1m6ΔHIEL were never performed because there is no evidence to suggest this transgene should affect viral replication. Other studies using CE-expressing replication-competent viruses did not report any effects of CE on adenovirus or herpes simplex virus replication (Stubdal et al., 2003; Tyminski et al., 2005). Returning to the *in vitro* efficacy experiment, since in the presence of CPT-11, CE virus is ~30% more toxic, this implies that ~20% of this increase in toxicity is due to CE conversion of CPT-11 to SN-38. A follow-up experiment where K-562 and U2OS were co-cultured, mimicking the heterogeneity of tumours, showed that CE-mediated production of SN-38 results in ~35% - 50% more cancer cell death. Differences in the magnitude of the benefit to encoding CE between direct K-562 infection and co-culture experiments may have arisen due to which cells were infected; in the direct K-562 infection, CE output is correlated to K-562 infection whereas in the co-culture experiment, it is, at first, determined by infection in U2OS and then subsequently in K-562. Since VV replicates very well in U2OS cells, in the co-culture experiment, there is a greater production of CE. Follow-up experiments could involve labeling the different cell types and altering the ratio of susceptible to resistant cells.

Although these experiments were hinting at efficacy, more dramatic results should be possible if K-562 persistent infection were taken into account. To verify claims of persistent infection, K-562 cells were infected and kept for 8 passages. Cell viability and YFP expression was determined at every passage (data not shown); although reduced at first, cell viability rebounded and roughly 10 – 30% of cells were YFP positive upon passaging, in line with Pogo et al. This suggests that VV persistent infection of K-562 cells is a chronic focal infection; infection is maintained by a small portion of the cells that are infected, release virus and are killed in the process (Boldogh et al., 1996). K-562's resistance to the induction of apoptosis by various agents (McGahon et al., 1994), including Dengue virus-induced apoptosis despite infection comparable to other susceptible cells lines (Brown et al., 2009), suggest that perhaps a reduction in virus-induced apoptosis may help in the establishment of persistent infection (Levine et al., 1993; Baixeras et al., 1998). Whether this resistance to apoptosis has biological significance in the context of VV-encoded anti-apoptotic genes has not formally been addressed. Interesting further studies would be to track gene expression, apoptosis and viral output in a population of infected K-562 cells over a long time course.

The last *in vitro* K-562 experiment occurred over 10 days. Conversion of CPT-11 to SN-38 by viral CE increased cancer cell death by ~70%. Since cells were treated with virus once, and the assay lasted over multiple passages, the fact that this particular assay yielded the best results suggest that the cells were making CE throughout the experiment and thus persistently infected. This could be verified by repeating the experiment but only adding drug to the cells in the first passage, and subsequently passaging the cells in drug-free media; if the cells were not persistently infected, CE would only be made during the first passage and efficacy would be very similar to that observed if drug were added at each passage. We suspect that this experiment was the most effective of all due to its drug replenishment and

duration. Since cells are likely persistently infected and continuously making CE, replenishing CPT-11 would produce more SN-38. Also, since SN-38 is an S-phase chemotherapeutic, the longer the experiment proceeds, the more cells enter S phase and become susceptible to the lethal effects of SN-38 (Hsiang et al., 1989; te Poele and Joel, 1999). Therefore, over multiple passages, although the majority of cells in the population remain uninfected, the production of CE, and thus SN-38, was able to reduce the viability of the remaining uninfected cells. Follow up experiments could involve using flow-cytometry to distinguish between infected and uninfected apoptotic cells, measuring the bystander effect more accurately.

In vivo K-562 models were subsequently attempted. CPT-11 and virus were given IT to ES1-SCID mice bearing K-562 solid tumours; viral CE did not provide an advantage in terms of tumour growth, although there is a trend towards it. Moreover, IHC staining did not show more intense active caspase-3 staining nor active caspase-3 staining extended beyond VV staining. However, from this IHC, it can be noted that the virus dose was sufficient: the large majority of tumours had easily detectable VV staining. Any more virus might make it difficult to see SN-38-mediated enhancements in active caspase-3 staining. Unfortunately, from this data, it cannot be inferred whether the CPT-11 dose was sufficient since PBS and CPT-11 alone control groups were absent. 0.3 mg/kg of CPT-11 was used based on literature where replication-competent adenovirus expressing CE was combined with CPT-11: survival of CPT-11-treated mice did not significantly differ from vehicle-treated mice, but mice treated with Ad-CE + CPT-11 survived significantly longer than all other groups, including Ad-CE on its own (Stubdal et al., 2003). However, there are a few points to note. Firstly, the Ad-CE paper did not use ES1-SCID mice. Also, they did not compare Ad-CE + CPT-11 to control Ad + CPT-11; although they are implying that CE is converting CPT-11 to SN-38

and that this is mediating efficacy, they cannot discount the possibility that this efficacy arose due to other non-CE synergistic interactions between Ad and CPT-11 in the tumour. Lastly, the Stubdal, H. et al paper had higher CE activity *in vitro*: 500 – 600 µmol/min/mg as opposed to our <300 µmol/min/ml of supernatant. Again this comparison is flawed; relative CE activity is typically lower in supernatant than it is in cell lysates (Wierdl et al., 2001) and CE activity is not a perfect marker of CPT-11 converting ability (Wierdl et al., 2001; Wierdl et al., 2008). Furthemore, Tyminski et al.'s studies also involved IT dosing of CPT-11, however, they used higher doses given less frequently. Perhaps the dose of 0.3 mg/kg of CPT-11 could be increased. Nevertheless, the hinting at tumour control towards the end of the experiment, combined with the *in vitro* data suggesting persistent infection, point towards benefits occurring later in the treatment course. Therefore, future experiments should have a longer timeline.

The *in vivo* situation encompasses a few elements that could potentially affect the phenomenon being examined. Reports have shown that CPT-11 can induce vessel normalization and increase perfusion, which may help the delivery of subsequent virus doses. Furthermore, it is suspected that SN-38 may be mediating vascular normalization (Kamiyama et al., 2005; Bocci et al., 2008; Verreault et al., 2011). In addition, it has been shown that SN-38 can antagonize HIF-1α (Kamiyama et al., 2005; Guérin et al., 2012; Murono et al., 2012). This reduction in tumour cell hypoxia may improve viral replication as hypoxia has been shown to reduce oncolytic virus replication (Pipiya et al., 2005; Shen et al., 2005; Shen et al., 2006; Friedman et al., 2012). However, VV Lister strain was shown unaffected by hypoxia (Hiley et al., 2010), whether this is the case for Copenhagen is unknown. Therefore, *in vivo*, CE-mediated conversion of CPT-11 to SN-38 may help normalize vessels and reduce hypoxia, advocating a regimen that encompasses multiple

treatments.

Conclusions

This work has shown that topoisomerase I inhibitors CPT-11 and SN-38 do not affect Copenhagen VV replication or spread. VV-CE recombinants produce functional CE, which provides a benefit in terms of *in vitro* K-562 cancer cell death in the presence of CPT-11. Virally-encoded CE potentiated the combination of VV and CPT-11 *in vitro*. Whether this proves to be the case *in vivo* has yet to be confirmed.

Given the obtained data, the ability of K-562s to be persistently infected *in vitro* and SN-38's role in vessel normalization and reduction of hypoxia, the next experiment to be performed would be IV dose-finding of CPT-11 and VV on their own, followed by a long-term efficacy experiment with multiple IV treatments. Also, CPT-11 and SN-38 distribution should be examined *in vivo*; ideally, at various time points, blood, tumour and normal tissue samples would be obtained and HPLC would be performed to quantify the amount of SN-38 and unconverted CPT-11, as done previously (Kaneda et al., 1990; Morton et al., 2000; Morton et al., 2005). It would also be beneficial to test this strategy *ex vivo* in heterogeneous patient tumour samples, which can be obtained through the Ottawa Hospital Research Institute, as described (Diallo et al., 2011).

Another interesting avenue to pursue would be the combination with immunotherapy; chemotherapy can make tumour cells more susceptible to immunotherapy. Major histocompatibility complex class I (MHC-1), which presents antigens to cytotoxic T cells and thus results in cell killing, can be downregulated in cancer as an immune escape mechanism (Garcia-Lora et al., 2003) Topotecan, another derivative of camptothecin, has been shown to induce MHC-1 and sensitize treated cells to effector T cells (Alagkiozidis et al., 2010; Wan et al., 2012). Moreover, it has been shown that CPT-11 treatment could induce Colo205 human colon cancer cells to overexpress cell-surface protein E48/Ly6D, a

marker for head and neck cancer (Rubinfeld et al., 2006). Following CPT-11 treatment, Rubinfeld et al. treated tumours with a monoclonal antibody against E48 conjugated to a cytotoxin and saw efficacy in preclinical models. Since oncolytic viruses, including VV, can create an inflammatory microenvironment that stimulates innate and adaptive anti-tumour responses (Melcher et al., 2011), perhaps CPT-11 induction of immune molecules would sensitize uninfected cells to oncolytic virus-mediated immunotherapy. At this point, it has yet to be determined if these effects are restricted to CPT-11 or if they include SN-38. If it is mediated by CPT-11, this effect would be present in all tumours treated with CPT-11. However, if it occurs via SN-38, this phenomenon would be more robust in VV-CE treated tumours.

If the combination of CPT-11 and CE-expressing virus proves beneficial *in vivo*, the potential implications of this project are powerful; virally-encoded CE may improve the safety of CPT-11 as lower doses can be administered yet its activity should remain high in the tumour. And since CPT-11 treatment is often curtailed due to side-effects, this strategy may prove useful. In addition, secreted versions of CE should allow for bystander killing of uninfected tumour cells, perhaps killing the cells VV has left behind.

PROJECT 2: THE EFFECT OF TUMOUR VASCULAR MODULATION ON ONCOLYTIC VIRUS ACTIVITY

Introduction

One of the barriers oncolytic viruses have to overcome is reaching tumour cells. Breitbach et al. found that treatment of murine CT26 colon adenocarcinoma tumours or human SW-620 colon carcinoma tumours with oncolytic versions of Vesicular stomatitis virus (VSV) or VV resulted in viral replication restricted to areas in the tumour rim or surrounding blood vessels. Specifically, infection triggered vascular shutdown, resulting in loss of blood flow to the tumour core (Breitbach et al., 2007). Although this induced apoptosis in the unperfused, uninfected tumour core, it would be interesting to see if increased perfusion would improve virus delivery and tumour infection enough to surpass the tumour destruction induced by vascular shutdown. This increase in perfusion could be brought about by vascular endothelial growth factor (VEGF).

VEGF is a secreted cytokine involved in normal and tumour-associated angiogenesis. Most of its effects are mediated via VEGF receptor 2 (VEGFR-2), which is generally found on endothelial cells (Hicklin and Ellis, 2005). The resulting signalling cascade induces endothelial cell survival, proliferation, migration and invasion, as well as vascular permeability, facilitating angiogenesis (Hicklin and Ellis, 2005). It has been well established that tumour vasculature provides tumour cells with oxygen, nutrients and a route for metastasis (Zhang et al., 2006). Moreover, VEGF signalling's role in cancer is supported by the association of VEGF overexpression with cancer progression as well as higher VEGFR-2 expression in tumour vasculature relative to normal vasculature (Plate et al., 1994). Blocking

VEGF signalling has been shown to inhibit tumour growth and metastasis (Prewett et al., 1999). However, recent studies indicate that blocking VEGF signalling may increase the incidence of metastasis; either through the upregulation of compensatory proangiogenic molecules (Crawford et al., 2009; Zaghloul et al., 2009) or through the induction of hypoxia, which is suspected to select for tumour cells capable of switching to a more invasive phenotype and thus able to escape their hypoxic environment (Paez-Ribes et al., 2009). As it stands, the literature contains contradictory information regarding VEGF's involvement in tumour progression and metastasis.

This project intends to address VEGF's role in tumour progression in the context of OV activity. The project stemmed from a former graduate student's work with Orf virus. Orf virus is a parapoxvirus that primarily affects goats and sheep resulting in lesions with massive capillary proliferation and dilation (Groves et al., 1991). In fact, this virus encodes a viral isoform of VEGF termed VEGF-E. The former graduate student in our laboratory found that wild type Orf and an OrfΔVEGF-E recombinant performed equally in a lung metastasis mouse model. With this in mind, it would be interesting to see if local VEGF production, which induces the formation of tumour vasculature, can help subsequent OV doses infiltrate tumours and access the cells at their core. However, this project involves characterizing the effect of VEGF-E in another virus, vvDD, an attenuated recombinant of Vaccinia virus that has been shown to inhibit tumour growth *in vitro* and *in vivo*, while remaining safe for healthy cells, even when administered systemically (Lun et al., 2009). Still, its efficacy could likely be improved. To this end, and with the contradictory state of VEGF literature in mind, insertion of the gene coding for VEGF-E, which binds to VEGFR-2 only, into vvDD would address the effects of VEGF-E on VV efficacy.

Hypothesis and objectives

We suspect that local VEGF production may help oncolytic virus delivery, spread and ultimately efficacy. Comparing vvDD-VEGF-E to parental vvDD *in vivo* in mice would comprise the first objective: to determine whether VEGF expression improves or reduces vvDD's oncolytic efficiency. The second objective would involve assessing tumour histology and viral distribution within the tumour to determine if the transgene increases delivery and/or spread.

Following the inception of this project, two exciting papers regarding the combination of OVs and VEGF were published. Tseng et al. showed that an oncolytic Sindbis viral vector carrying murine VEGF enhanced tumour vasculature leakiness, in mice, and that this corresponded with an increase in virus delivery and transduction (Tseng et al., 2010). Kottke et al. showed that systemic murine VEGF injections increased the delivery of subsequent Reovirus treatments to the tumour more so than normal tissues, in mice. They also concluded that VEGF renders endothelial cells permissive for Reovirus replication which can provide virus to underlying tumour cells (Kottke et al., 2010). Furthermore, a very recent study has shown that VEGF increases VV internalization leading to augmented replication and cytotoxicity (Hiley et al., 2012). All three of these papers demonstrate a supportive role for VEGF in oncolytic virus activity. Furthermore, the proposed research involves VEGF-E, which binds VEGFR-2 only, as opposed to VEGF, which was used in the three aforementioned studies and which binds both VEGFR-1 and VEGFR-2. VEGFR-1 induces immunostimulatory effects, therefore, perhaps the viral VEGF-E evolved to avoid the receptor in order to maximize viral replication (Wise et al., 2003; Inder et al., 2008; Shibuya, 2009). Therefore, use of VEGF-E should avoid eliciting immune activity.

Results

Recombinant vvDD-VEGF-E was constructed in order to better examine the effect of VEGF-E on tumours in the context of oncolytic VV infection. The recombinant, Appendix IX, was cloned successfully, verified by sequencing, rescued and partially plaque purified. Despite many rounds of plaque purification, 100% recombinant plaques were never observed. This is further examined in project 3 of the thesis. vvDD-VEGF-E was never used in experiments.

Initially, Orf viruses were used as a source of VEGF-E. BALB/c mice bearing syngeneic CT26LacZ SQ tumours were treated with either WT Orf or OrfΔVEGF-E followed by vvDD treatment, hoping that previous WT Orf treatments would have increased angiogenesis and thus improved vvDD delivery and spread, Figure 2.1A. None of the treatment regimens significantly affected tumour volume (Figure 2.1B) or tumour mass (Figure 2.1C). Moreover, no differences in virus recovery were observed when vvDD was given IV or IT, as measured by infectious viral particles in the tumour (Figure 2.1D) or expressed in infectious virus particles per mg of tumour tissue (Figure 2.1E). Aware that using virus as a source of VEGF-E not only precludes the control of how much VEGF-E is produced but can also further alter the tumour microenvironment, commercial recombinant VEGF-E protein was subsequently selected as a source of VEGF-E.

To focus on viral spread throughout the tumour, BALB/c mice bearing syngeneic CT26WT tumours were treated with VEGF-E or vehicle IT and then followed up with vvDD IT, Figure 2.2A. Tumours were excised and titered 3 days post-infection; there is a trend, although insignificant, towards VEGF-E tumours having more virus (Figure 2.2C). There are

Figure 2.1: In this model, pre-treatment of CT26LacZ tumours with Orf virus ± VEGF-E, does not affect tumour virus recovery of a subsequent vvDD dose. A) BALB/c mice bearing palpable CT26LacZ tumours were treated according to the schedule shown. B) Tumour volume was measured on days 0, 2, 4 and 7. Volume was calculated by (length × width^2)/2. Data points are means ± SD. n = 12 on days 0, 2 and 4; n = 4 on day 7. (C), (D) and (E) Excised tumours were weighed (C), homogenized in PBS and titered on U2OS cells, (D) and (E). Data represents means ± SD, n = 4. ns $P > 0.05$ (one way ANOVA with Bonferroni's Multiple Comparison Test).

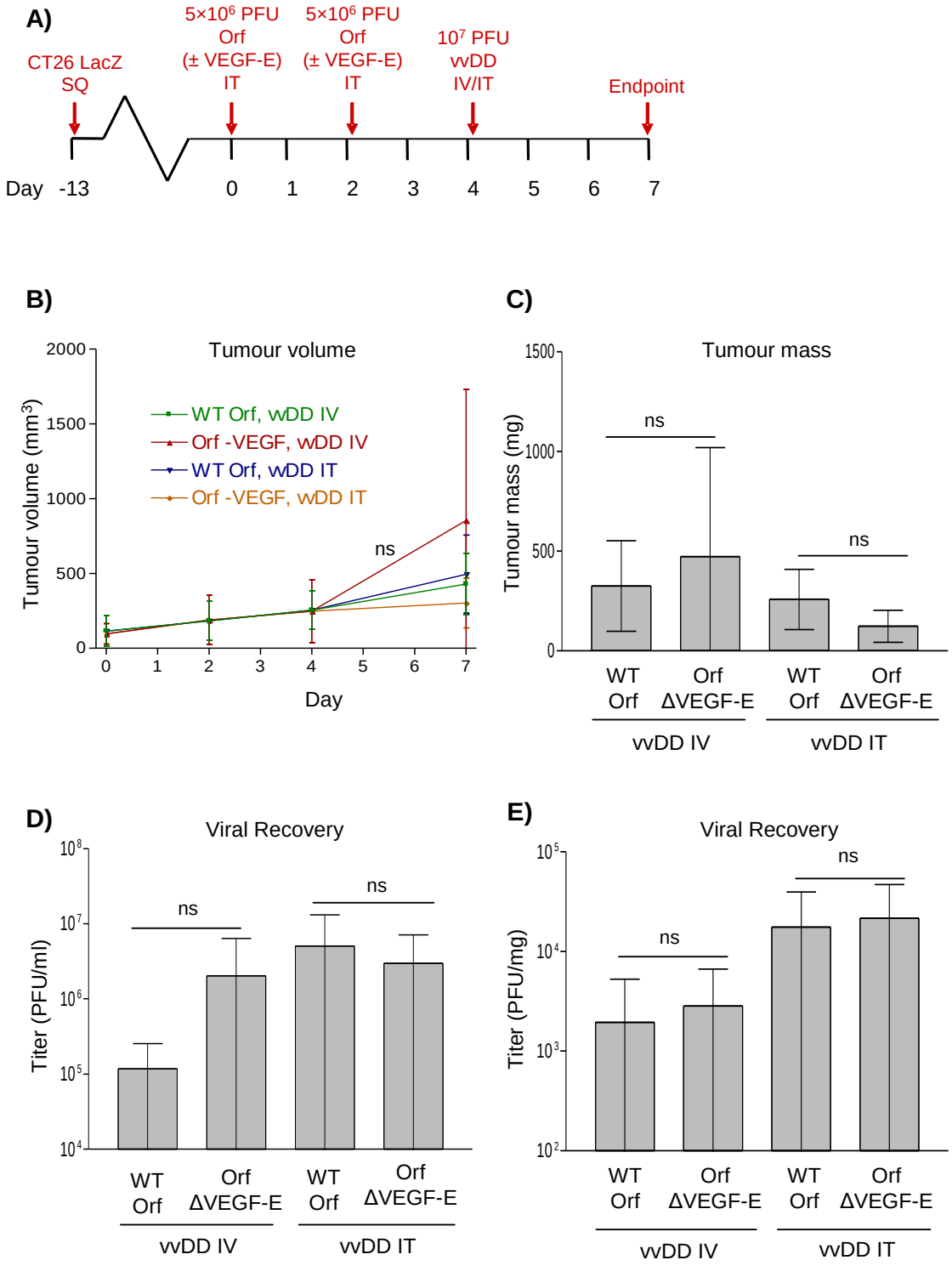
A)
5×10⁶ PFU Orf (± VEGF-E) IT
5×10⁶ PFU Orf (± VEGF-E) IT
10⁷ PFU vvDD IV/IT
CT26 LacZ SQ
Endpoint
Day -13 0 1 2 3 4 5 6 7
B)
Tumour volume
Tumour volume (mm³)
WT Orf, wDD IV
Orf -VEGF, wDD IV
WT Orf, wDD IT
Orf -VEGF, wDD IT
ns
Day
C)
Tumour mass
Tumour mass (mg)
ns
ns
WT Orf
Orf ΔVEGF-E
WT Orf
Orf ΔVEGF-E
vvDD IV
vvDD IT
D)
Viral Recovery
Titer (PFU/ml)
ns
ns
WT Orf
Orf ΔVEGF-E
WT Orf
Orf ΔVEGF-E
vvDD IV
vvDD IT
E)
Viral Recovery
Titer (PFU/mg)
ns
ns
WT Orf
Orf ΔVEGF-E
WT Orf
Orf ΔVEGF-E
vvDD IV
vvDD IT

Figure 2.2: In this model, pre-treatment of CT26WT tumours with recombinant VEGF-E protein does not affect tumour virus recovery of a subsequent vvDD dose. A) BALB/c mice bearing palpable CT26WT tumours were treated according to schedule shown. Tumours were weighed (B), homogenized in PBS and titered on U2OS cells, (C) and (D). Data represents means ± SD, n = 3. ns $P > 0.05$ (Welch's corrected unpaired t test)

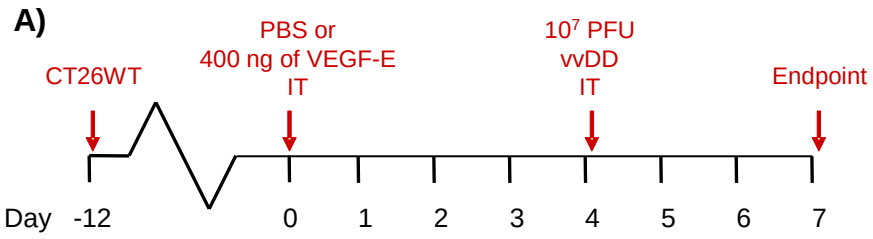
A)
CT26WT
PBS or
400 ng of VEGF-E
IT
10^7 PFU
vvDD
IT
Endpoint
Day -12 0 1 2 3 4 5 6 7

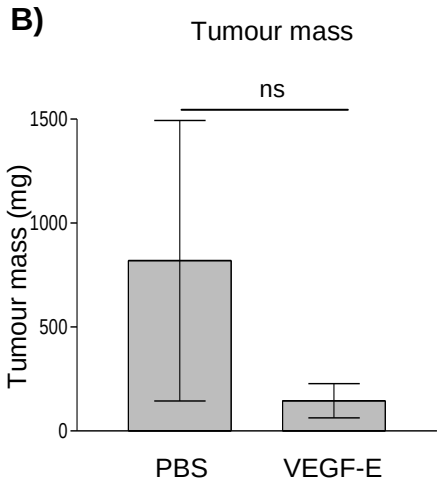
B)
Tumour mass
ns
Tumour mass (mg)
1500
1000
500
0
PBS
VEGF-E

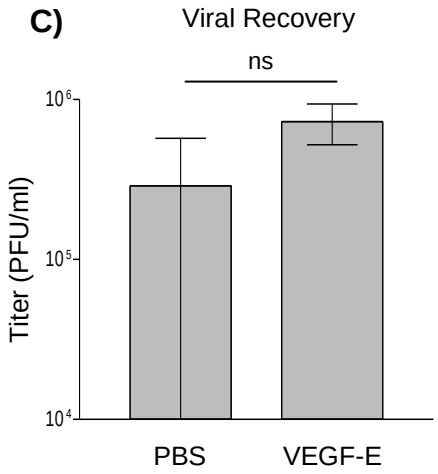
C)
Viral Recovery
ns
Titer (PFU/ml)
10^6
10^5
10^4
PBS
VEGF-E

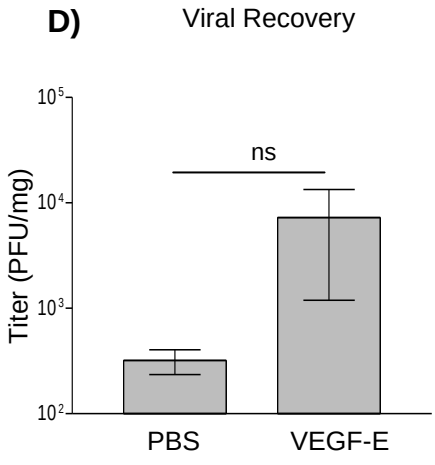
D)
Viral Recovery
ns
Titer (PFU/mg)
10^5
10^4
10^3
10^2
PBS
VEGF-E

also insignificant trends towards VEGF-E tumours being smaller, Figure 2.2B, and having more virus per mg of tumour tissue, Figure 2.2D.

To focus on viral delivery to the tumour, BALB/c mice bearing CT26WT tumours were treated with VEGF-E or vehicle IT followed with vvDD IV, Figure 2.3A. Treatment groups did not differ in tumour volume, Figure 2.3B. Some mice were sacrificed on day 4, without receiving virus, and their tumours were excised, sectioned and hematoxylin & eosin stains (H & Es) were performed, Figure 2.3C. A pathologist within the cancer centre, Dr. Manijeh Daneshmand, pointed out how to identify blood vessel structures and then the obvious ones were subsequently counted; quantification is conservative. However, the increase in tumour blood vessels did not translate into an increase in perfusion, as observed by the distribution of fluorescent microspheres, Figure 2.3D. This is reflected in the mice that were sacrificed one day after virus injection; VEGF-E did not alter tumour mass, Figure 2.3E, nor viral recovery, Figure 2.3F and 2.3G.

The lack of efficacy in these preliminary experiments and the difficulties plaque purifying recombinant virus lead to switching to the CE project.

Figure 2.3: In this model, pre-treatment of CT26WT tumours with VEGF-E does not affect viral delivery of a subsequent vvDD dose. A) BALB/c mice bearing palpable CT26WT tumours were treated according to the schedule shown. Mice either received virus on day 4 and were scarified on day 5, or they were sacrificed on day 4 to see tumour histology and perfusion at the time point when the other mice received virus. B) Tumours were measured on days 0, 4 and 5. Volume was calculated by (length × width^2)/2. n = 8 on days 0 and 4; n = 5 on day 5. Data points are means ±SD. C) Representative images of hematoxylin and eosin stains of tumour sections from mice sacrificed on Day 4. Arrows indicate blood vessels, which were counted at 10X zoom using Aperio ScanScope software. Quantification, on the right, represents the mean of 3 mice (±SD), each having its tumour vessels counted in 5 random fields. (D) For the mice that were sacrificed on day 4, five minutes preceding endpoint, mice were injected IV with fluorescent microspheres. Their tumours were excised and tumour sections were scanned with a microarray scanner to analyze the distribution of the microspheres (shown as black), representative images are shown. For mice that received virus and were sacrificed on day 5, excised tumours were also weighed (E), homogenized in PBS and titered on U2OS cells, (F) and (G). Data represents means ± SD, n = 5. ns $P > 0.05$, *** $P < 0.001$ (Welch's corrected unpaired t test; two-tailed).

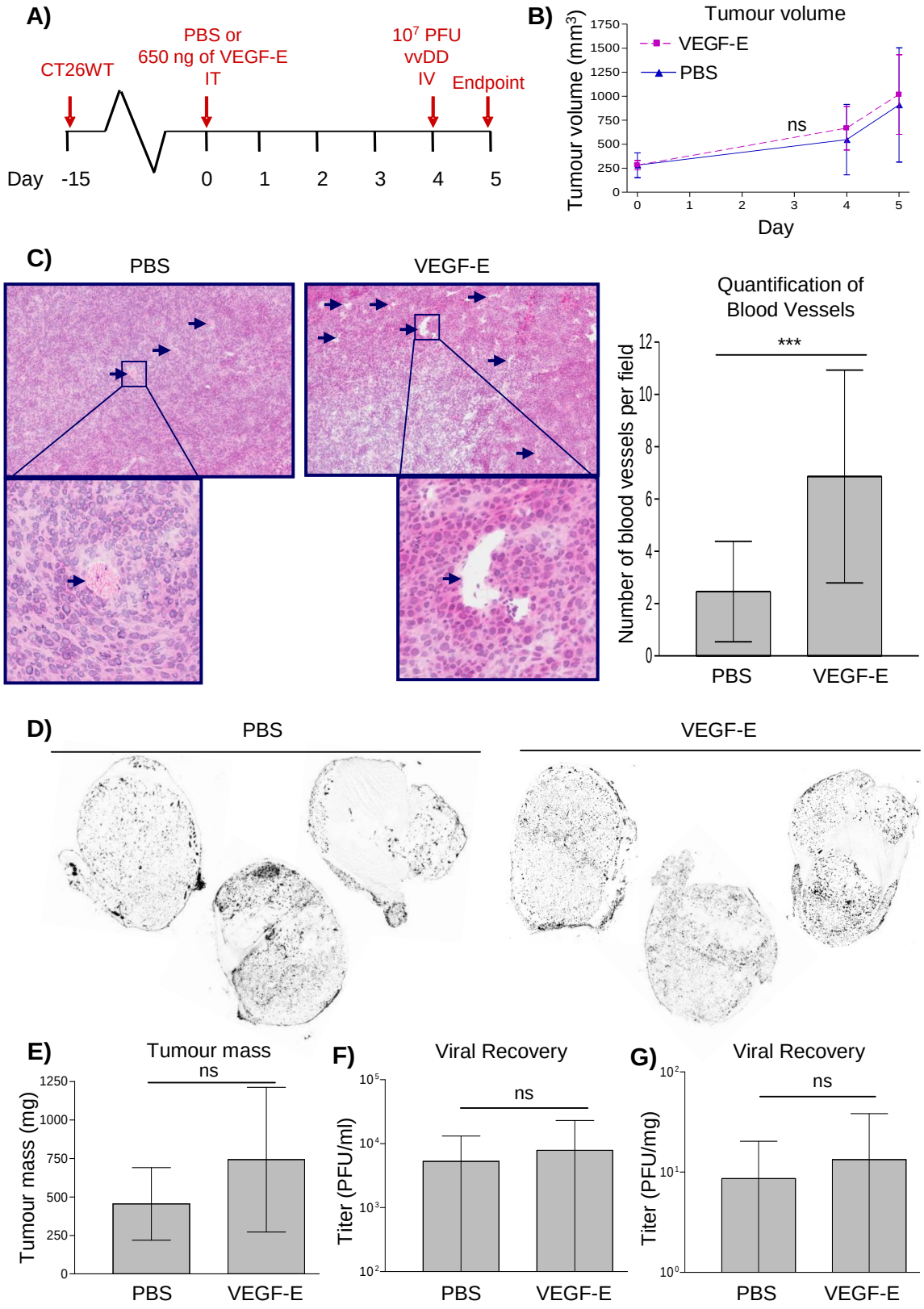
A)
CT26WT
PBS or
650 ng of VEGF-E
IT
10^7 PFU
vvDD
IV
Endpoint
Day -15 0 1 2 3 4 5
B)
Tumour volume
VEGF-E
PBS
Tumour volume (mm3)
ns
Day
C)
PBS
VEGF-E
Quantification of
Blood Vessels
***
Number of blood vessels per field
PBS
VEGF-E
D)
PBS
VEGF-E
E)
Tumour mass
ns
Tumour mass (mg)
PBS
VEGF-E
F)
Viral Recovery
ns
Titer (PFU/ml)
PBS
VEGF-E
G)
Viral Recovery
ns
Titer (PFU/mg)
PBS
VEGF-E

Discussion

The pilot experiment where mice bearing CT26LacZ SQ tumours were pre-treated with either WT Orf or OrfΔVEGF-E prior to treatment with vvDD failed to show any differences in efficacy. As stated previously, this pilot experiment did have some limitations; firstly, how much VEGF-E is produced by Orf cannot be controlled. CT26LacZ tumours were chosen because Orf replicates in this cell line (Rintoul et al., 2012), however it is unknown whether biologically significant amounts of VEGF-E protein were ever reached. Also, although VEGF-E is expressed early in Orf virus infection (Lyttle et al., 1994), perhaps there simply was not enough time for the VEGF-E to be made, secreted and exert its functions. While waiting longer after Orf treatment might allow more angiogenesis to occur, VEGF-E induced angiogenesis needed to be capitalized on as soon as possible given VEGF is a pro-tumourigenic factor (Folkman, 1995); waiting longer likely would result in larger tumours that are more difficult to treat. Savory et al. infected sheep, Orf's natural host, with either WT Orf or OrfΔVEGF-E and found that infection with OrfΔVEGF-E produced less vascularized lesions, a less intense influx of inflammatory cells and infection resolved more quickly. At 2 days post-infection, they did not see any differences in vascularization but at 6 days post-infection, only WT Orf lesions showed intense vascularization. How significant this effect would be at 4 days is unknown. On one hand, at 6 days post-infection, which would have been 2 days post vvDD treatment and one day prior to endpoint, only WT Orf tumours should have been vascularized in which case an increase in vascularization could have resulted in an increase in viral spread throughout the tumour. On the other hand, viral kinetics may be different in sheep skin compared to a mouse tumour.

Returning to the pilot experiment with Orf pre-treatments, mice pre-treated with vehicle should have been included to better dissect the effects of the pre-treatments. At the dose used, Orf is cleared from CT26LacZ tumours two days post-infection (unpublished data, Dr. Julia Rintoul). Even if Orf is completely cleared from the tumours by the time vvDD is given, Orf treatments likely changed the local microenvironment. Orf is known to create a response reminiscent of a sustained wound healing response (Savory et al., 2000). Given Savory et al. found that OrfΔVEGF-E, in addition to producing less vascularized lesions, produced less intense inflammation and pathology, it is possible that these latter effects, in addition to those associated with having replicating virus present, may affect parameters such as perfusion (Breitbach et al., 2007; Sun et al., 2007) and vascular permeability (Joris et al., 1990), which may cloud the effect being observed. Aware that the presence of replicating Orf virus complicated the experiment, commercial recombinant VEGF-E protein was subsequently used as a source of VEGF-E.

In addition, CT26WT tumours were selected for ensuing experiments: they are less perfused and more resistant to vvDD than CT26LacZ (unpublished data from our lab), but are still considered intermediate so it should be possible to see improvements in perfusion and viral spread. Moreover, CT26WT tumour angiogenesis has been shown to be VEGF-dependent (Basu et al., 2008) and there have been reports where various treatments induced CT26WT tumour angiogenesis (Kollmar et al., 2006; Kollmar et al., 2007; Rupertus et al., 2007; Basu et al., 2008; Valcárcel et al., 2008), therefore, it is physiologically possible for these tumours to increase in vasculature. Viral treatment was maintained at 4 days post VEGF treatment because a study showed that recombinant VEGF was able to induce angiogenesis in the mouse cornea in just four days (Kenyon et al., 1996). The Orf virus VEGF-E also induced angiogenesis in just 4 days in mice (Ogawa et al., 1998). However, the

latter paper used Matrigel, which likely would have accelerated angiogenesis due to high local concentrations of proangiogenic factors (Vukicevic et al., 1992; Kenyon et al., 1996).

To focus on the effect of VEGF-E on virus spread within the tumour, 400 ng of VEGF-E was used (Ogawa et al., 1998). Although the trend for virus recovery was in the desired direction, failure to take tumour measurements throughout the experiment precluded the distinction between VEGF-E treated tumours shrinking due to enhanced virus spread or simply the tumours were smaller when treatment was initiated. Moreover, the lack of proof of VEGF-E function means that failure to see an effect could be because VEGF-E treatment was not sufficient to alter tumour microenvironment or that it was sufficient but that the altered microenvironment did not increase viral recovery.

The effect of VEGF-E on virus delivery was then examined. In an effort to increase the effect of VEGF-E, the dose was raised to 650 ng. This time, tumour volume, histology and perfusion were observed. Although tumour volume was unchanged, VEGF-E treated tumours showed a statistically significant increase in blood vessels. However, this did not result in an increase in perfusion. One interpretation is that the increase in blood vessels, although statistically significant, was not biologically significant. Another interpretation is that the VEGF-E induced blood vessels were of poor quality and functionality. (Benjamin et al., 1999; Jain, 2005) Either way, the similar perfusion among control and VEGF-E tumours is reflected in the lack of difference in virus delivery.

Conclusions

Unfortunately, the first objective, to determine whether VEGF-E improves or reduces vvDD's oncolytic efficiency, was never properly accomplished due to difficulties with the tumour model. Therefore, whether local VEGF production would help oncolytic virus delivery, spread and/or efficacy remains to be elucidated.

If the project were to be restarted, the following changes would be made: the first experiment would be to optimize VEGF-E treatment; treating tumours with increasing doses of VEGF-E and waiting for different periods time. H & E stains of tumour sections would be used to see blood vessels, confirming by performing IHC for CD31 to stain these vessels (Breitbach et al., 2011a) and looking at perfusion via microspheres. Furthermore, vessel quality could be examined by staining for pericytes (Bergers and Song, 2005; Fakhrejahani and Toi, 2012). Then, after determining the VEGF-E treatment regimen, performing efficacy experiments in the context of delivery and spread, as attempted above. IHC looking at virus distribution throughout the tumour could be done. If these results were promising, the vvDD-VEGF-E recombinant would be constructed as outlined in the next chapter. This recombinant would be examined as described above; perhaps continuous production of VEGF-E may have different effects on tumour progression or VV activity.

Interesting avenues to pursue would be to look at increases in vessel permeability (Tseng et al., 2010), vessel infection (Breitbach et al., 2011a) and the effect of increasing angiogenesis on infiltration of immune cells into the tumour (Martinotti et al., 1995; Björkdahl et al., 1997; Breitbach et al., 2007) and metastasis (Kollmar et al., 2006; Kollmar et al., 2007; Rupertus et al., 2007; Valcárcel et al., 2008).

The implications of this project would be broad: perhaps VEGF-E expression could produce a microenvironment that increases the delivery, spread and efficacy of many OVs.

PROJECT 3: THE DISAGGREGATION OF VACCINIA VIRUS PARTICLES FOR IMPROVED PLAQUE PURIFICATION OF RECOMBINANT VIRUSES

Introduction

Difficulties encountered throughout vvDD-VEGF-E plaque purification could have arisen for a number of reasons. Although a linearized cloning vector was used and proper cloning was verified by sequencing, perhaps the recombinant virus was unstable, reverting to parental virus, even though the size of the insert can easily be accommodated by VV. Another possibility is that the luciferase gene, which was used as a marker for recombinant virus, was causing problems. After all, it was never entirely sequenced. If this enzyme, which converts luciferin to oxyluciferin – which releases a photon, were functioning inconsistently, recombinant plaques may have looked like parental plaques. A third possibility was that viral particle aggregation was complicating plaque purification. Perhaps plaques that were picked actually contained cells infected with both types of virus. This was further studied in order to determine if particle aggregation is a significant problem with VV throughout this particular procedure and, if so, strategies for disaggregating viral particles would be applied to it.

VV lysate preparations are known to contain aggregates; in the 1950s, electron microscopy (EM) was applied to the evaluation of particle dispersion in virus preparations (Sharp and Buckingham, 1956) and shortly thereafter, it was shown that crude extracts of VV-infected cells contained virus particle aggregates and that sonication could improve dispersion (Overman and Sharp, 1959). It was estimated that approximately 60% of virus

particles obtained from untreated cell lysates were aggregated (Galasso and Sharp, 1962). The frequency of singlets was greatest and the frequency of aggregates decreased with increasing number of particles within the aggregate. Furthermore, both sonicated and filtered lysates greatly reduced the number and the size of aggregates. (Galasso et al., 1964).

The D. G. Sharp group went on to show that sonication did not have destructive effects on VV particles (Kim and Sharp, 1966), and that proteolytic enzymes trypsin and chymotrypsin enhanced VV titer (Kim et al., 1969).

Hypothesis and objectives

We suspect that disaggregation methods could be applied to the plaque picking procedure to reduce the incidence of picking plaques that have arisen from more than one virus particle, which should reduce the number of rounds of plaque purification necessary. The first objective was to determine the most effective disaggregation method. The second was to verify that a disaggregation technique could be applied to the plaque picking procedure.

Results

Parental and recombinant plaques were modeled with vvDD-eGFP and vvDD-mCherry; that way, the sites of replication of each virus could be distinguished. Equal amounts of sucrose purified vvDD-eGFP and vvDD-mCherry preparations were mixed and used to infect cells. Cells were topped with an agarose overlay, given this type of overlay is used for plaque purification. Plaque fluorescence was then observed by microscopy. Figure 3.1A shows that purified preparations produce very few plaques that are both red and green. To more closely mimic the plaque purification procedure, purified virus preparations were substituted with infected cell lysate, given picked plaques are infected cells that are lysed by freeze/thawing. Specifically, cells infected with a mixture of vvDD-GFP and vvDD-mCherry were collected and freeze/thawed 3 times. This infected cell lysate was used to infect cells and resulting plaque colours were observed. Figure 3.1B shows that as much as ~16.8 % of plaques are mixed or "yellow", suggesting they arose from aggregated virus particles. Please note that this assay does have its caveats, further discussed in the next section. Various disaggregation methods were applied but only benzonase + Tryp-LE + sonication and filtration using a 0.65 µM pore resulted in a significant decrease in % aggregation. Filtration also significantly outperformed benzonase + Tryp-LE + sonication (1.2% aggregations vs. 9.5%, respectively). However, viral titers showed that filtering the lysate resulted in approximately one log loss of virus.

To learn more about aggregation throughout the VV infection cycle, lysate collected at 48 hrs post-infection, as done above and throughout the plaque purification procedure, was compared to supernatant collected 16 hrs post-infection, which would contain some viral particles which have budded from infected cells as opposed to mostly consisting of large

Figure 3.1: Viral particle aggregates in infected cell lysates produce mixed plaques but can be removed by filtration. A) Equal amounts of sucrose-purified vvDD-GFP and vvDD-mCherry were mixed and used to infect U2OS cells. Two days later, resulting plaques were observed by microscopy to determine which virus created the plaque. B) The entire contents of the well from cells infected with a mixture of equal amounts of vvDD-GFP and vvDD-mCherry were collected two days post-infection. Following 3 freeze/thaw cycles, this infected cell lysate was either left untreated or treated with the indicated disaggregation method prior to being used to infect U2OS cells. Two days later, plaque colour was observed. % aggregation is on the top panel and titer is on the bottom. For "1", n = 7; for "2", "3" and "4", n = 2; for "5", n = 5. * $P < 0.05$, ** $P < 0.01$, *** $P < 0.001$ (one way ANOVA with Bonferroni's Multiple Comparison Test). C) Cells were infected with a vvDD-GFP and vvDD-mCherry mixture and either the entire contents of the well were collected at 48 hrs post-infection or just the supernatant was collected 16 hrs post-infection. Following 3 freeze thaw cycles, this infected cell lysate or supernatant was either left untreated or filtered prior to being used to infect U2OS cells. Data is from one independent experiment.

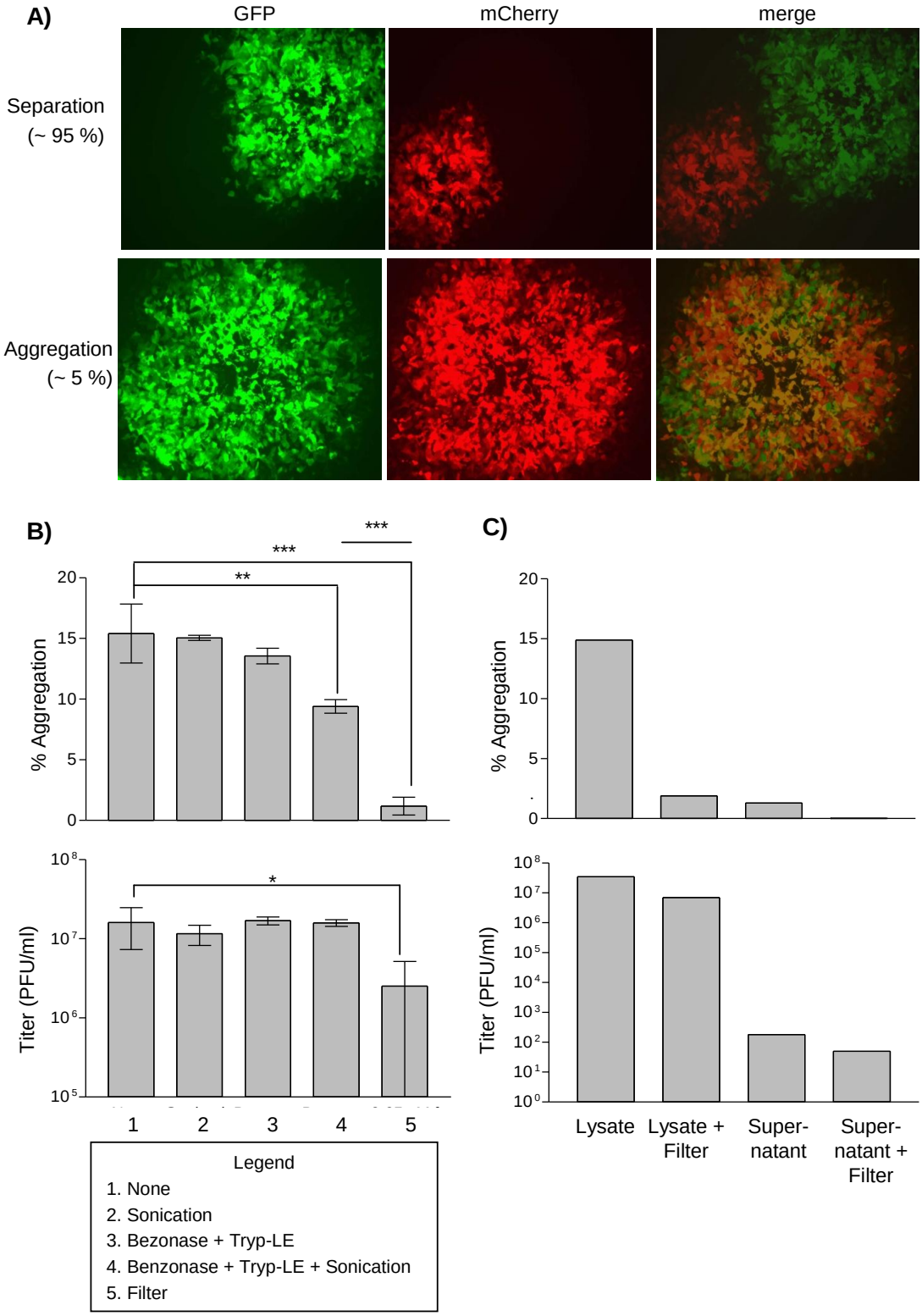
A)
GFP
mCherry
merge
Separation
(~ 95 %)
Aggregation
(~ 5 %)
B)
C)
% Aggregation
Titer (PFU/ml)
***
**
*
1
2
3
4
5
Legend
1. None
2. Sonication
3. Bezonase + Tryp-LE
4. Benzonase + Tryp-LE + Sonication
5. Filter
Lysate
Lysate + Filter
Super-natant
Super-natant + Filter

amounts of virus released from lysed cells. Figure 3.1C shows that supernatant collected 16 hrs post-infection produced significantly fewer viral aggregates than the lysate at 48 hrs. As previously observed, filtering significantly reduced aggregation and showed a trend towards reducing viral titer by approximately one log. As expected, the supernatant from an early time point had much less virus than lysate collected at a later time point; 5 logs less.

To see if virus particles would reaggregate after filtering, infected cell lysate was split into fractions which were filtered at different time points prior to infection. Figure 3.2A shows that reagreggation does not occur over 7 days. To see if freeze/thawing a virus preparation would cause reaggregation, infected cell lysate was filtered and then freeze/thawed for the indicated number of cycles. Figure 3.2B shows that 3 freeze/thaw cycles did not result in particle reaggregation.

To learn more about the plaque picking procedure, 3 green plaques, 3 red plaques and 3 mixed plaques were picked, according to the laboratory's plaque picking procedure. Figure 3.3A shows that green plaques mostly produce green progeny plaques, red plaques mostly produce red progeny plaques (although one of the plaques was lost – picked incorrectly) and mixed plaques produce green, red and mixed progeny plaques (~68%, ~26% and ~6%, respectively). Therefore, even when picking a mixed plaque, progeny plaques arise mostly from a single virus.

Finally, a filtration step was applied to the plaque picking procedure; mixed plaques were picked and each resuspended plaque was split into two fractions: one was filtered and the other remained unfiltered prior to infection. The bottom panel of Figure 3.3B, shows that, for 2 of the 3 plaques picked (Plaques 1 and 3), filtration removed all virus particles completely, given the amount of virus in those particular picked plaques was low to begin

Figure 3.2: After filtration, viral particles in infected cell lysates do not reaggregate over time or freeze/thaw cycles. A) vvDD-GFP and vvDD-mCherry infected cell lysate was split into 6 fractions, which were stored at 4°C. At different times prior to infection, fractions were filtered and put back at 4°C. Two days after infection, resulting plaques were observed. Data is from one independent experiment. B) vvDD-GFP and vvDD-mCherry infected cell lysate was split into 5 fractions. Four of these were filtered, and then freeze/thawed for the indicated number of freeze/thaw cycles prior to infection. Two days after infection, resulting plaques were observed. Data is from one independent experiment.

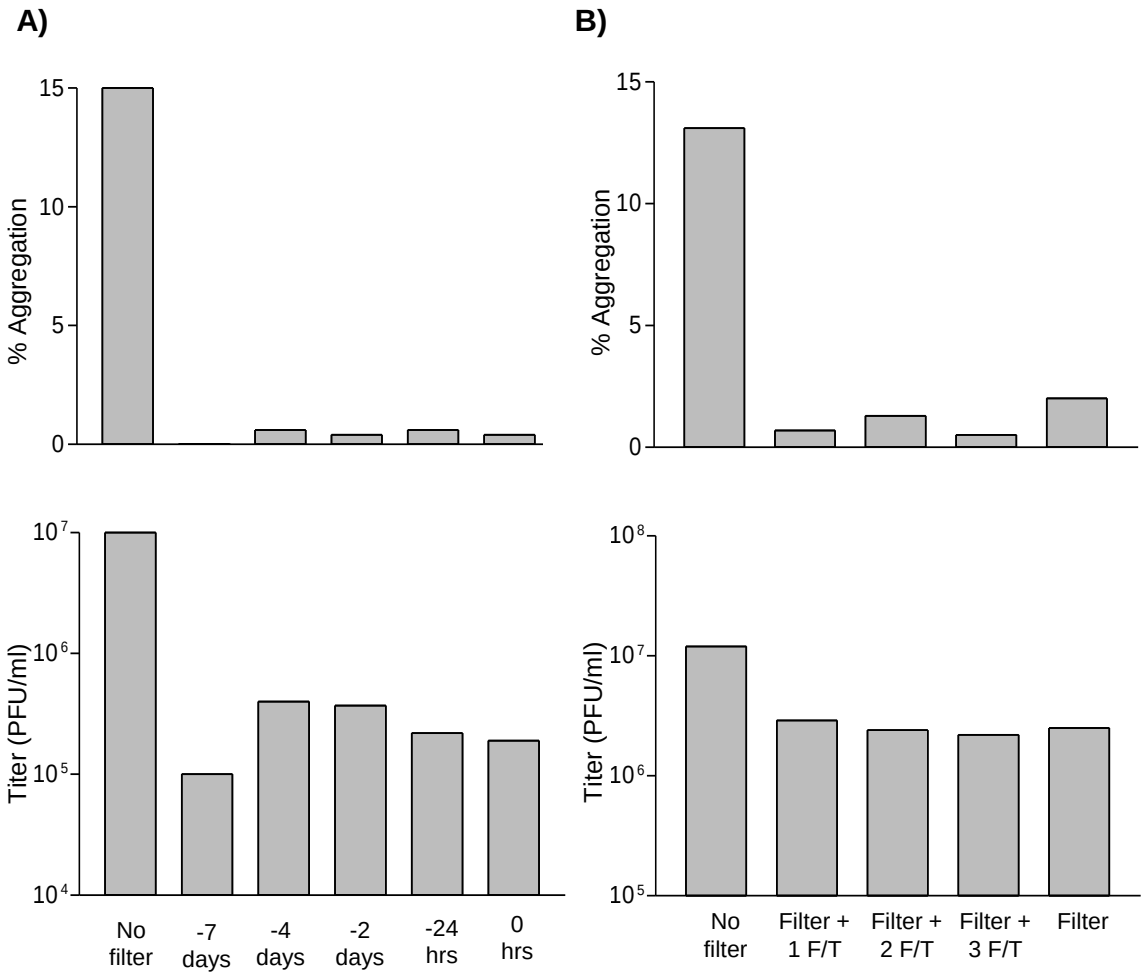
A)
B)
% Aggregation
15
10
5
0
Titer (PFU/ml)
10^7
10^6
10^5
10^4
10^8
No filter
-7 days
-4 days
-2 days
-24 hrs
0 hrs
Filter + 1 F/T
Filter + 2 F/T
Filter + 3 F/T
Filter

Figure 3.3: Addition of a filtration step to the plaque picking procedure removes aggregates but may also remove all virus. A vvDD-GFP and vvDD-mCherry infected cell lysate was used to infect U2OS cells. Two days after infection, resulting plaques were observed and 3 green plaques, 3 red plaques and 3 mixed plaques were picked according to the lab's plaque picking procedure. A) These plaques were used to infect subsequent U2OS cells. Two days later, resulting plaques were observed. Data is from one independent experiment. B) The 3 mixed plaques were split into two fractions, one of which was filtered. These filtered and unfiltered fractions were then used to infect subsequent U2OS cells. Two days later, resulting plaques were observed. Data is from one independent experiment.

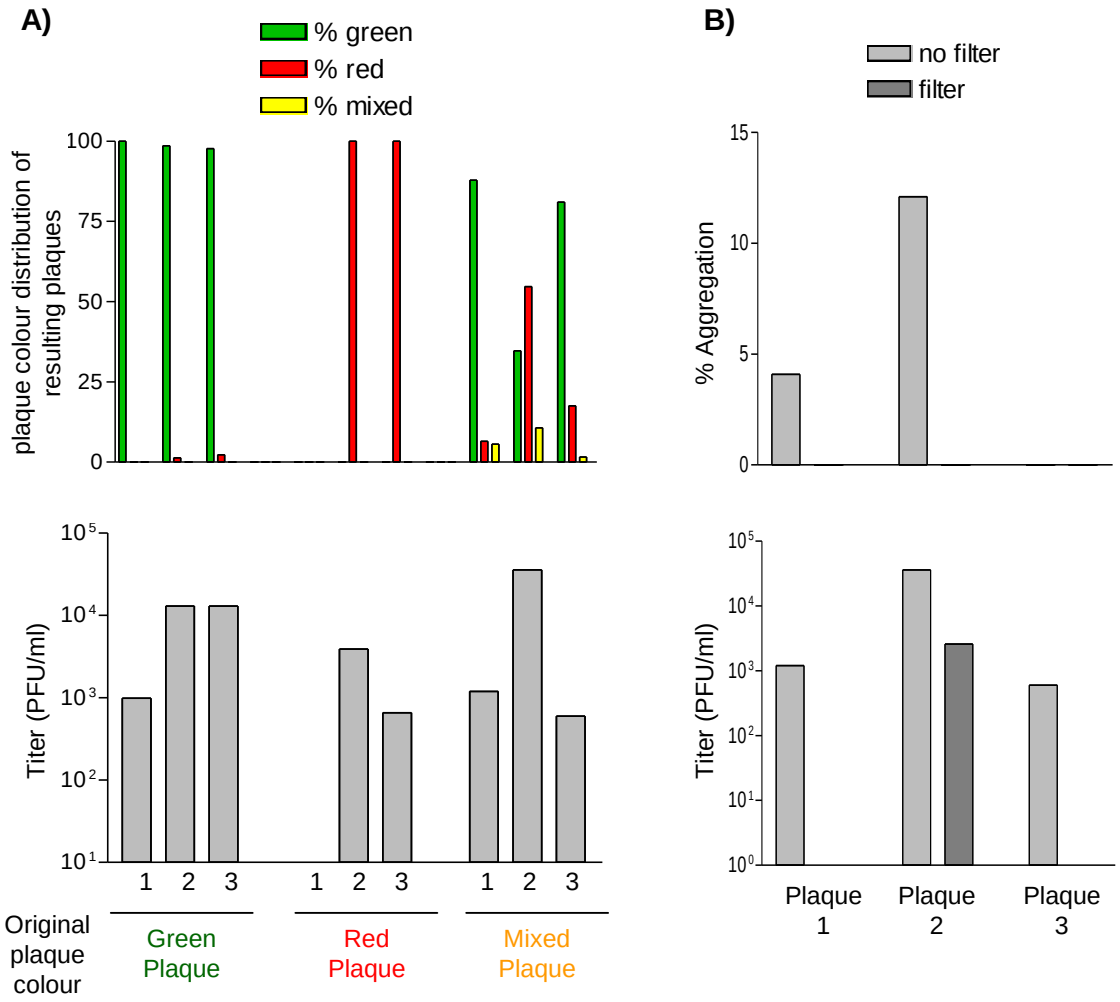
A)
% green
% red
% mixed
plaque colour distribution of resulting plaques
100
75
50
25
0
Titer (PFU/ml)
10^5
10^4
10^3
10^2
10^1
1 2 3 1 2 3 1 2 3
Original plaque colour
Green Plaque
Red Plaque
Mixed Plaque
B)
no filter
filter
% Aggregation
15
10
5
0
Titer (PFU/ml)
10^5
10^4
10^3
10^2
10^1
10^0
Plaque 1
Plaque 2
Plaque 3

with. Picked plaque 2, which had more virus to begin with, still had virus particles following filtration (bottom panel) and was aggregate-free (top panel).

Discussion

Aggregation was modeled by working with a mixture of vvDD-GFP and vvDD-mCherry; that way, it would be obvious which virus particle(s) produced each plaque. This model has limitations; only mixed, or "yellow" plaques would be detected as aggregates while aggregates of multiple GFP encoding virions or multiple mCherry encoding virions would appear as a single virion. Although this would lead us to believe that this assay only detects one third of viral aggregates, this in fact depends on how many virus particles are in each aggregate and this information can be estimated by looking at the ratios of the different plaques colours. If every plaque arose from a single virus particle, 0% of plaques would be yellow. If every plaque resulted from the aggregation of two viral particles, 33% of plaques would be yellow. Assuming every plaque resulted from the aggregation of three virus particles, 1 of 4 combinations results in green plaques, 1 of 4 in red plaques and 2 of 4 in yellow plaques, which means 50% of observed plaques would be yellow. The larger the size of the aggregates, the more yellow plaques would be observed. 16.8% yellow plaques were observed; this is somewhere between that expected if the population were made up entirely of singlets (0% yellow) and if it were entirely doublets (33% yellow). This indicates that most of the population of virus particles are singlets and doublets but does not exclude the possibility of triplets or larger aggregates being present. Findings in the literature also stipulate that VV is mostly found in singlets and doublets: EM examining VV particles in an unpurified lysate showed ~58% of particles were singlets, 13% were doublets and the remaining 29% were aggregates consisting of 3 to 150 virus particles (Galasso et al., 1964). The larger the aggregate, the less frequently it was observed. Although it seems like aggregates were much more prominent in the literature, ~42% and ~60% (Galasso and

Sharp, 1962), EM looks at all particles while looking at plaque colour only looks at infectious virus. It is estimated that only 1 in 50 VV particles are infectious (Overman and Sharp, 1959; Contreras and Ohlbaum, 1968; Moss et al., 1973). As it stands, infectious and non-infectious particles cannot be morphologically distinguished (Overman and Sharp, 1959; Nitsche et al., 2006; Condit, 2007: 40-41), and there is no evidence to suggest that one type of particle is more likely to aggregate. Therefore, whether infectious or non-infectious particles are being considered, the proportion of singlets, doublets, triplets, etc. should be the same; this assay simply looks at one fiftieth of the total population. The only exception is the case of aggregates containing only one infectious particle; EM would show these as aggregates while our assay would report them as singlets. Our model thus underestimates the real amount of aggregation. For the remainder of the report, infectious virus only is considered unless stated otherwise.

Knowing that the virus preparation consists mostly of singlets, doublets, etc., the accuracy of the assay can be inferred. If the population were entirely singlets, the assay would be 100% accurate at reporting singlets as singlets. If the population was entirely made up of doublets, 33% of plaques would be yellow and the assay would detect 33% of doublets. If the population were made up entirely of triplets, 50% of plaques would be yellow and 50% of aggregates would be detected and so forth; the larger the aggregates, the higher the accuracy. Therefore, the observed 16.8% aggregation is an underestimate; although the singlets were reported accurately, only a fraction of the aggregates were detected. Assuming the population of virus particles were entirely made up of doublets, the condition in which the assay is the least accurate, the % aggregation would have to be tripled: 16.8% aggregation would actually mean 50.4% aggregation. But, since singlets, triplets and higher order aggregates are reported more accurately than doublets, the actual %

aggregation of infectious particles is somewhere between 16.8 and 50.4 %, but could be even higher if non-infectious virus were included. In short, aggregation is present in cell lysate preparations.

Sucrose-purified virus preparations have few aggregates likely because they have very little cell debris (Smallwood et al., 2010) and "[…] aggregates of virus and cell debris are believed to occur due to the membrane-associated nature of the poxviruses." (Newman et al., 2003; Overman and Sharp, 1959).

In cell lysate, ~16.8% aggregation was observed. Various disaggregation methods were applied; sonication was used to disperse particles (Galasso and Sharp, 1962; Galasso et al., 1964; Kim and Sharp 1966), benzonase nuclease to degrade nucleic acids as host cell nucleic acid debris may be mediating aggregation, Tryp-LE to digest "cementing substances" (Ichihashi and Oie, 1980; Planterose et al., 1962; Kim et al., 1969; Moss et al., 1973) and finally filtration with a 0.65 µM pore (Galasso et al., 1964; Ver et al., 1968), which does not disaggregate particles but simply removes the aggregates. 0.65 µM was selected because it is roughly twice the size of a VV particle, 360 × 270 × 250 nm (Cyrklaff et al., 2005), anything smaller may reduce the amount of particles that go through the filter due to adsorption onto the membrane (Ver et al., 1968). Filtration was the most effective method of removing aggregates, however, it resulted in one log less of virus; 90% of virus was removed. This does not imply that 90% of the prep was aggregated, but indicates that aggregates were removed along with some singlets, perhaps due to interactions with the untreated membrane (Ver et al., 1968). Although increasing pore size would improve virus recovery, it would also increase the amount of aggregates that pass through the pores. Since aggregation is being examined in the context of plaque purification, it is more important that a preparation be aggregate-free than it be of high virus yield.

Supernatant collected 16 hours post-infection had much fewer aggregates, advocating the role of cell debris in aggregation; supernatant collected earlier, when fewer cells would have lysed from viral infection, would have much less cell debris. The 16 hrs supernatant and 48hrs cell lysate, in theory, would also differ in terms of their distribution of the virion types: EEV, although a very small portion of total virions, is first liberated from infected cells around 4 to 6 hours and plateaus around 16 hours post-infection (Payne et al., 1979) while IMV is only released upon cell lysis. Therefore, the 16 hrs supernatant would have a higher EEV to IMV ratio than the 48 hr lysate. Not much is known about the two particles' tendency to aggregate; one relevant report mentioned that their EEV preparation had a greater tendency to aggregate in a particular VV entry assay, but cited "unpublished data" (Locker et al., 2000). Although this disagrees with the obtained data, the situations are a little different: our samples are not pure IMV or EEV, they are a mixture and they also contain varying amounts of cell debris. Thus, overall, although two EEV particles might be more likely to aggregate than two IMV particles, obtained data suggests that supernatant collected at a point when virus particles are being released from infected cells contains fewer aggregates than samples collected after a larger fraction of cells have burst open and spewed out virus.

Further tests revealed that after filtration, particles did not reaggregate over time nor freeze/thaw cycles; perhaps once most of the cell debris is removed, there is simply nothing to "cement" (Ichihashi and Oie, 1980) virus particles together.

Finally, using this model to examine the lab's plaque purification procedure revealed that when picking a single-coloured plaque, progeny plaques are mostly of that plaque colour (>97%) and that when picking mixed plaques, only a small percentage of progeny plaques are mixed. This speaks to the quality of the plaque purifying procedure as is and implies that

very few rounds of plaque purification are, in theory, needed to obtain a single type of virus. In practice, at least five or six rounds are needed. Given how few mixed progeny plaques were produced after picking a mixed plaque, the fact that the vvDD-VEGF-E virus was not pure after many more than 6 rounds of plaque purification infers that aggregation was not the major cause of difficulties plaque purifying. Insert instability or luciferase mutations are thus likely the cause.

Adding a filtration step to the plaque picking procedure completely removed aggregates and thus should reduce the number of rounds of plaque purification required. Although filtration may completely remove virus from preparations with a low titer, picking many plaques should avoid complete loss of recombinant virus. One hundred percent purity of recombinant virus is required in downstream applications not just to attribute any effects to the recombinant with complete certainty but also because a mixed population may change under different selective pressures. Moreover, if a recombinant virus reaches clinical trials, it is very important that it does not contain contaminating virus.

The following is recommended for plaque purification; proceed as is, then, after a couple of rounds of purification, once the recombinant is starting to become the more prevalent type of virus in the population, a filtration step should be added to the final round of plaque purification. The final plaque picked, which should be a singlet since the inoculum was filtered, should be free of parental virus. To ensure 100% purity, this plaque should be used to infect a last round of plates, to make sure every resulting plaque is a recombinant plaque. If so, this plaque can proceed to be amplified to make up the recombinant virus stock.

Conclusions

In conclusion, both objectives were met: filtration was identified as an effective method for removing viral aggregates and was applied to the plaque picking procedure. An interesting final test would be to compare how many rounds of plaque purification are needed to reach 100% purity with and without filtration; we suspect filtration would reduce the number of rounds.

After having completed this side project, looking back on the plaque purification of vvDD-VEGF-E, the following changes should have been made: in addition to adding a filtration step to the plaque purification method, the parental virus should have a different marker, such as mCherry, in order to track its disappearance. This would allow the distinction between recombinant, parental and a third population of marker-less plaques, which may have arisen from the virus kicking out the foreign DNA. This third population could have been confused with parental virus in the luciferase system and thus did not give any information about the underlying problem. Finally, in addition to sequencing the gene of interest and the regions flanking the insert to ensure proper recombination, the entire genomic insert should be sequenced to make sure that all incorporated genes are unchanged.

Future experiments should include pre-coating filters to improve viral yield, as done by Ver et al. Increasing virus recovery would allow the technique to be applied to earlier rounds of plaque purification and would thus reduce the number of rounds necessary. Furthermore, methods of breaking up the aggregates, as opposed to simply removing them, could be investigated. Such methods could include the addition of citrate (Peterson et al., 2006) or glycerol (Wang et al., 2007) or the use of different medias (Leibovitz et al., 1983; Han et al., 2006), which have helped disaggregate other viruses or cells. It has yet to be determined if these methods would work with VV.

The low virus yield limits the application of the filtration technique to plaque purification, however, a method to physically disaggregate particles would be beneficial for manufacturing purposes.

GENERAL CONCLUSIONS

Both main projects, CE and VEGF-E expression from VV, were aimed at increasing the efficacy of VV.

Clinical trials have shown that OVs produce limited toxicities, rendering them a safe alternative to current therapies. However, clinical trials have also shown that there is an opportunity to increase antitumour efficacy. Cancer's heterogeneity and ability to adapt require clever multi-pronged attacks in order to treat this deadly disease. VV's large cloning capacity means that several transgenes may be expressed, providing the opportunity for multi-modality killing from a single targeted virus (Thorne and Kirn, 2004). In addition, the viruses' reduced systemic toxicities allow for combinations with other standard treatments, which would increase the impact of treatment on this elusive disease.

REFERENCES

Aghi, M. and Martuza, R. L. (2005) Oncolytic viral therapies - the clinical experience. *Oncogene* **24**(52): 7802-16.

Alagkiozidis, I. et al. (2011) Time-dependent cytotoxic drugs selectively cooperate with IL-18 for cancer chemo-immunotherapy. *Journal of Translational Medicine* **9**:77.

Alberts, B. et al. Molecular Biology of the Cell. 4th edition. New York: Garland Science; 2002. Cancer as a Microevolutionary Process. Available from: http://www-ncbi-nlm-nih-gov.proxy.bib.uottawa.ca/books/NBK26891/

Arkenau, H.-T. et al. (2008) Targeted agents in cancer therapy. *Medicine* **36**(1): 33-37.

Baixeras, E. et al. (1998) Vaccinia virus-induced apoptosis in immature B lymphocytes: role of cellular Bcl-2. *Virus Research* **58**(1-2): 107-13.

Baker, J. H. et al. (2008) Irinophore C, a novel nanoformulation of irinotecan, alters tumor vascular function and enhances the distribution of 5-fluorouracil and doxorubicin. *Clinical Cancer Research* **14**(22): 7260-71.

Baskar, R. et al. (2012) Cancer and radiation therapy: current advances and future directions. *International Journal of Medical Science* **9**(3): 193-9.

Basu, A. et al. (2008) Overexpression of vascular endothelial growth factor and the development of post-transplantation cancer. *Cancer Research* **68**(14): 5689-98.

Baxevanis, C. N. et al. (2009) Cancer immunotherapy. *Critical Reviews in Clinical Laboratory Sciences* **46**(4): 167-189.

Begg, A. C. et al. (2011) Strategies to improve radiotherapy with targeted drugs. *Nature Reviews Cancer* **11**(4): 239-53.

Bell, J. (2010) Oncolytic viruses: an approved product on the horizon? *Molecular Therapy* **18**(2): 233-4.

Benjamin, L. E. et al. (1999) Selective ablation of immature blood vessels in established human tumors follows vascular endothelial growth factor withdrawal. *Journal of Clinical Investigation* **103**(2):159-65.

Bergers, G. and Song, S. (2005) The role of pericytes in blood-vessel formation and maintenance. *Neuro-Oncology* **7**(4):452-64.

Bertram, J. S. (2000) The molecular biology of cancer. *Molecular Aspects of Medicine* **21**(6): 167-223.

Björkdahl, O. et al. (1997) Gene transfer of a hybrid interleukin-1 beta gene to B16 mouse melanoma recruits leucocyte subsets and reduces tumour growth in vivo. *Cancer Immunology Immunotherapy* **44**(5): 273-81.

Bocci, G. et al. (2008). Antiangiogenic and anticolorectal cancer effects of metronomic irinotecan chemotherapy alone and in combination with semaxinib. *British Journal of Cancer* **98**(10): 1619-29.

Boldogh, I. et al. Persistent Viral Infections. In: Baron S, editor. Medical Microbiology. 4th edition. Galveston (TX): University of Texas Medical Branch at Galveston; 1996. Chapter 46. Available from: http://www.ncbi.nlm.nih.gov/books/NBK8538/

Breitbach, C. J. et al. (2007) Targeted inflammation during oncolytic virus therapy severely compromises tumor blood flow. *Molecular Therapy* **15**(9):1686-93.

Breitbach, C. J. et al. (2011a) Targeting tumor vasculature with an oncolytic virus. *Molecular Therapy* **19**(5):886-94.

Breitbach, C. J. et al. (2011b) Intravenous delivery of a multi-mechanistic cancer-targeted oncolytic poxvirus in humans. *Nature* **477**(7362): 99-102.

Bridle, B.W. et al. (2010) Combining oncolytic virotherapy and tumour vaccination. *Cytokine & Growth Factor Reviews* **21**(2-3): 143-8.

Brown, M. G. et al. (2009) Dramatic caspase-dependent apoptosis in antibody-enhanced dengue virus infection of human mast cells. *Journal of Leukocyte Biology* **85**(1): 71-80.

Byfield, J. E. et al. (1977) Molecular interactions between adriamycin and x-ray damage in mammalian tumor cells. *International Journal of Cancer* **19**(2): 186-93.

Canadian Cancer Society's Steering Committee on Cancer Statistics. *Canadian Cancer Statistics 2012*. Toronto, ON: Canadian Cancer Society; 2012.

Casas, S. et al. (2003) Changes in apoptosis-related pathways in acute myelocytic leukemia. *Cancer Genetics and Cytogenetics* **146**(2): 89-101.

Catimel, G. et al. (1995) Phase I and pharmacokinetic study of irinotecan (CPT-11) administered daily for three consecutive days every three weeks in patients with advanced solid tumors. *Annals of Oncology* **6**(2):133-40.

Chabot, G. G. et al. (1995) Population pharmacokinetics and pharmacodynamics of irinotecan (CPT-11) and active metabolite SN-38 during phase I trials. *Annals of Oncology* **6**(2):141-51.

Chaffer, C. L. and Weinberg, R. A. (2011) A perspective on cancer cell metastasis. *Science* **331**(6024): 1559-64.

Cheever, M. A. et al. (2009) The prioritization of cancer antigens: a national cancer institute pilot project for the acceleration of translational research. *Cancer Research* **15**(17): 5323-37.

Chen, R. and Plunkett, W. (2010) Strategy to induce apoptosis and circumvent resistance in chronic lymphocytic leukaemia. *Best Practice and Research: Clinical Haematology* **23**(1): 155-166.

Chiocca, E. A. (2002) Oncolytic viruses. *Nature Reviews Cancer* **2**(12): 938-50.

Chou, T. C. and Talaly, P. (1977) A simple generalized equation for the analysis of multiple inhibitions of Michaelis-Menten kinetic systems. *Journal of Biological Chemistry* **252**(18): 6438-42.

Ciavarella, S. et al. (2010) Targeted therapies in cancer. *BioDrugs* **24**(2): 77-88.

Cohen, G. M. (1997) Caspases: the executioners of apoptosis. *The Biochemical Journal* **326**(Pt 1): 1-16.

Condit, R. C. "Principles of Virology." *Fields Virology*. 5th ed. Vol 1. Philadelphia: Lippincott Williams & Wilkins, 2007. Print.

Contreras, G. and Ohlbaum, A. (1968) Target Volume Analysis of Vaccinia Virus: Influence of Virus Dispersion and Noninfectious Particles. *Journal of Virology* **2**(10): 1102-1106.

Cotter, T. G. (1995) BCR-ABL: an anti-apoptosis gene in chronic myelogenous leukemia. *Leukemia and Lymphoma* **18**(3-4): 231-6.

Crawford, Y. et al. (2009) PDGF-C mediates the angiogenic and tumorigenic properties of fibroblasts associated with tumors refractory to anti-VEGF treatment. *Cancer Cell* **15**(1): 21-34.

Cryns, V. and Yuan, J. (1998) Proteases to die for. *Genes and Development* **12**(11): 1551-70.

Cyrklaff, M. et al. (2005) Cryo-electron tomography of vaccinia virus. *Proceedings of the National Academy of Sciences of the United States of America* **102**(8): 2772-7.

Danks, M. K. et al. (1998) Overexpression of a rabbit liver carboxylesterase sensitizes human tumor cells to CPT-11. *Cancer Research* **58**(1): 20-2.

Danks, M. K. et al. (1999) Comparison of activation of CPT-11 by rabbit and human carboxylesterases for use in enzyme/prodrug therapy. *Clinical Cancer Research* **5**(4): 917-24.

de Forni, M. et al. (1994) Phase I and pharmacokinetic study of the camptothecin derivative irinotecan, administered on a weekly schedule in cancer patients. *Cancer Research* **54**(16): 4347-54.

De Silva, N. et al. (2010) Double trouble for tumours: exploiting the tumour microenvironment to enhance anticancer effect of oncolytic viruses. *Cytokine &Growth Factor Reviews* **21**(2-3): 135-41.

Diallo, J. S. et al. (2011) Ex vivo infection of live tissue with oncolytic viruses. *Journal of Visualized Experiments* (52) pii: 2854.

Donovan, D. et al. (2001) Comparison of three in vitro human 'angiogenesis' assays with capillaries formed in vivo. *Angiogenesis* **4**(2):113-21.

Dunn, G. P. et al. (2002) Cancer immunoediting: from immunosurveillance to tumor escape. *Nature Immunology* **3**(11): 991-8.

Fakhrejahani, E. and Toi, M. (2012) Tumor angiogenesis: pericytes and maturation are not to be ignored. *Journal of Oncology* **2012**:261750.

Fenner, F. et al. *Smallpox and its eradication*. Geneva: World Health Organization, 1988. Print.

Ferguson, M. S. et al. (2012) Systemic delivery of oncolytic viruses: hopes and hurdles. *Advances in Virology* 805629.

Fernández, J. L. and Gosálvez, J. (2002) Application of FISH to detect DNA damage. DNA breakage detection-FISH (DBD-FISH). *Methods in Molecular Biology* **203**: 203-16.

Fidler, I. J. (2003) The pathogenesis of cancer metastasis: the 'seed and soil' hypothesis revisited. *Nature Reviews Cancer* **3**(6): 453-8.

Folkman J. (1995) Angiogenesis in cancer, vascular, rheumatoid and other disease. *Nature Medicine* **1**(1):27-31.

Folkman, J. (1986) How is blood vessel growth regulated in normal and neoplastic tissue? G.H.A. Clowes memorial Award lecture. *Cancer Research* **46**(2): 467-73.

Friedman, G. K. et al. (2012) Hypoxia Moderates γ(1)34.5-Deleted Herpes Simplex Virus Oncolytic Activity in Human Glioma Xenoline Primary Cultures. *Translational Oncology* **5**(3): 200-7.

Froelich, J. J. et al. (1999) The influence of radiation and chemotherapy-related DNA strand breaks on carcinogenesis: an evaluation. *Clinical Chemistry and Laboratory Medicine* **37**(4): 403-8.

Fry, T. J. and Lankester, A. C. (2010) Cancer immunotherapy: will expanding knowledge lead to success in pediatric oncology? *Hematoly/Oncology Clinics of North America* **24**(1): 109-27.

Fu, Z. et al. (2007) Inhibition of five xenografted human cancers and two murine cancers by the tripeptide tyroservatide. *Anticancer Drugs* **8***(*4):467-70.

Galasso, G. J. and Sharp, D. G. (1962) Virus particle aggregation and the plaque-forming unit. *The Journal of Immunology*. **88**: 339-347.

Galasso, G. J. et al. (1964) The influence of degree of aggregation and virus quality on the plaque titer of aggregated Vaccinia virus. *The Journal of Immunology* **92**: 870-878.

Gao, W. et al. (2011) Inhibition of K562 leukemia angiogenesis and growth by selective Na+/H+ exchanger inhibitor cariporide through down-regulation of pro-angiogenesis factor VEGF. *Leukemia Research* **35**(11):1506-11.

Garber, K. (2006) China approves world's first oncolytic virus therapy for cancer treatment. *Journal of the National Cancer Institute* **98**(5): 298-300.

Garcia-Lora, A. et al. (2003) MHC class I antigens, immune surveillance, and tumor immune escape. *Journal of Cellular Physiology* **195**(3):346-55.

Gerlinger, M. N. et al. (2012) Intratumor heterogeneity and branched evolution revealed by multiregion sequencing. *New England Journal of Medicine* **366**(10): 883-92.

Goldenberg, G. J. et al. (1986) Resistance to adriamycin: relationship of cytotoxicity to drug uptake and DNA single- and double-strand breakage in cloned cell lines of adriamycin-sensitive and -resistant P388 leukemia. *Cancer Research* **46**(6):2978-83.

Groves, R. W. et al. (1991) Human orf and milkers' nodule: a clinicopathologic study. *Journal of the American Academy of Dermatology* **25**(4): 706-11.

Guérin, E. et al. (2012) In vivo topoisomerase I inhibition attenuates the expression of hypoxia-inducible factor 1α target genes and decreases tumor angiogenesis. *Molecular Medicine* **18**(1): 83-94.

Guichard, S. et al. (1999) CPT-11 converting carboxylesterase and topoisomerase I activities in tumour and normal colon and liver tissues. *British Journal of Cancer* **80**(3/4): 364–370.

Gupta, M. et al. (1992) An engineered mutant of vaccinia virus DNA topoisomerase I is sensitive to the anti-cancer drug camptothecin. *Journal of Biological Chemistry* **267**(34): 24177-80.

Guse, K. et al. (2011) Oncolytic vaccinia virus for the treatment of cancer. *Expert Opinion on Biological Therapy* **11**(5): 595-608.

Han, Y. et al. (2006) Cultivation of recombinant Chinese hamster ovary cells grown as suspended aggregates in stirred vessels. *Journal of Bioscience and Bioengineering* **102**(5): 430-5.

Hanahan, D. and Weinberg, R. A. (2000) The hallmarks of cancer. *Cell* **100**(1): 57-70.

Hanahan, D. and Weinberg, R. A. (2011) Hallmarks of cancer: the next generation. *Cell* **144**(5): 646-74.

He, R. et al. (2003) Inhibition of K562 leukemia angiogenesis and growth by expression of antisense vascular endothelial growth factor (VEGF) sequence. *Cancer Gene Therapy* **10**(12):879-86.

Hicklin, D. J. and Ellis, L. M. (2005) Role of the vascular endothelial growth factor pathway in tumor growth and angiogenesis. *Journal of Clinical Oncology* **23**(5): 1011-1027.

Hiley, C. T. et al. (2010) Lister strain vaccinia virus, a potential therapeutic vector targeting hypoxic tumours. *Gene Therapy* **17**(2): 281-7.

Hiley, C. T. et al. (2012) Vascular endothelial growth factor-A promotes Vaccinia virus entry into host cells via activation of the Akt pathway. *Journal of Virology* 2012 Dec 26. [Epub ahead of print]

Hsiang, Y. H. et al. (1989) Arrest of replication forks by drug-stabilized topoisomerase I-DNA cleavable complexes as a mechanism of cell killing by camptothecin. *Cancer Research* **49**(18): 5077-82.

Ichihashi, Y. and Oie, M. (1980) Adsorption and penetration of the trypsinized vaccinia virion. *Virology* **101**(1): 50-60.

Imai, T. (2006) Human Carboxylesterase Isozymes: Catalytic Properties and Rational Drug Design. *Drug Metabolism and Pharmacokinetics* **21**(3):173-85.

Inder, M. K. et al. (2008) The C-terminus of viral vascular endothelial growth factor-E partially blocks binding to VEGF receptor-1. *The FEBS Journal*. **275**(1): 207–217.

Iqbal Ahmed, C.M. et al. (2001) Interferon alpha2b gene delivery using adenoviral vector causes inhibition of tumor growth in xenograft models from a variety of cancers. *Cancer Gene Therapy* **8**(10):788-95.

Jain, R. K. (2005) Normalization of tumor vasculature: an emerging concept in antiangiogenic therapy. *Science* **307**(5706):58-62.

Jansen, W. M. et al. (1997) CPT-11 in human colon-cancer cell lines and xenografts: characterization of cellular sensitivity determinants. *International Journal of Cancer* **70**(3): 335-340.

Jones, S. et al. (2008) Core signaling pathways in human pancreatic cancers revealed by global genomic analyses. *Science* **321**(5897): 1801-6.

Joris, I. et al. (1990) Capillary leakage in inflammation. A study by vascular labeling. *American Journal of Pathology* **137**(6):1353-63.

Kamiyama, H. et al. (2005) Anti-angiogenic effects of SN38 (active metabolite of irinotecan): inhibition of hypoxia-inducible factor 1 alpha (HIF-1alpha)/vascular endothelial growth factor (VEGF) expression of glioma and growth of endothelial cells. *Journal of Cancer Research and Clinical Oncology* **131**(4): 205-13.

Kaneda, N. et al. (1990) Metabolism and Pharmacokinetics of the Camptothecin Analogue CPT-11 in the Mouse. *Cancer Research* **50**:1715-1720.

Kawato, Y. et al. (1991) Intracellular roles of SN-38, a metabolite of the camptothecin derivative CPT-11, in the antitumor effect of CPT-11. *Cancer Research* **51**(16):4187-91.

Kelly, E. and Russell, S. J. (2007) History of oncolytic viruses: genesis to genetic engineering. *Molecular Therapy* **15**(4):651-9.

Kenyon, B. M. et al. (1996) A model of angiogenesis in the mouse cornea. *Investigational Ophthalmology and Visual Science* **37**(8): 1625-32.

Khanna, R. et al. (2000) Proficient Metabolism of Irinotecan by a Human Intestinal Carboxylesterase. *Cancer Research* **60**: 4725–4728.

Kim, K. S. et al. (1969) Effect of some proteolytic enzymes on the plaque titer of vaccinia and rabbitpox viruses. *Virology* **38**(4):503-11.

Kim, K.S. and Sharp, D. G. (1966) Electron microscopic observations on the nature of Vaccinia virus particle aggregation. *The Journal of Immunology* **97**(2): 197-202.

Kim, M. et al. (2010) The viral tropism of two distinct oncolytic viruses, reovirus and myxoma virus, is modulated by cellular tumor suppressor gene status. *Oncogene* **29**(27): 3990-6.

Kirn, D. H. and Thorne, S. H. (2009) Targeted and armed oncolytic poxviruses: a novel multi-mechanistic therapeutic class for cancer. *Nature Reviews Cancer* **9**(1): 64-71.

Kobayashi, K. et al. (1999) pH-dependent uptake of irinotecan and its active metabolite, SN-38, by intestinal cells. *International Journal of Cancer* **83**(4): 491-6.

Kollmar, O. et al. (2006) Macrophage inflammatory protein-2 promotes angiogenesis, cell migration, and tumor growth in hepatic metastasis. *Annals of Surgical Oncology* **13**(2): 263-75.

Kollmar, O. et al. (2007) Stromal cell-derived factor-1 promotes cell migration and tumor growth of colorectal metastasis. *Neoplasia* **9**(10): 862-70.

Kottke, T. et al. (2010) Antiangiogenic cancer therapy combined with oncolytic virotherapy leads to regression of established tumors in mice. *The Journal of Clinical Investigation* **120**(5): 1551-1560.

Le Boeuf, F. and Bell, J. C. (2010) United virus: the oncolytic tag-team against cancer! *Cytokine & Growth Factor Reviews* **21**(2-3): 205-11.

Leibovitz, A. et al. (1983) A hypo-osmotic medium to disaggregate tumor cell clumps into viable and clonogenic single cells for the human tumor stem cell clonogenic assay. *International Journal of Cell Cloning* **1**(6): 478-85.

Levine, B. et al. (1993) Conversion of lytic to persistent alphavirus infection by the bcl-2 cellular oncogene. *Nature* **361**(6414): 739-42.

Li, X. et al. (2005) The hepoxilin analog, PBT-3, inhibits growth of K-562 CML solid tumours in vivo in nude mice. *In Vivo* **19**(1):185-9.

Locker, J. K. et al. (2000) Entry of the two infectious forms of Vaccinia virus at the plasma membrane is signaling-dependent for the IMV but not the EEV. *Molecular Biology of the Cell* **11**(7):2497-511.

Lozzio, B.B. et al. (1983) Proliferation of human malignant hematopoietic cells in immunodeficient mice: suppression by antibody to pluripotent K-562 leukemia cells involves direct cytolysis and effector cells. *Blood* **61**(6):1045-53.

Lun, X. Q. et al. (2009) Efficacy of systemically administered oncolytic vaccinia virotherapy for malignant gliomas is enhanced by combination therapy with rapamycin or cyclophosphamide. *Clinical Cancer Research* **15**(8): 2777- 2788.

Lyttle, D. J. et al. (1994) Homologs of vascular endothelial growth factor are encoded by the poxvirus orf virus. *Journal of Virology* **68**(1): 84-92.

Martinotti, A. et al. (1995) CD4 T cells inhibit in vivo the CD8-mediated immune response against murine colon carcinoma cells transduced with interleukin-12 genes. *European Journal of Immunology* **25**(1):137-46.

Mastrangelo, M. J. et al. (1999) Intratumoral recombinant GM-CSF-encoding virus as gene therapy in patients with cutaneous melanoma. *Cancer Gene Therapy* **6**(5): 409-22.

McCart, J. A. et al. (2000) Complex interactions between the replicating oncolytic effect and the enzyme/prodrug effect of vaccinia-mediated tumor regression. *Gene Therapy* **7**(14): 1217-23.

McCart, J. A. et al. (2001) Systemic cancer therapy with a tumor-selective vaccinia virus mutant lacking thymidine kinase and vaccinia growth factor genes. *Cancer Research* **61**(24): 8751-7.

McGahon, A. et al. (1994) BCR-ABL maintains resistance of chronic myelogenous leukemia cells to apoptotic cell death. *Blood* **83**(5): 1179-87.

Melcher, A. et al. (2011) Thunder and lightning: immunotherapy and oncolytic viruses collide. *Molecular Therapy* **19**(6):1008-16.

Morton, C. L. et al. (2000) Activation of CPT-11 in Mice: Identification and Analysis of a Highly Effective Plasma Esterase. *Cancer Research* **60**: 4206–4210.

Morton, C. L. et al. (2005) Activation and antitumor activity of CPT-11 in plasma esterase-deficient mice. *Cancer Chemotherapy and Pharmacology* **56**(6): 629-36.

Moss, B. 2001. Poxviridae: The Viruses and Their Replication. In Knipe, D. M. and Howley, P. M., eds., Fields Virology, 4th ed., pp. 2849-2871. Lippincott-Raven, Philadelphia.

Moss, B. et al. (1973) Glycoprotein synthesis in cells infected with Vaccinia virus. 3. Purification and biosynthesis of the virion glycoprotein. *Virology* **55**(1):143-56.

Mukherjee, S et al. (2000) Replication-restricted vaccinia as a cytokine gene therapy vector in cancer: persistent transgene expression despite antibody generation. *Cancer Gene Therapy* **7**(5): 663-70.

Mullen, J. T. and Tanabe, K. K. (2002) Viral oncolysis. *The Oncologist* **7**(2): 106-19.

Murono, K. et al. (2012) SN-38 overcomes chemoresistance of colorectal cancer cells induced by hypoxia, through HIF1alpha. *Anticancer Research* **32**(3): 865-72.

Neeman, E. and Ben-Eliyahu, S. (2012) Surgery and stress promote cancer metastasis: New outlooks on perioperative mediating mechanisms and immune involvement. *Brain, Behaviour and Immunity* Available online 4 April 2012

Newman, F. K. et al. (2003) Improved assay to detect neutralizing antibody following vaccination with diluted or undiluted vaccinia (Dryvax) vaccine. *Journal of Clinical Microbiology* **41**(7): 3154-7.

Nitsche, A. et al. (2006) Detection of infectious poxvirus particles. *Emerging Infectious Diseases* **12**(7): 1139–1141.

Ogawa, S. et al. (1998) A novel type of vascular endothelial growth factor, VEGF-E (NZ-7 VEGF), preferentially utilizes KDR/Flk-1 receptor and carries a potent mitotic activity without heparin-binding domain. *Journal of Biological Chemistry* **273**(47): 31273-82.

Ottolino-Perry, K. et al. (2010) Intelligent design: combination therapy with oncolytic viruses. *Molecular Therapy* **18**(2): 251-63.

Overman, J. R. and Sharp, D. G. (1959) Ratios of Vaccinia virus particles to virus infectious units; studies of ratio changes during growth and adaptation in eggs, guinea pigs, and rabbits. *Journal of Experimental Medicine* **110**:461-80.

Paez-Ribes, M. et al. (2009) Antiangiogenic therapy elicits malignant progression of tumors to increased local invasion and distant metastasis. *Cancer Cell* **15**(3): 220-231.

Parato, K. A. et al. (2005) Recent progress in the battle between oncolytic viruses and tumours. *Nature Reviews Cancer* **5**(12): 965-76.

Parato, K. A. et al. (2012) The oncolytic poxvirus JX-594 selectively replicates in and destroys cancer cells driven by genetic pathways commonly activated in cancers. *Molecular Therapy* **20**(4): 749-58.

Park, B. H. et al. (2008) Use of a targeted oncolytic poxvirus, JX-594, in patients with refractory primary or metastatic liver cancer: a phase I trial. *The Lancet Oncology* **9**(6): 533-42.

Payne, L. G. et al. (1979) Mechanism of vaccinia virus release and its specific inhibition by N1-isonicotinoyl-N2-3-methyl-4-chlorobenzoylhydrazine. *Journal of Virology* **32**(2): 614-22.

Peterson, S. E. et al. (2006) Citrate-mediated disaggregation of rotavirus particles in RotaTeq vaccine. *Antiviral Research* **69**(2):107-15.

Pipiya, T. et al. (2005) Hypoxia reduces adenoviral replication in cancer cells by downregulation of viral protein expression. *Gene Therapy* **12**(11): 911-7.

Pitot, H. C. et al. (2000) Phase I dose-finding and pharmacokinetic trial of irinotecan hydrochloride (CPT-11) using a once-every-three-week dosing schedule for patients with advanced solid tumor malignancy. *Clinical Cancer Research* **6**(6):2236-44.

Planterose, D. N. et al. (1962) The purification of vaccinia virus from cell cultures. *Virology* **18**:294-301.

Plate, K. H. et al. (1994) Vascular endothelial growth factor and glioma angiogenesis: coordinate induction of VEGF receptors, distribution of VEGF protein and possible in vivo regulatory mechanisms. *International Journal of Cancer* **59**(4): 520-9.

Pogo, B. G. et al. (1991) Changes in cell gene expression in human leukemic cells persistently infected with vaccinia virus. *Virus Research* **19**(2-3): 131-8.

Potter, P. M. et al. (1998) Cellular Localization Domains of a Rabbit and a Human Carboxylesterase: Influence on Irinotecan (CPT-11) Metabolism by the Rabbit Enzyme. *Cancer Research* **58**: 3627-3632.

Power, A. T. and Bell, J. C. (2007) Cell-based delivery of oncolytic viruses: a new strategic alliance for a biological strike against cancer. *Molecular Therapy* **15**(4): 660-5.

Prewett, M. et al. (1999) Antivascular endothelial growth factor receptor (fetal liver kinase 1) monoclonal antibody inhibits tumor angiogenesis and growth of several mouse and human tumors. *Cancer Research* **59**(20): 5209-5218.

Riley, L.B. and Desai, D.C. (2009) The Molecular Basis of Cancer and the Development of Targeted Therapy. *Surgical Clinics of North America* **89**(1): 1-15.

Rintoul, J. L. et al. (2012) ORFV: a novel oncolytic and immune stimulating parapoxvirus therapeutic. *Molecular Therapy* **20**(6):1148-57.

Rivory, L. P. et al. (1997) Pharmacokinetic interrelationships of irinotecan (CPT-11) and its three major plasma metabolites in patients enrolled in phase I/II trials. *Clinical Cancer Research* **3**(8):1261-6.

Rogakou, E. P. et al. (1998) DNA double-stranded breaks induce histone H2AX phosphorylation on serine 139. *Journal of Biological Chemistry* **273**(10): 5858-5868.

Rothenberg, M. L. et al. (2001) Phase I dose-finding and pharmacokinetic trial of irinotecan (CPT-11) administered every two weeks. *Annals of Oncology* **12**(11):1631-41.

Rubinfeld, B. et al. (2006) Identification and immunotherapeutic targeting of antigens induced by chemotherapy. *Nature Biotechnology* **24**(2): 205-9.

Rupertus, K. et al. (2007) Major but not minor hepatectomy accelerates engraftment of extrahepatic tumor cells. *Clinical and Experimental Metastasis* **24**(1):39-48.

Satoh, T. and Hosokawa, M. (1998) The Mammalian Carboxylesterases: From Molecules to Functions. *Annual Review of Pharmacology and Toxicology* **38**: 257–288.

Savory, L. J. et al. (2000) Viral vascular endothelial growth factor plays a critical role in orf virus infection. *Journal of Virology* **74**(22):10699-706.

Sharp, D. G. and Buckingham, M. J. (1956) Electron microscopic measure of virus particle dispersion in suspension. *Biochimica et Biophysica Acta* **19**(1): 13-21.

Shen, B. H. et al. (2005) Effect of hypoxia on Ad5 infection, transgene expression and replication. *Gene Therapy* **12**(11): 902-10.

Shen, B. H. et al. (2006) The effect of hypoxia on the uptake, replication and lytic potential of group B adenovirus type 3 (Ad3) and type 11p (Ad11p). *Gene Therapy* **13**(12): 986-90.

Shen, Y. and Nemunaitis, J. (2004) Fighting cancer with vaccinia virus: teaching new tricks to an old dog. *Molecular Therapy* **11**(2): 180-95.

Sheng, W.-Y. and Huang, L. (2011) Cancer immunotherapy and nanomedicine. *Pharmaceutical Research* **28**(2): 200-214.

Shibuya, M. (2009) Unique signal transduction of the VEGF family members VEGF-A and VEGF-E. *Biochemical Society Transactions*. **37**(6):1161-6.

Shuman, S. et al. (1988) Characterization of vaccinia virus DNA topoisomerase I expressed in Escherichia coli. *Journal of Biological Chemistry* **263**(31): 16401-7.

Skeel, R.T. et al. (1997) Common cancers - Immunotherapy and multidisciplinary therapy: Parts III and IV. *Disease-a-Month* **43**(11): 749-808

Slee, E. A. et al. (1999) Serial killers: ordering caspase activation events in apoptosis. *Cell Death and Differentiation* **6**(11): 1067-74.

Smallwood, S. E. et al. (2010) Myxoma virus: propagation, purification, quantification, and storage. *Current Protocols in Microbiology* **Chapter 14**: Unit 14A.1.

Smith, G. L. and Moss, B. (1983) Infectious poxvirus vectors have capacity for at least 25 000 base pairs of foreign DNA. *Gene* **25**(1): 21-8.

Soares, E. R. (1979) Identification of a new allele of Es-1 segregating in an inbred strain of mice. *Biochemical Genetics* **17**(7-8):577–583

Stefanko, E. and Wróbel, T. (2010) Mechanisms of resistance to cancer chemotherapy. *Advances in Clinical and Experimental Medicine* **19**(1): 5-12.

Stubdal, H. et al. (2003) A prodrug strategy using ONYX-015-based replicating adenoviruses to deliver rabbit carboxylesterase to tumor cells for conversion of CPT-11 to SN-38. *Cancer Research* **63**(20): 6900-8.

Subarsky, P. and Hill, R. P. (2003) The hypoxic tumour microenvironment and metastatic progression. *Clinical and Experimental Metastasis* **20**(3): 237-50.

Sun, C. et al. (2007) Non-uniform plasma leakage affects local hematocrit and blood flow: implications for inflammation and tumor perfusion. *Annals of Biomedical Engineering* **35**(12):2121-9

te Poele, R. H. and Joel, S. P. (1999) Schedule-dependent cytotoxicity of SN-38 in p53 wild-type and mutant colon adenocarcinoma cell lines. *British Journal of Cancer* **81**(8): 1285-93.

Thorne, S. H. and Kirn, D. H. (2004) Future directions for the field of oncolytic virotherapy: A perspective on the use of vaccinia virus. *Expert Opinion on Biological Therapy* **4**(8): 1307-1321

Thorne, S. H. et al. (2007) Rational strain selection and engineering creates a broad-spectrum, systemically effective oncolytic poxvirus, JX-963. *Journal of Clinical Investigation* **117**(11): 3350-8.

Tseng, J. C. et al. (2010) Enhanced specific delivery and targeting of oncolytic Sindbis viral vectors by modulating vascular leakiness in tumor. *Cancer Gene Therapy* **17**(4):244-55.

Tucker, M. A. et al. (1987) Bone sarcomas linked to radiotherapy and chemotherapy in children. *New England Journal of Medicine* **317**(10): 588-93.

Tucker, M. A. et al. (1988) Risk of second cancers after treatment for Hodgkin's disease. *New England Journal of Medicine* **318**(2): 76-81.

Tyminski, E. et al. (2005) Brain tumor oncolysis with replication-conditional herpes simplex virus type 1 expressing the prodrug-activating genes, CYP2B1 and secreted human intestinal carboxylesterase, in combination with cyclophosphamide and irinotecan. *Cancer Research* **65**(15): 6850-7.

Ueno, H. et al. (2007) A phase II study of weekly irinotecan as first-line therapy for patients with metastatic pancreatic cancer. *Cancer Chemotherapy and Pharmacology* **59**(4): 447-54.

Valcárcel, M. et al. (2008) Three-dimensional growth as multicellular spheroid activates the proangiogenic phenotype of colorectal carcinoma cells via LFA-1-dependent VEGF: implications on hepatic micrometastasis. *Journal of Translational Medicine* **6**:57.

Ver, B.A. et al. (1968) Efficient Filtration and Sizing of Viruses with Membrane Filters. *Journal of Virology* **2**(1): 21–25.

Verreault, M. et al. (2011) Vascular normalization in orthotopic glioblastoma following intravenous treatment with lipid-based nanoparticulate formulations of irinotecan (Irinophore C™), doxorubicin (Caelyx®) or vincristine. *BMC Cancer* **11**:124.

Vukicevic, S. et al. (1992) Identification of multiple active growth factors in basement membrane Matrigel suggests caution in interpretation of cellular activity related to extracellular matrix components. *Experimental Cell Research* **202**(1): 1-8.

Wan, S. et al. (2012) Chemotherapeutics and radiation stimulate MHC class I expression through elevated interferon-beta signaling in breast cancer cells. *PLoS One* **7**(3): e32542.

Wang, P. et al. (2007) Glycerol facilitates the disaggregation of recombinant adeno-associated virus serotype 2 on mica surface. *Colloids and Surfaces* **60**(2):264-7.

Weitzman, M. D. et al. (2010) Genomes in conflict: maintaining genome integrity during virus infection. *Annual Review of Microbiology* **64**: 61-81.

Wierdl, M. et al. (2001) Sensitization of human tumor cells to CPT-11 via adenoviral-mediated delivery of a rabbit liver carboxylesterase. *Cancer Research* **61**(13):5078-82.

Wierdl, M. et al. (2008) An improved human carboxylesterase for enzyme/prodrug therapy with CPT-11. *Cancer Gene Therapy* **15**(3): 183-92.

Wildner, O. (2001) Oncolytic viruses as therapeutic agents. *Annals of Medicine* **33**(5): 291-304.

Williams, J. et al. (2003) Nanoparticle drug delivery system for intravenous delivery of topoisomerase inhibitors. *Journal of Controlled Release* **91**(1-2): 167-72.

Wise, L. M. et al. (2003) Viral Vascular Endothelial Growth Factors Vary Extensively in Amino Acid Sequence, Receptor-binding Specificities, and the Ability to Induce Vascular Permeability yet Are Uniformly Active Mitogens *The Journal of Biological Chemistry*. **278**(39): 38004–38014.

Wise, L. M. et al. (2007) Major amino acid sequence variants of viral vascular endothelial growth factor are functionally equivalent during Orf virus infection of sheep skin. *Virus Research* **128**(1-2): 115-25

Yu, Y. A. et al. (2004) Visualization of tumors and metastases in live animals with bacteria and vaccinia virus encoding light-emitting proteins. *Nature Biotechnology* **22**(3): 313-20.

Zaghloul, N. et al. (2009) Vascular endothelial growth factor blockade rapidly elicits alternative proangiogenic pathways in neuroblastoma. *International Journal of Oncology* **34**(2): 401-7.

Vascular endothelial growth factor blockade rapidly elicits alternative proangiogenic pathways in neuroblastoma.

Zaghloul N,

Zeng, Y. et al. (2012) Knockdown of ZNF268, which is transcriptionally downregulated by GATA-1, promotes proliferation of K562 cells. *PLoS One* **7**(1):e29518

Zhang, L. et al. (2006) Vascular endothelial growth factor overexpression by soft tissue sarcoma cells: implications for tumor growth, metastasis, and chemoresistance. *Cancer Research* **66**(17): 8770-8778.

CONTRIBUTIONS OF COLLABORATORS

Christopher Storbeck, PhD, a post-doc in the lab, designed and cloned VV-YFP and the VV-CE recombinants. In addition, he optimized the CE colourimetric assay.

Phillip Potter, PhD, a collaborator, licensed the CE technology, provided our laboratory with plasmids encoding rCE and hCES1m6, as well as ES1-SCID mice from which to start our colony.

Julia Rintoul, PhD, a former graduate student, provided Orf virus DNA as well as WT Orf and OrfΔVEGF-E virus stocks.

Theresa Falls, a technician in the lab, performed all injections for *in vivo* studies.

Judith Paget and Madison Foster, a technician in the lab and a co-op student, respectively, assisted with the optimization of supernatant CE concentration and desalting as well as grew up concentrated stocks of VV-YFP and the VV-CE recombinants.

Marianne Stanford, PhD, a former post-doc in the lab, performed preliminary experiments that inspired the project (data not shown but major findings were stated).

Appendix I: CE activity of supernatant collected 72 hrs following infection of U2OS cells with the indicated VV recombinant at an MOI of 0.1, as assessed by ability to convert *o*-nitrophenyl acetate to *o*-nitrophenol

Supernatant source	CE activity (µmol *o* -nitrophenol/min/ml of supernatant)
Mock-infected	0.0 ± 68
VV-YFP	-114.4 ± 73
VV-rCEΔHIEL	256.2 ± 59 **
VV-hCES1m6 FL	-154.2 ± 18
VV-hCES1m6ΔHIEL	2.5 ± 30
Mock-infected + hCES2	1065.9 ± 67 ***
Media + 1% FBS	33.6 ± 78
Media + 10% FBS	522.4 ± 19 ***

Results are obtained from one experiment done in triplicate. Data represents mean ± SD. **P < 0.01, *** P < 0.001 (one way ANOVA with Bonferroni's Multiple Comparison Test, comparing samples to "no virus sup").

Appendix II: CPT-11 and SN-38 are stable *in vitro*, as seen by greater efficacy with early CPT-11 addition in the modified supernatant transfer assay. Original cells were either mock infected or infected with the indicated virus at an MOI of 0.1, as well as treated with either vehicle, 0.1 µM CPT-11 or 0.1 µM SN-38 at the indicated time pre-transfer. Three days following infection, supernatant was collected, filtered to remove virus and added to target cells, at a final volume of 50%. Three days following supernatant transfer, target cell metabolic activity was assessed by Alamar Blue. Viability was normalized to target cells receiving supernatant from mock infected cells that were treated with vehicle. Results were obtained from one experiment done with 6 replicates. Data represents mean ± SD. ns P > 05, *** P < 0.001 (one way ANOVA with Bonferroni's Multiple Comparison Test).

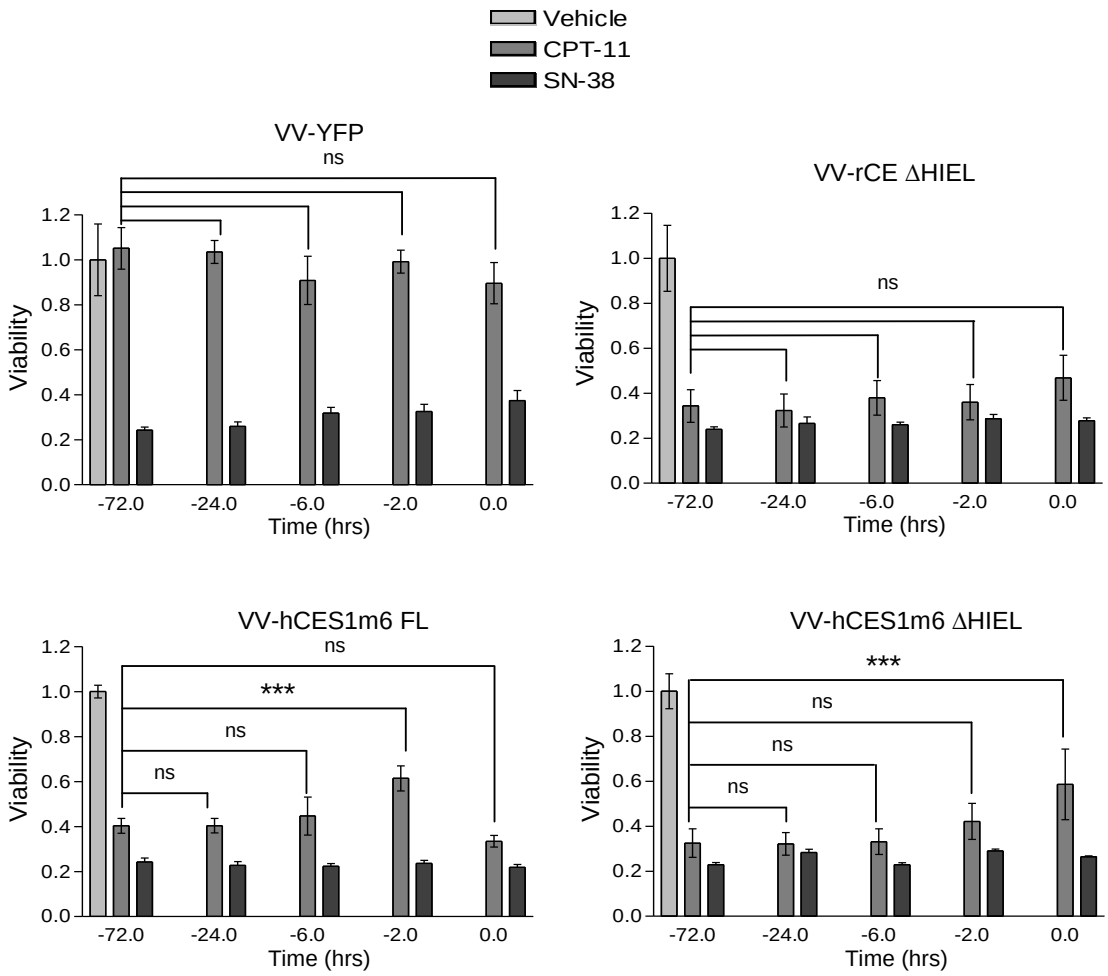
Vehicle
CPT-11
SN-38
VV-YFP
ns
Viability
1.2
1.0
0.8
0.6
0.4
0.2
0.0
-72.0
-24.0
-6.0
-2.0
0.0
Time (hrs)
VV-rCE ΔHIEL
ns
VV-hCES1m6 FL
ns
***
ns
ns
VV-hCES1m6 ΔHIEL
***
ns
ns
ns

Appendix III: Virally-encoded CE does not reduce CPT-11 LC50 *in vitro* in SW-620 cells, as seen by a lack of leftward shift in the curve. SW-620 cells were either mock infected or infected with the indicated virus at an MOI of 0.01 or 3, as well as treated with various CPT-11 concentrations. The drugs and virus were left on the cells for the duration of the experiment. At the indicated day post-treatment, metabolic activity was assessed by Alamar Blue. All values are normalized to the untreated control. Results are obtained from one experiment done with 6 replicates. Data points are means ± SD.

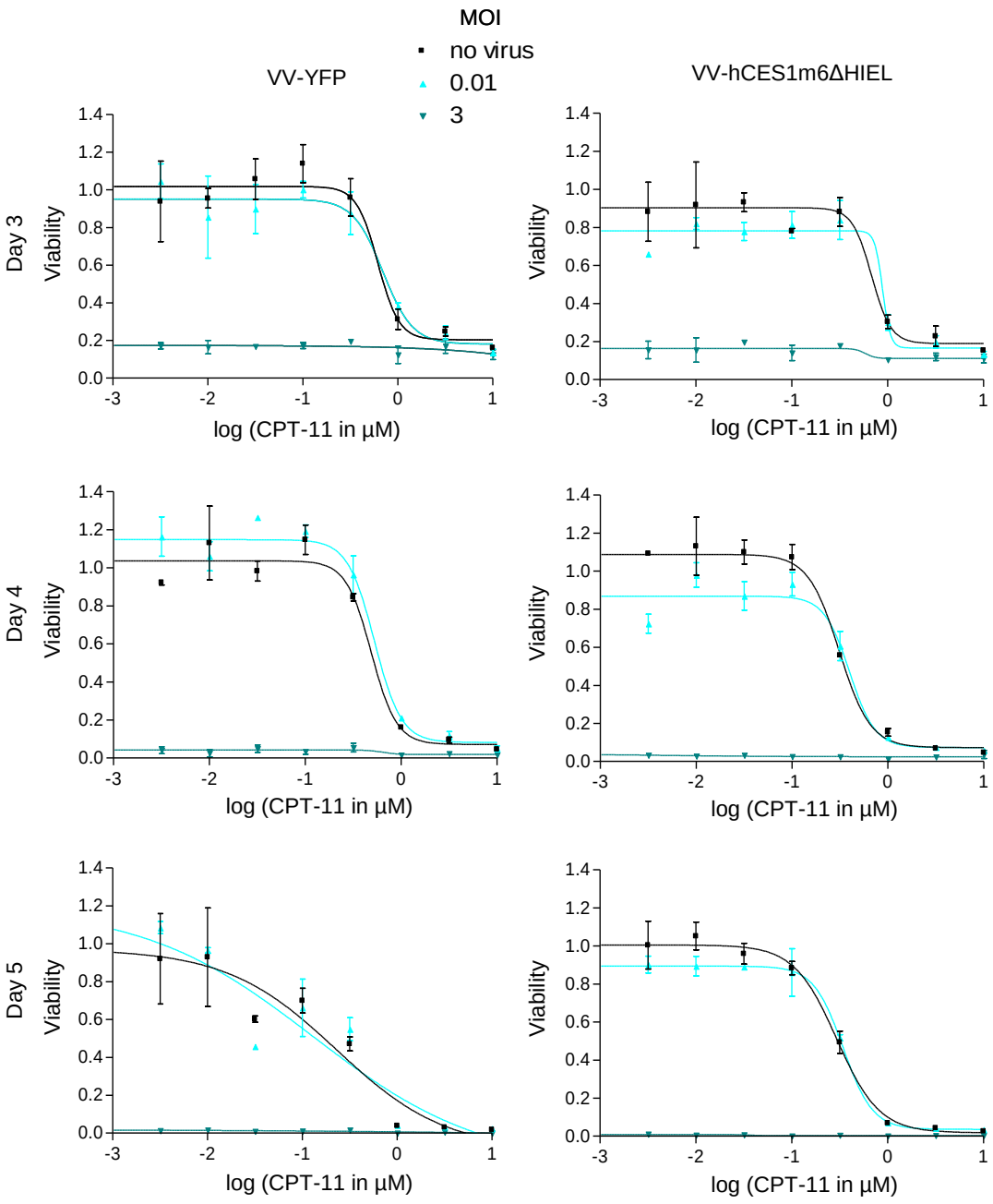
MOI
no virus
0.01
3
VV-YFP
VV-hCES1m6ΔHIEL
Day 3
Day 4
Day 5
Viability
log (CPT-11 in μM)

Appendix IV: Virally-encoded CE does not enhance target SW-620 cell death in the presence of CPT-11 in an *in vitro* transwell system. Both the top and bottom layers of a transwell system, where pores are too small to allow VV to cross the insert, were plated with SW-620 cells. The bottom layer was either mock infected or infected with the indicated virus at an MOI of 0.1 as well as treated with either vehicle, 0.1 µM CPT-11 or 0.03 µM SN-38. The drug remained in the media for the remainder of the experiment. Five days later, metabolic activity was assessed by Alamar Blue. Viability was normalized to that of the sample from that particular layer that was mock infected and treated with vehicle only. Results were obtained from one experiment and viability readings were done in duplicate for the bottom layer and triplicate for the top layer. Data represents mean ± SD. ** $P < 0.01$, *** $P < 0.001$ (one way ANOVA with Bonferroni's Multiple Comparison Test).

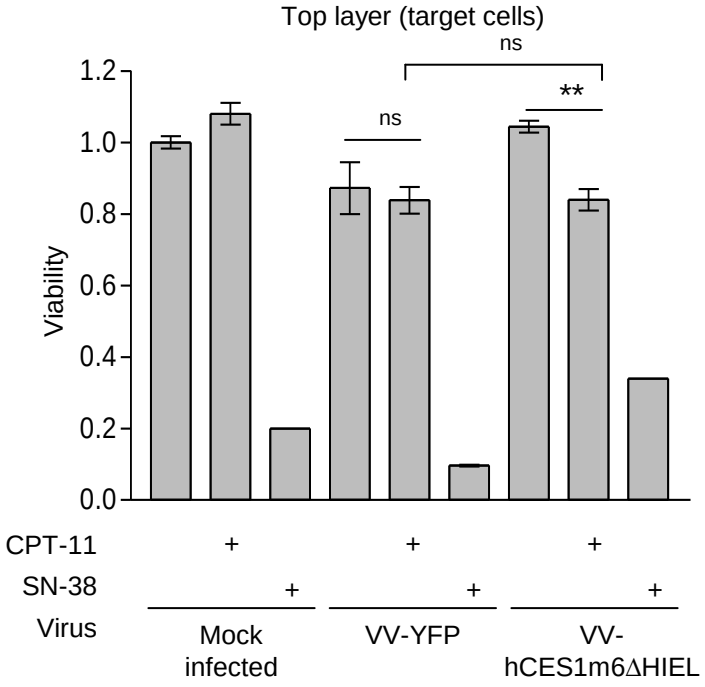
Top layer (target cells)
ns
**
ns
1.2
1.0
0.8
0.6
0.4
0.2
0.0
Viability
CPT-11
SN-38
Virus
+
+
+
+
+
+
Mock infected
VV-YFP
VV-hCES1m6ΔHIEL

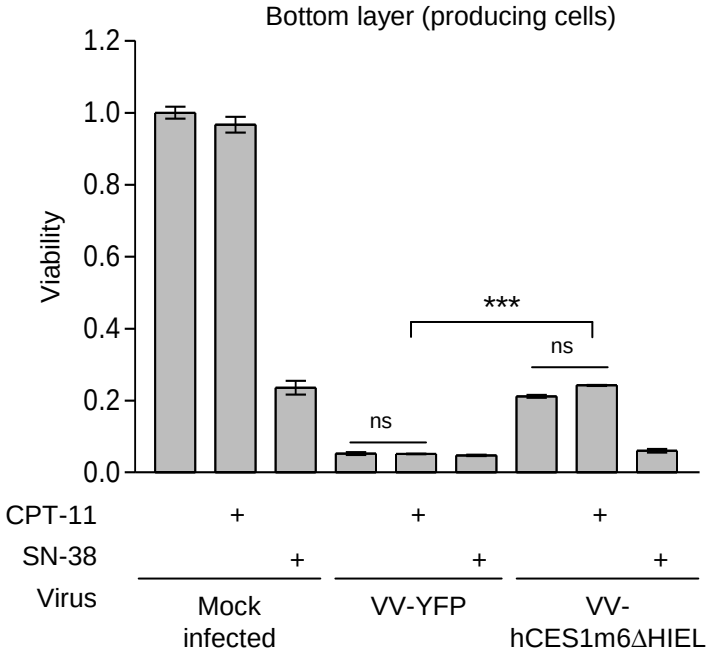
Bottom layer (producing cells)
***
ns
ns
1.2
1.0
0.8
0.6
0.4
0.2
0.0
Viability
CPT-11
SN-38
Virus
+
+
+
+
+
+
Mock infected
VV-YFP
VV-hCES1m6ΔHIEL

Appendix V: VV-CE recombinants do not provide an advantage when combined with CPT-11 in an *in vitro* SW-620 spheroid model. SW-620 spheroids, which were produced using the hanging drop method, were treated with the indicated number of pre-infected SW-620 cells, or mock infected cells, as well as either vehicle, 0.01 µM CPT-11 or 0.01 µM SN-38. The pre-infected cells were infected at an MOI of 1 and added to the spheroids immediately after infection. Four days post-treatment, YFP expression was assessed and the percentage of YFP positive spheroids is indicated above each bar. Spheroids from the same condition were combined (20 spheroids / condition), disaggregated and viability was assessed by trypan blue exclusion. For samples that were treated with infected cells, only YFP positive spheroids were collected and counted. The viable cell count was normalized to that of spheroids treated with mock infected cells and vehicle.

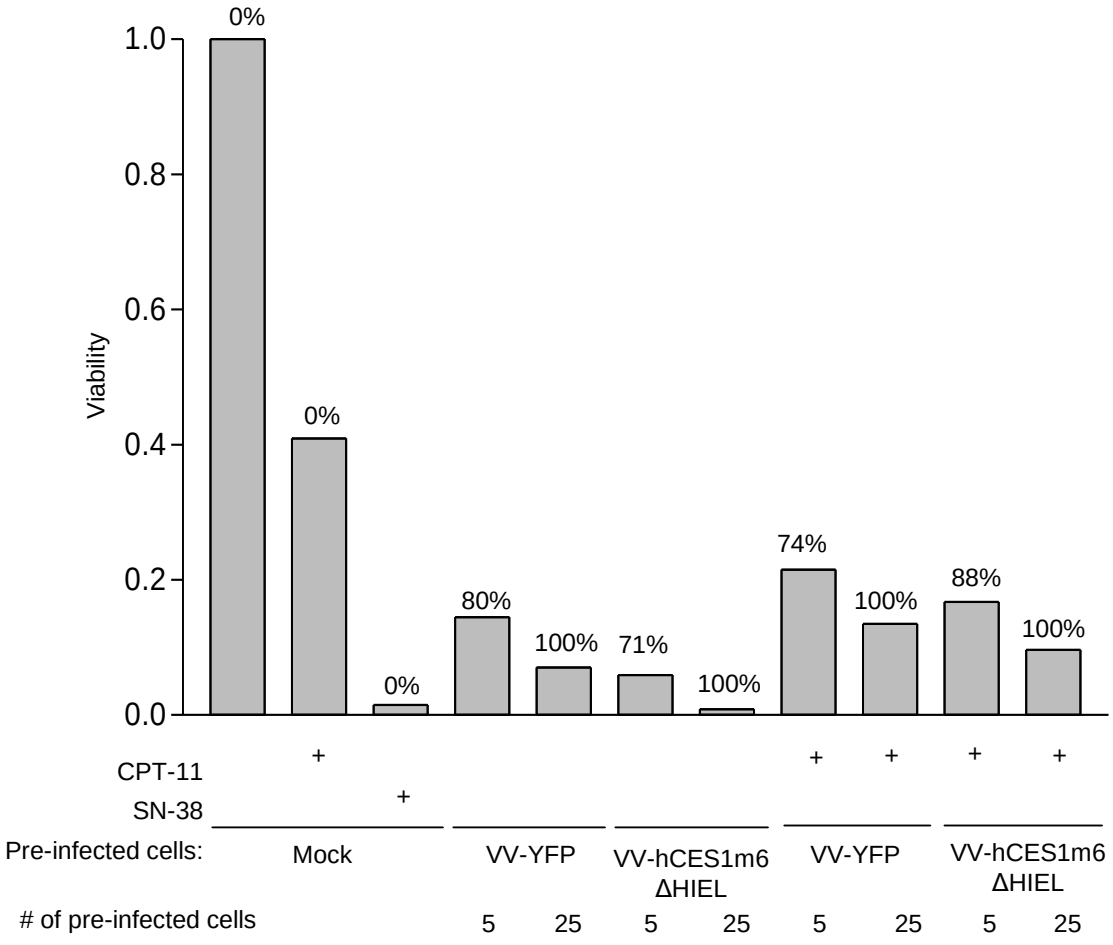
0%
0%
0%
80%
100%
71%
100%
74%
100%
88%
100%
1.0
0.8
0.6
0.4
0.2
0.0
Viability
CPT-11
SN-38
+
+
+
+
+
+
Pre-infected cells:
Mock
VV-YFP
VV-hCES1m6 ΔHIEL
VV-YFP
VV-hCES1m6 ΔHIEL
# of pre-infected cells
5
25
5
25
5
25
5
25

Appendix VI: Virally-encoded CE does not consistently provide an advantage in an *in vitro* cover slip spreading assay on 786-0 cells in the presence of CPT-11. A cover slip containing a monolayer of U2OS cells was either mock infected or infected with the indicated virus at an MOI of 3. Following the infection, the cover slip was immediately added to a monolayer of 786-0 cells and topped with agarose overlay containing either vehicle, 0.1 µM CPT-11 or 0.1 µM SN-38. Four days later, wells were fixed with Carnoy's Fix and stained with Coomassie Blue. Each column represents an independent experiment. For simplicity, only one replicate was shown for mock infected cover slips as well as for wells containing SN-38 in the overlay. Data represents 5 independent experiments.

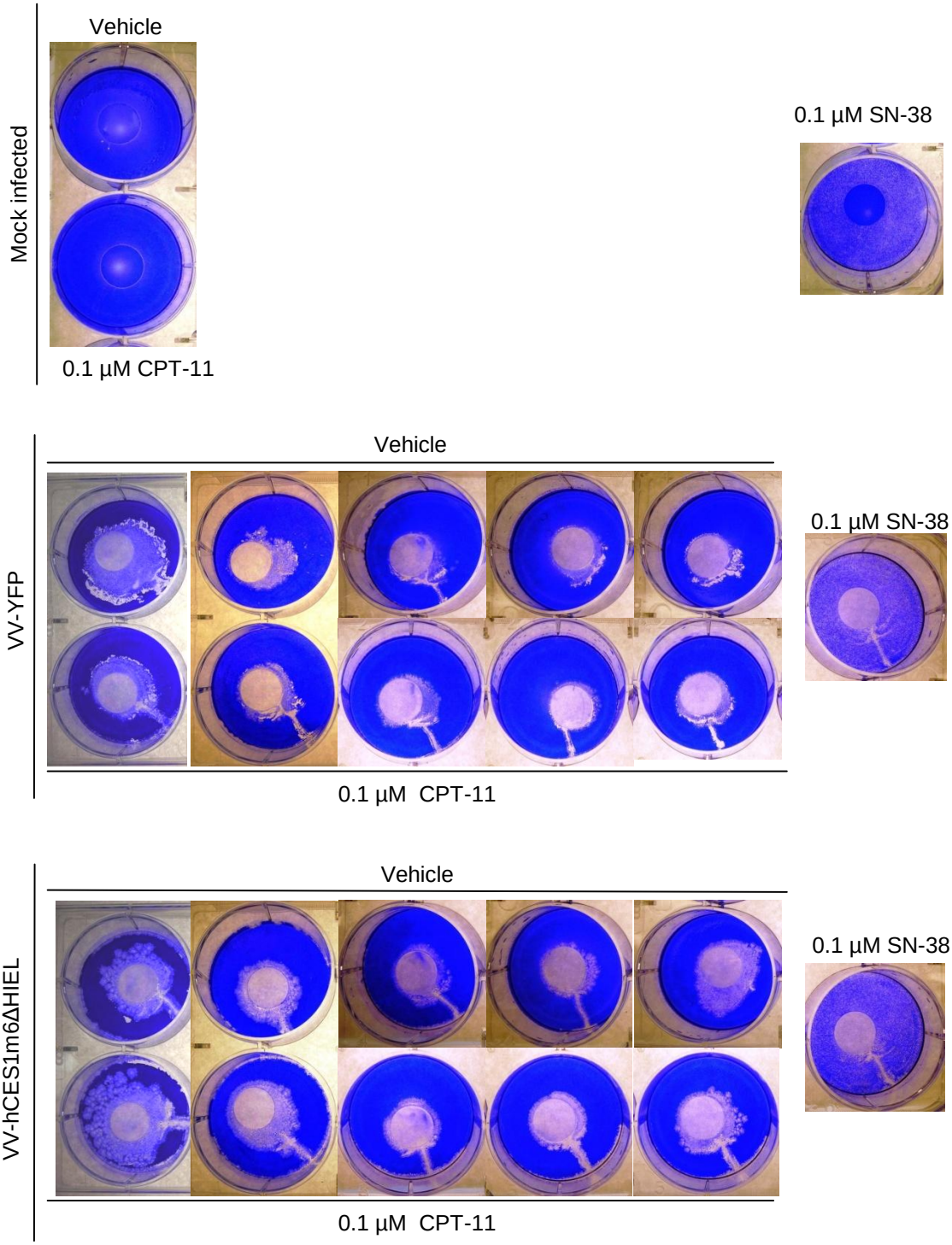
Vehicle
Mock infected
0.1 µM SN-38
0.1 µM CPT-11
Vehicle
VV-YFP
0.1 µM SN-38
0.1 µM CPT-11
Vehicle
VV-hCES1m6ΔHIEL
0.1 µM SN-38
0.1 µM CPT-11

Appendix VII: 10^6 PFU of VV-YFP is a good starting point for follow-up IV VV-YFP dose escalation experiments in ES1-SCID mice bearing SW-620 tumours. A dose of 10^6 PFU results in replicating virus within the tumour but does not significantly shrink tumour volume on its own. A) Two ES1-SCID mice bearing palpable SQ SW-620 tumours were treated according to the schedule shown. B) Tumour volume was measured on days 0, 6 and 9. Volume was calculated by (length × width2)/2. C) Excised tumours were weighed, homogenized in PBS and titered on U2OS cells.

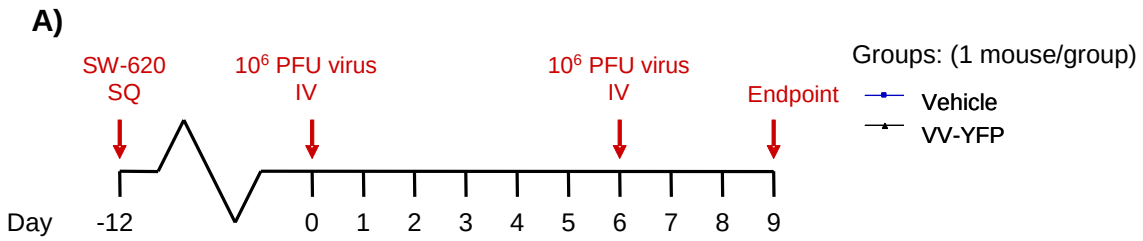
A)
SW-620
SQ
10^6 PFU virus
IV
10^6 PFU virus
IV
Endpoint
Groups: (1 mouse/group)
Vehicle
VV-YFP
Day
-12
0
1
2
3
4
5
6
7
8
9

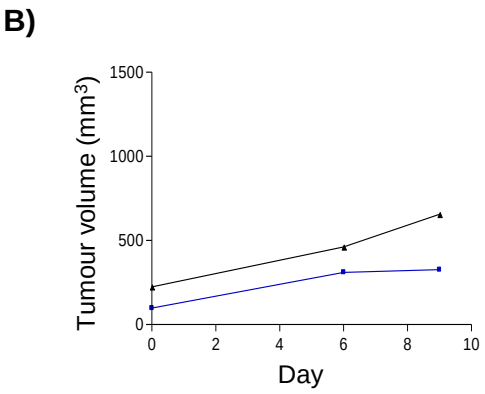
B)
Tumour volume (mm3)
1500
1000
500
0
0
2
4
6
8
10
Day

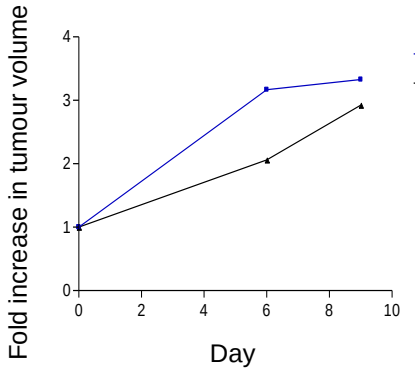
Fold increase in tumour volume
4
3
2
1
0
0
2
4
6
8
10
Day

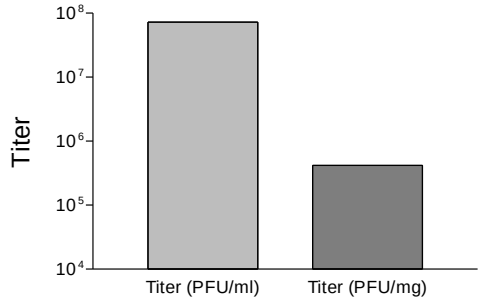
C)
Titer
10^8
10^7
10^6
10^5
10^4
Titer (PFU/ml)
Titer (PFU/mg)

Appendix VIII: Virally-encoded CE does not provide an advantage when combined with CPT-11 for the treatment of SW-620 tumours, as assessed by the restriction of active caspase-3 staining to areas of VV staining in both treatment groups. A) ES1-SCID mice bearing palpable SW-620 SQ tumours were treated according to the schedule shown. B) Tumour volume was measured on days 0, 2, 7 and 9. Volume was calculated by (length × width^2)/2. Data points are means ± SD, n = 2. ns P > 0.05 (Welch's corrected unpaired t test). (C) Excised tumours were sectioned, frozen and IHC staining for VV and active caspase-3 was performed. Image is representative of tumours from both groups.

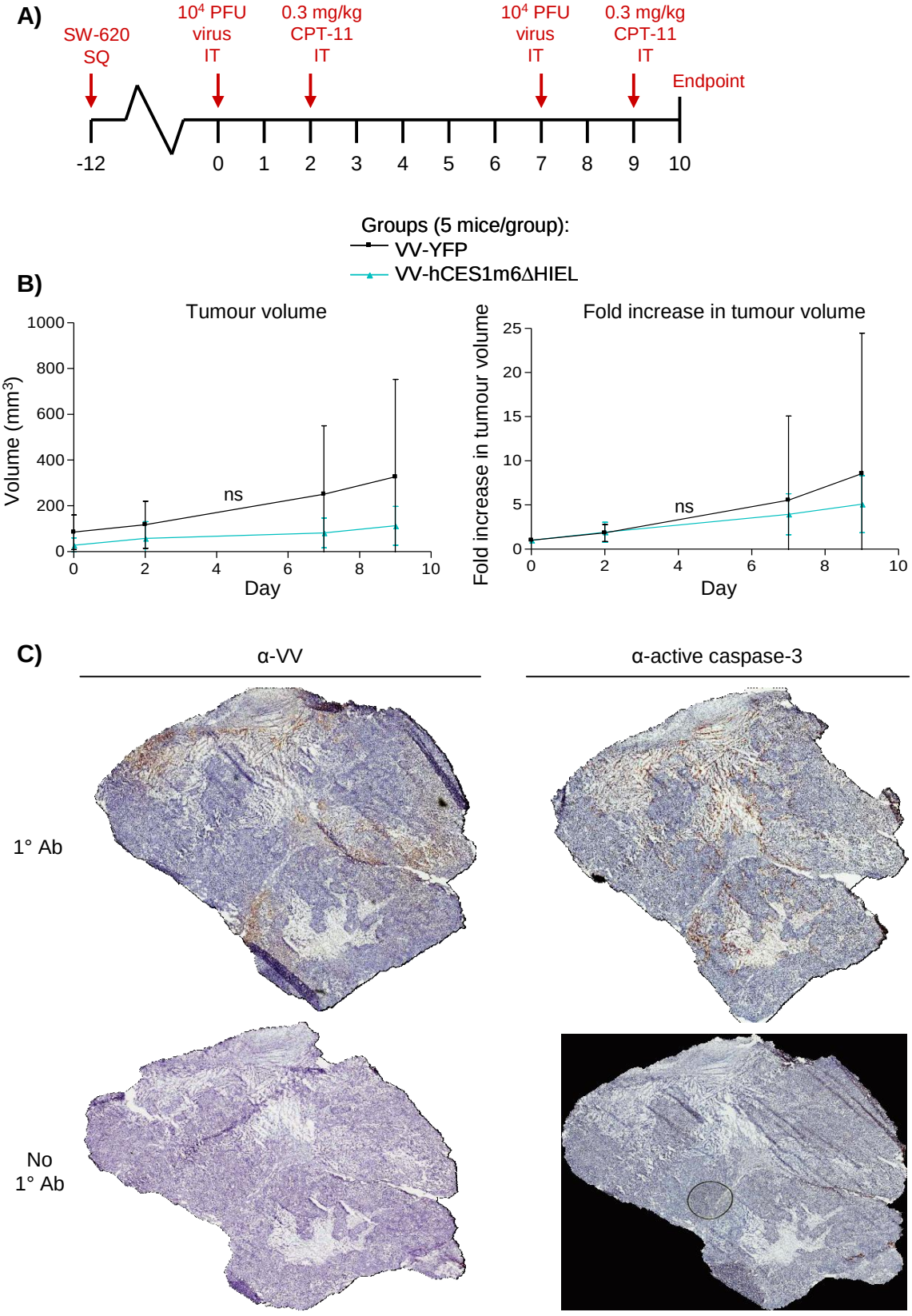
A)
SW-620 SQ
10^4 PFU virus IT
0.3 mg/kg CPT-11 IT
10^4 PFU virus IT
0.3 mg/kg CPT-11 IT
Endpoint
-12
0
1
2
3
4
5
6
7
8
9
10
Groups (5 mice/group):
VV-YFP
VV-hCES1m6ΔHIEL
B)
Tumour volume
Volume (mm3)
ns
Day
Fold increase in tumour volume
Fold increase in tumour volume
ns
Day
C)
α-VV
α-active caspase-3
1° Ab
No 1° Ab

Appendix IX: Schematic representation of the recombinant vvDD-VEGF-E construct. Orf virus VEGF-E gene was subcloned into the pSC65-Luc plasmid and then recombined into vvDD's TK location, disrupting the TK gene. pSel is the VV synthetic early/late promoter and p7.5 is the Vaccinia 7.5K early/late promoter.

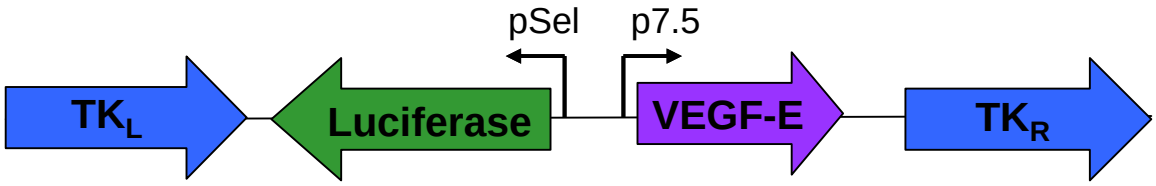
pSel
p7.5
TK$_L$
Luciferase
VEGF-E
TK$_R$

Michelle Caitlin Becker

EDUCATION

2009 – *present* **University of Ottawa**
Master of Science in Biochemistry with Specialization in Human and Molecular Genetics
- Thesis: The combination of carboxylesterase-expressing oncolytic Vaccinia virus and irinotecan

2005 – 2009 **University of Ottawa**
Bachelor of Science, Honours with Specialization in Biochemistry
- Graduated Summa Cum Laude
- Thesis: The construction of three attenuated Semliki Forest virus derivatives

PUBLICATIONS

Vaha-Koskela, M.; Le Boeuf, F.; Lemay, C.; De Silva, N.; Diallo, J. S.; Cox, J.; **Becker, M**.; Choi, Y.; Ananth, A.; Sellers, C.; Breton, S.; Roy, D.; Falls, T.; Brun, J.; Hemminki, A.; Hinkkanen, A. and Bell, J. C. (2012) Resistance to two heterologous neurotropic oncolytic viruses in experimental glioma. *Journal of Virology* [Epub ahead of print]
- Accepted

PRESENTATIONS

The following seminar was presented at the following meetings:
- Title: The effect of tumour vascular modulation on oncolytic virus activity

February 2011 **University of Ottawa BMI Seminar Day**

The following poster was presented at the following meetings:
- Title: The combination of carboxylesterase-expressing oncolytic Vaccinia virus and irinotecan

May 2012 **University of Ottawa BMI Poster Day**
November 2011 **1st Canadian Cancer Research Conference**
November 2011 **11th Annual Ottawa Hospital Research Institute's Research Day**

The following poster was presented at the following meetings:
- Title: The effect of tumour vascular modulation on oncolytic virus activity

March 2011 **6th International Conference on Oncolytic Viruses As Cancer Therapeutics**
November 2010 **10th Annual Ottawa Hospital Research Institute's Research Day**
June 2010 **XVIII International Poxvirus, Asfivirus, and Iridovirus Symposium**
May 2010 **University of Ottawa BMI Poster Day**

February/March 2010 **3rd Annual Ontario Institute for Cancer Research's Annual Scientific Meeting**
November 2009 **9th Annual Ottawa Hospital Research Institute's Research Day**

GRANTS AND FELLOWSHIPS

2011 – 2012 **Ontario Graduate Scholarship (PhD level)**, refused
2010 – 2011 **Ontario Graduate Scholarships in Science and Technology (Master's Level)**
2010 – 2011 **University of Ottawa Admission Scholarship**
2009 – 2010 **CIHR Frederick Banting and Charles Best Canada Graduate Scholarships - Master's Award**
2009 – 2010 **University of Ottawa Excellence Scholarship**
2005 – 2009 **University of Ottawa Admission Scholarship**

AWARDS AND HONOURS

2009 Graduated Bachelor's program **Summa Cum Laude**
2005 – 2009 **Dean's Honour List** for undergraduate studies

WORK EXPERIENCE

Summer 2009, 2008 **Ottawa Health Research Institute's Center for Cancer Therapeutics** Student Research Assistant in Dr. John Bell's lab

Summer 2007 **VHA Health and Home Support** Administrative Assistant / Receptionist

Summer 2006 **Math tutor**